

MOLECULAR GENETICS OF THE LONG QT SYNDROME

by

Igor Splawski

A dissertation submitted to the faculty of  
The University of Utah,  
in partial fulfillment of the requirements for the degree of

Doctor of Philosophy

Department of Human Genetics

The University of Utah

May 1999

Copyright © Igor Splawski 1999

All Rights Reserved

THE UNIVERSITY OF UTAH GRADUATE SCHOOL

## SUPERVISORY COMMITTEE APPROVAL

of a dissertation submitted by

**Igor Splawski**

This dissertation has been read by each member of the following supervisory committee and by majority vote has been found to be satisfactory.

  
\_\_\_\_\_

  
\_\_\_\_\_

Chair: Mark T. Keating

  
\_\_\_\_\_

  
\_\_\_\_\_

Mark F. Leppe

  
\_\_\_\_\_

  
\_\_\_\_\_

Richard S. Le

  
\_\_\_\_\_

  
\_\_\_\_\_

Louis J. Ptacek

  
\_\_\_\_\_

  
\_\_\_\_\_


THE UNIVERSITY OF UTAH GRADUATE SCHOOL

**FINAL READING APPROVAL**


To the Graduate Council of the University of Utah:

I have read the dissertation of \_\_\_\_\_ in its final form and I have found that (1) its format, citations and bibliographic style are consistent and acceptable; (2) its illustrative materials including figures, tables and charts are in place; and (3) the final manuscript is satisfactory to the supervisory committee and is ready for submission to The Graduate School.

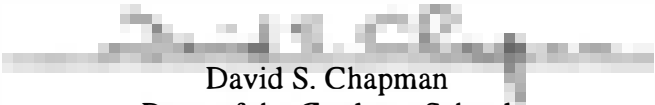
\_\_\_\_\_  
Date

  
Chair, Supervisory Committee

Approved for the Major Department

  
Chair/Dean

Approved for the Graduate Council

  
David S. Chapman  
Dean of the Graduate School

## ABSTRACT

Long QT syndrome (LQT) is a cardiovascular disorder that causes syncope, seizures and sudden death. Two forms of inherited LQT have been identified, autosomal dominant and autosomal recessive. The autosomal dominant form is the most common form and is not associated with other known phenotypic abnormalities. Autosomal recessive LQT is associated with congenital neural deafness. The symptoms of LQT result from cardiac arrhythmias, specifically ventricular tachyarrhythmias, like *torsade de pointes* and ventricular fibrillation.

In 1991, a gene for autosomal dominant LQT was localized to chromosome 11p15.5 (*LQT1*) in our laboratory. We employed linkage analyses, using PCR-based polymorphic markers regularly spaced throughout the human genome, to identify two new loci for autosomal dominant LQT - 7q35-36 (*LQT2*) and 3p21-24 (*LQT3*). Positional-candidate gene approach showed that mutations in a putative potassium channel gene, *HERG*, caused LQT2 and that LQT3 was caused by mutations in *SCN5A*, the cardiac sodium channel gene. Positional cloning methods were used to isolate a novel gene, *KVLQT1*, from the physical map encompassing the LQT1 region. Multiple mutations in *KVLQT1* were implicated in arrhythmia susceptibility and sudden death. MinK, a potassium channel subunit, was shown to assemble with KVLQT1 to form cardiac  $I_{Ks}$  channels. Thus, *minK* became a candidate gene for LQT. We demonstrated that mutations in *minK* cosegregated with the disease phenotype in two families.

Coexpression of mutant and normal minK demonstrated that mutations suppress  $I_{Ks}$  channel function.

*KVLQT1*, *HERG*, *SCN5A* and *minK* encode ion channel subunits involved in the generation of the cardiac action potential. Mutations can lead to channel dysfunction and delayed myocellular repolarization. The aberrant cardiac repolarization creates a substrate for arrhythmia. *KVLQT1* and *minK* are also expressed in the inner ear. We demonstrated that homozygous mutations in *KVLQT1* can cause deafness and the severe cardiac phenotype associated with Jervell and Lange-Nielsen syndrome. Loss of functional channels in the ear disrupts the production of endolymph, leading to deafness.

Finally, we defined the complete genomic structure of *KVLQT1*, *HERG* and *minK* and designed primers for the amplification of each exon. This information was used to identify 138 new LQT-associated mutations. This enables presymptomatic diagnosis of LQT in the affected families and has implications for the prevention and treatment of this life-threatening disorder.

## TABLE OF CONTENTS

ABSTRACT .....	iv
Chapter	
1. INTRODUCTION .....	1
References .....	11
2. TWO LONG QT SYNDROME LOCI MAP TO CHROMOSOMES 3 AND 7 WITH EVIDENCE FOR FURTHER HETEROGENEITY.....	15
Introduction.....	16
Results .....	17
Discussion .....	19
Acknowledgments .....	21
References .....	22
3. A MOLECULAR BASIS FOR CARDIAC ARRHYTHMIA: <i>HERG</i> MUTATIONS CAUSE LONGQTSYNDROME.....	23
Summary.....	24
Introduction.....	24
Results .....	25
Discussion .....	29
Experimental Procedures.....	30
Acknowledgments .....	31
References .....	31
4. <i>SCN5A</i> MUTATIONS ASSOCIATED WITH AN INHERITED CARDIAC ARRHYTHMIA, LONG QT SYNDROME.....	33
Summary.....	34
Introduction.....	34
Results .....	35
Discussion .....	37
Experimental Procedures.....	38
Acknowledgments .....	39
References .....	39
5. POSITIONAL CLONING OF A NOVEL POTASSIUM CHANNEL GENE: <i>KVLQT1</i> MUTATIONS CAUSE CARDIAC ARRHYTHMIAS.....	41

	Introduction.....	42
	Results .....	42
	Discussion.....	46
	Methods.....	47
	Acknowledgments .....	48
	References .....	48
6.	MUTATIONS IN <i>HMINK</i> GENE CAUSE LONG QT SYNDROME AND SUPPRESS $I_{Ks}$ FUNCTION.....	49
	Abstract .....	50
	Results and Discussion.....	50
	Methods.....	52
	Acknowledgments .....	52
	References .....	52
7.	MOLECULAR BASIS OF THE LONG-QT SYNDROME ASSOCIATED WITH DEAFNESS.....	53
	Introduction.....	54
	Methods.....	54
	Results .....	55
	Discussion.....	57
	Acknowledgments .....	59
	References .....	59
8.	GENOMIC STRUCTURE OF THREE LONG QT SYNDROME GENES: <i>KVLQT1</i> , <i>HERG</i> , AND <i>KCNE1</i> .....	60
	Abstract .....	61
	Introduction.....	61
	Materials and Methods .....	62
	Results .....	66
	Discussion.....	70
	Acknowledgments .....	71
	References .....	71
9.	NOVEL MUTATIONS IN LONG QT SYNDROME GENES: <i>KVLQT1</i> , <i>HERG</i> , <i>SCN5A</i> AND <i>MINK</i> .....	73
	Introduction.....	73
	Methods.....	75
	Results .....	76
	Discussion.....	100
	References .....	105



## ACKNOWLEDGMENTS

I would like to thank my parents Weneta Splawska and Jozef Splawski, and my brother Wlodzimierz Splawski for their unconditional support through the 23 years of my schooling. I will always appreciate their love and devotion, and the effort to create a freethinking and encouraging atmosphere from which I drew my confidence.

Mark Keating established an environment in which team success led to individual success and *vice versa*. With his guidance and especially with his personal example, Mark helped to develop my concentration, persistence, and at the same time impatience - all of which are so important in the world of science. I realize now how contagious were his enthusiasm and optimism for setting higher goals and standards. Thank you, Mark!

I am thankful to my committee members, Dr. Jean-Marc Lalouel, Dr. Mark Leppert, Dr. Louis Ptacek and Dr. Richard Lemons for their time and advice. I also wish to thank my master's thesis advisor, Dr. Luben Dolapchiev at the Institute of Molecular Biology in Sofia, Bulgaria, for my first steps into the biology of macromolecules.

The findings described here would not have been possible without the help of many collaborators. Katherine Timothy was tireless in her search for patients and phenotypic details, which are an inseparable part of the human genetics field and provide clues for numerous experiments. Mike Sanguinetti took our discoveries to another level by showing physiologically how mutations in cardiac ion channels cause arrhythmia. It is difficult to adequately express my gratitude to Donald Atkinson for the countless hours

he spent trying to transplant his experience upon me and for his invaluable help with computers. My other labmates, Qing Wang, Mark Curran, Shannon Odelberg, Amanda Ewart, Mike Frangiskakis, Dean Li, Xun Meng, Lisa Urness, Beth Boak, Xiaojun Lu, Tim Olson and Jiaxiang Shen were a never ending source of information.

I am grateful to the experienced personnel and for the modern research facilities available at the University of Utah. Ed Meenen at the nucleotide synthesis core, Tena Varvil at the DNA core facility, Wendy Bahr at the Clinical Research Center and the DNA sequencing core provided many of the tools that led to the discoveries in this thesis.

Funding from government and private institutions such as the National Institutes of Health, the American Heart Association, the University of Utah, the Howard Hughes Medical Institute and Bristol-Myers Squibb was essential and is appreciated. I am indebted to the journals *Cell*, *Nature Genetics*, *New England Journal of Medicine* and *Genomics* for giving me permission to reprint published work.

I thank my friends Krassimire Vatev and Pamela Arneson for standing by me in difficult moments and for helping me go through the inevitable ups and downs associated with work of this kind.

Lastly, but most importantly, I would like to thank the hundreds of individuals with cardiac arrhythmias and their family members for agreeing to participate in this study.

## CHAPTER 1

### INTRODUCTION

Sudden death claims more than 300,000 lives in the United States each year and ventricular arrhythmias are responsible for most of these deaths (Kannel et al., 1987; Willich et al., 1987). Despite their importance, presymptomatic diagnosis and treatment of life-threatening arrhythmias are difficult and in some cases medical therapy has increased the occurrence of arrhythmia. Until recently, the molecular mechanisms of cardiac arrhythmias were poorly understood.

Long QT syndrome (LQT) is a cardiovascular disorder characterized by an abnormality in cardiac repolarization leading to prolonged QT interval on surface electrocardiograms. LQT causes episodic and abrupt loss of consciousness (syncope), seizures and sudden death, usually in young, otherwise healthy, individuals. The clinical features of LQT result from the episodic cardiac tachyarrhythmia, *torsade de pointes*, named for the characteristic undulating nature of the electrocardiogram (Moss et al., 1991; Schwartz et al., 1975). *Torsade de pointes* may degenerate into ventricular fibrillation, a particularly lethal arrhythmia. Although LQT is not a common diagnosis, ventricular arrhythmias are very common and aberrant cardiac repolarization may be the

underlying mechanism in many cases. LQT, therefore, provides a unique opportunity to study life-threatening cardiac arrhythmias at the molecular level.

Long QT syndrome can be inherited or acquired. Acquired LQT typically results from treatment with antiarrhythmics (quinidine, sotalol), antidepressants (amitriptyline), antihistamines (astemizole), antibiotics (erythromycin) and other drugs. QT prolongation can also be induced by electrolyte abnormalities like hypomagnesemia and hypokalemia. Various medical conditions, such as bradycardia, myocarditis, encephalitis and intracranial bleeding can cause acquired LQT as well.

Two inherited forms of LQT exist: Jervell and Lange-Nielsen syndrome (JLN) and Romano-Ward syndrome (RW). JLN is characterized by the presence of deafness, a phenotypic abnormality inherited as an autosomal recessive trait. In 1957, Jervell and Lange-Nielsen reported a Norwegian family with six children, four of whom had congenital sensory deafness and prolonged QT interval (Jervell and Lange-Nielsen, 1957). Affected children had multiple syncopal episodes and three died suddenly at ages 4, 5 and 9 years. Since 1957, other examples of long-QT syndrome associated with deafness have been described (Fraser et al., 1964; Jervell et al., 1966; Tesson et al., 1996). In all cases the apparent mode of inheritance was autosomal recessive. This syndrome is rare with estimated incidence of 1.6 to 6 per million (Fraser et al., 1964). Affected individuals are susceptible to recurrent syncope with a high incidence of sudden death and short life expectancy.

Romano-Ward syndrome is the autosomal dominant form of LQT and is not associated with deafness or other phenotypic abnormalities. Romano et al. in 1963 and Ward in 1964 described the presence of prolonged QT intervals, syncopal episodes and

sudden death in members of two families (Romano et al., 1963; Ward, 1964). Multiple reports followed describing additional families with autosomal dominant inheritance. Once viewed as a rare disorder, Romano-Ward syndrome is now increasingly recognized. The incidence of Romano-Ward is higher than Jervell and Lange-Nielsen syndrome, but affected individuals generally have milder symptoms (Moss et al., 1985; Moss et al., 1991).

In 1991, our laboratory reported tight genetic linkage between autosomal dominant LQT and a DNA marker within the Harvey *ras-1* gene on chromosome 11p15.5 (Keating et al., 1991). This finding was confirmed in six additional families bringing the combined LOD (logarithm of odds) score to 21.69, indicating odds greater than  $10^{21}$  to 1 in favor of linkage (Keating et al., 1991). Phenotypically, members of families were divided in three categories based on their QTc (QT interval corrected for heart rate) and presence of symptoms. The categories clearly distinguished affected individuals ( $QTc > 0.45$  sec with symptoms or  $QTc > 0.47$  sec without symptoms) from unaffected ( $QTc < 0.41$  sec) and uncertain ( $0.42 < QTc < 0.46$  without symptoms) individuals. Only affected and unaffected individuals were used for linkage. A DNA marker linked to the disease phenotype was then used for genotypic analysis in all members of these families.

The study showed the shortcomings of LQT diagnosis based only on QTc interval, especially in asymptomatic individuals with QTc between 0.42 and 0.46 sec. In the past, diagnosis of LQT was based on electrocardiographic findings of QTc greater than 0.44 sec, presence of symptoms (syncope, seizures, and sudden death), and family history. Many LQT gene carriers have prolonged QT intervals on electrocardiograms, but diagnosis of LQT based solely on these criteria is difficult. Gender, age, drug

treatment, electrolytic abnormalities and presence of other disease can influence the QT interval. Furthermore, the presence of symptoms and family history are not completely indicative of LQT. Genetic studies show overlap between QTc in LQT carriers and control populations. In one study, using 0.44 sec as a critical value resulted in a misclassification rate of 11% (Vincent et al., 1992). The rate was 20% in another study (Splawski et al., 1997). Misclassification leads to false-positive diagnosis with potential for unnecessary treatment. Misclassification can also result in false-negatives. The latter group (LQT carriers with QTc of 0.44 sec or less) is more important as these patients may be at risk for tachyarrhythmias and sudden death. Additionally, young people, the age group most often affected by arrhythmia in LQT, rarely undergo electrocardiographic screening.

In 1993, two groups, including our laboratory, reported kindreds that were not linked to 11p15.5, defining genetic heterogeneity for LQT (Benhorin et al., 1993; Curran et al., 1993). This discovery initiated new linkage studies. Simultaneously, using refined linkage mapping or direct sequencing, we excluded several chromosome 11 genes, which had become candidates based on physiologic rationale and position of the gene.

Two physiologic models for repolarization abnormalities in LQT existed. The first suggested that abnormally high left or abnormally low right sympathetic cardiac innervation could cause in abnormal repolarization and predisposition to arrhythmia. This hypothesis was supported by experiments showing induction of arrhythmia in dogs after removal of the right stellate ganglion or stimulation of the left stellate ganglion (Abildskov, 1991). In a few cases, left sympathectomy seemed to reduce the risk of developing ventricular tachyarrhythmias in human subjects.

The second theoretical model proposed that cardiac repolarization abnormalities were due to mutations in cardiac ion channels or ion channel modulators. Evidence supporting this model came from trials demonstrating that administration of potassium channel blockers, like quinidine and sotalol, lengthened the QT interval and induced *torsade de pointes* in human and animal models. Excessive prolongation of cardiac repolarization could result in reactivation of L-type calcium or sodium channels causing secondary depolarizations, a likely mechanism of *torsade de pointes* (Antzelevitch and Sicouri, 1994).

In 1994, we used genetic linkage analysis to map two new LQT loci (Chapter 2). Initial linkage studies in two kindreds, not linked to chromosome 11, excluded 35% of the genome. A marker on the long arm of chromosome 7 then showed a maximal LOD score of 4.25 at a recombination fraction ( $\Theta$ ) of 0.001 in these two families. The hypothesis that an LQT gene maps between markers at *D7S483* and *D7S505* on 7q35-36 was confirmed after demonstrating that seven additional families were linked to this locus. The combined LOD score for the nine families at this locus (designated *LQT2*) was 19.41. Six families, however, remained unlinked indicating the existence of another LQT locus. Continued genotype analyses mapped another LQT locus (*LQT3*) to chromosome 3p21-24. Three of the unlinked families showed positive LOD scores for markers at *D3S1100* (LOD score of 6.72 at  $\Theta$  of 0.001) and *D3S1298* (LOD score of 6.39 at  $\Theta$  of 0.001). Negative LOD scores for all known loci were obtained in three families, evidence for further genetic heterogeneity of this disorder.

In 1995, using fluorescence in situ hybridization, we mapped a putative potassium channel gene, *HERG* (human *ether-a-go-go* related gene) to 7q35-36. Genotypic

analyses showed complete linkage between two nucleotide polymorphisms from *HERG* and the disease phenotype in the chromosome 7-linked families. Moreover, *HERG* was highly expressed in heart tissue. The last and most important line of evidence that *HERG* is *LQT2* came from single strand conformational polymorphism (SSCP) analyses which demonstrated that mutations in *HERG* were associated with the LQT disease phenotype. One of the mutations arose *de novo*. This work is described in detail in Chapter 3.

Shortly after the localization of *LQT2* and *LQT3*, George et al. mapped *SCN5A*, the cardiac sodium channel gene, to chromosome 3p21. Based on physiologic rationale and position this gene became an obvious candidate for *LQT3* (George et al., 1995). It encoded an ion channel involved in the action potential duration of cardiac myocytes and mapped to the same region as *LQT3*. We accumulated evidence that strongly implicated *SCN5A* as the *LQT3* gene (Chapter 4). We showed that there were no recombination events between two *SCN5A* polymorphisms and LQT in the three unrelated families linked to chromosome 3. Identical intragenic deletions in *SCN5A* were identified in two of the families. The deletions disrupted a region known to be important for sodium channel inactivation (West et al., 1992). Delayed inactivation of the cardiac sodium channel would prolong action potential duration.

A fourth long QT syndrome gene was mapped in 1995 (Schott et al., 1995). DNA markers localized *LQT4* to chromosome 4q25-27 in a large French kindred with 19 affected individuals. The phenotype in this family differed from common LQT in that affected family members also presented with bradycardia, occurrence of atrial fibrillation and unusual T-wave morphology.



Positional cloning methods employed in the identification of the chromosome 11 LQT gene succeeded in 1996 (Chapter 5). Newly developed DNA markers genotyped in Utah kindred 1532, the kindred used in the original linkage report, narrowed the critical region to 700 kb. A novel gene (named *KVLQT1*), showing homology to voltage-gated potassium channels, was isolated from genomic clones covering the interval of interest. Northern blot analyses showed high levels of *KVLQT1* mRNA in heart. *KVLQT1* mutations cosegregated with the disease phenotype in six large families and were found in ten small families or sporadic cases. Taken together, the data lead to the conclusion that *KVLQT1* is *LQT1*, the gene causing chromosome 11-linked LQT.

Expression studies demonstrated that *HERG* and *KVLQT1* encode potassium channel alpha subunits. Four HERG subunits form  $I_{Kr}$  channels which underlie the rapidly activating delayed rectifier potassium current in the heart (Sanguinetti et al., 1995; Trudeau et al., 1995). Four KVLQT1 subunits coassemble with minK (a beta subunit) to form  $I_{Ks}$  channels underlying the slowly activating delayed rectifier potassium current (Barhanin et al., 1996; Sanguinetti et al., 1996). Coexpression of wild type and mutant channels (affected individual are heterozygous for mutations in these genes) causes reduction in  $I_{Kr}$  or  $I_{Ks}$  by a dominant-negative mechanism or loss of function (Chouabe et al., 1997; Sanguinetti et al., 1996; Shalaby et al., 1997; Splawski et al., 1997; Wollnik et al., 1997). Mutations in *SCN5A*, responsible for cardiac  $I_{Na}$ , lead to gain of function (Bennett et al., 1995; Dumaine et al., 1996). The destabilized inactivation gate of *SCN5A* causes delayed channel inactivation and dispersed reopenings. The reduction of  $I_{Kr}$  and  $I_{Ks}$ , and the increased activity of  $I_{Na}$  prolongs the cardiac action potential leading to increased risk of arrhythmia.

The findings that minK coassembles with KVLQT1 to form  $I_{Ks}$  channels and that mutations in *KVLQT1* cause LQT lead us to hypothesize that mutations in *minK* also cause this disorder. We identified *minK* mutations cosegregating with LQT in two families. These mutations were not observed in unaffected members of families or in 200 unrelated control individuals. When mutant minK subunits were coexpressed with normal minK (and normal KVLQT1), the biophysical properties of  $I_{Ks}$  channels were altered. Both mutants caused a positive shift in the voltage-dependence of channel activation (opening) and increased the rate of channel deactivation (closure). One of the mutants also had a dominant-negative effect. We concluded that *minK* mutations reduce  $I_{Ks}$  which leads to delayed myocellular repolarization and arrhythmia susceptibility. This study is described in Chapter 6.

In a study presented in Chapter 7, we hypothesized that Jervell and Lange-Nielsen syndrome (the autosomal recessive form of LQT) results from mutations affecting both alleles of an autosomal dominant LQT gene. We ascertained and phenotypically characterized a family in which the proband had long QT syndrome and sensory deafness. Some family members also had LQT with an autosomal dominant pattern of inheritance, but these patients had normal hearing. The gene responsible for LQT in this family was mapped to chromosome 11p15.5 using linkage analyses. Mutation analyses revealed a single base pair insertion in *KVLQT1*, the potassium channel gene responsible for chromosome 11-linked LQT syndrome. This mutation caused a premature stop codon. All individuals with LQT, except the proband, were heterozygous for the mutation. The proband with Jervell and Lange-Nielsen syndrome resulted from a consanguineous marriage and was homozygous for the *KVLQT1* mutation. We

concluded that homozygous mutation of *KVLQT1* causes Jervell and Lange-Nielsen syndrome and that members of JLN families, even if they have normal hearing, should be examined for long QT syndrome.

Expression of *KVLQT1* and *minK* was demonstrated in the inner ear. (Neyroud et al., 1997; Vetter et al., 1996) Other groups showed that homozygous or compound heterozygous mutations not only in *KVLQT1* but also in *minK* can cause deafness and the severe cardiac phenotype of the Jervell and Lange-Nielsen syndrome (Neyroud et al., 1997; Schulze-Bahr et al., 1997; Tyson et al., 1997). Lack of functional channels disrupts the production of endolymph leading to degeneration of the organ of Corti.

The identification of 4 LQT genes enabled clinicians to use linkage analysis in determining the genetic cause underlying LQT and to diagnose all individuals in some families. But linkage analysis, although a powerful technique, has its limitations. In small families, the number of meioses is insufficient to definitely implicate or eliminate a gene. In sporadic cases the proband might be the only individual to show QTc prolongation or symptoms in a family. Alternatively, the mutation might have arisen *de novo*.

Genetic screening using mutational analysis can improve presymptomatic diagnosis. The presence of a mutation would unequivocally distinguish affected individuals and identify the gene causing LQT even in small families and sporadic cases. To assist the identification of LQT-associated mutations, we determined the genomic structure of *KVLQT1*, *HERG* and *minK* and designed primer pairs for the amplification of all exons. SSCP analyses identified additional mutations in *KVLQT1* and *HERG*. The

results of this study are presented in chapter 8. The genomic structure and primer pairs for *SCN5A* were reported earlier (Wang et al., 1996).

To facilitate genetic testing and enable genotype-phenotype correlation studies in long QT syndrome, we screened a pool of 350 unrelated individuals with inherited, sporadic or acquired LQT for mutations in the four defined genes. Chapter 9 describes the identification of 138 mutations associated with LQT, 89 of which are novel. Most mutations were found in *KVLQT1* and *HERG* followed by *SCN5A* and *minK*. Multiple mutations were detected in previously undefined regions of the genes. This investigation has implications for effective drug therapy as well. Potassium channel openers may be beneficial in patients with *KVLQT1*, *HERG* and *minK* mutations while sodium channel blockers could be helpful in patients with *SCN5A* mutations. Expression of mutant channels in model systems, on the other hand, will provide better understanding of the mechanisms of disease and help further elucidate structure-function relationships in ion channels.

## References

- Abildskov, J. (1991). The sympathetic imbalance hypothesis of QT interval prolongation. *J. Cardiovasc. Electrophysiol.* 2, 355-359.
- Antzelevitch, C., and Sicouri, S. (1994). Clinical relevance of cardiac arrhythmias generated by afterdepolarizations. *JACC* 23, 259-277.
- Barhanin, J., Lesage, F., Guillemare, E., Fink, M., Lazdunski, M., and Romey, G. (1996). KvLQT1 and IsK (minK) proteins associate to form the  $I_{Ks}$  cardiac potassium current. *Nature* 384, 78-80.
- Benhorin, J., Kalman, Y. M., Medina, A., Towbin, J., Rave-Harel, N., Dyer, T. D., Blangero, J., MacCluer, J. W., and Kerem, B. (1993). Evidence of genetic heterogeneity in the long QT syndrome. *Science* 260, 1960-1961.
- Bennett, P. B., Yazawa, K., Makita, N., and George, A. L. (1995). Molecular mechanism for an inherited cardiac arrhythmia. *Nature* 376, 683-685.
- Chouabe, C., Neyroud, N., Guicheney, P., Lazdunski, M., Romey, G., and Barhanin, J. (1997). Properties of KvLQT1  $K^+$  channel mutations in Romano-Ward and Jervell and Lange-Nielsen inherited cardiac arrhythmias. *EMBO J.* 16, 5472-5479.
- Curran, M., Atkinson, D., Timothy, K., G, V., Moss, A., Leppert, M., and Keating, M. (1993). Locus heterogeneity of autosomal dominant long QT syndrome. *J. Clin. Invest.* 92, 799-803.
- Dumaine, R., Wang, Q., Keating, M. T., Hartmann, H. A., Schwartz, P. J., Brown, A. M., and Kirsch, G. E. (1996). Multiple mechanisms of sodium channel-linked long QT syndrome. *Circ. Res.* 78, 914-924.
- Fraser, G. R., Froggatt, P., and James, T. N. (1964). Congenital deafness associated with electrocardiographic abnormalities, fainting attacks and sudden death. *Quart. J. Med.* 33, 361-385.
- George, A., Varkony, T., Drabkin, H., Han, J., Knops, J., Finley, W., Brown, G., Ward, D., and Haas, M. (1995). Assignment of the human heart tetrodotoxin-resistant voltage-gated  $Na^+$  channel  $\alpha$ -subunit gene (SCN5A) to band 3p21. *Cytogenet. Cell. Genet.* 68, 67-70.
- Jervell, A., and Lange-Nielsen, F. (1957). Congenital deaf-mutism, functional heart disease with prolongation of the QT interval, and sudden death. *Am. Heart J.* 54, 59-68.
- Jervell, A., Thingstad, R., and Endsjo, T. O. (1966). Three new cases of congenital deafness with syncopal attacks and Q-T prolongation in the electrocardiogram. *Am. Heart J.* 72, 582-593.

- Kannel, W. B., Cupples, A., and D'Agostino, R. B. (1987). Sudden death risk in overt coronary heart diseases: the Framingham study. *Am. Heart J.* 113, 799-804.
- Keating, M., Atkinson, D., Dunn, C., Timothy, K., Vincent, G. M., and Leppert, M. (1991). Linkage of a cardiac arrhythmia, the long QT syndrome, and the Harvey *ras-1* gene. *Science* 252, 704-706.
- Keating, M., Dunn, C., Atkinson, D., Timothy, K., Vincent, G. M., and Leppert, M. (1991). Consistent linkage of the long QT syndrome to the Harvey *ras-1* locus on chromosome 11. *Am. J. Hum. Genet.* 49, 1335-1339.
- Moss, A., Schwartz, P., Crampton, R., Locati, E., and Carleen, E. (1985). The long QT syndrome: a prospective international study. *Circulation* 57, 654-658.
- Moss, A., Schwartz, P., Crampton, R., Tzivoni, D., Locati-Heilbron, E., MacCluer, Hall, W., Weitkamp, L., Vincent, G. M., Garson, A., Robinson, J., and Benhorin, J. (1991). The long QT syndrome: prospective longitudinal study of 328 families. *Circulation* 84, 1136-1144.
- Neyroud, N., Tesson, F., Denjoy, I., Leibovici, M., Donger, C., Barhanin, J., Faure, S., Gary, F., Coumel, P., Petit, C., Schwartz, K., and Guicheney, P. (1997). A novel mutation in the potassium channel gene *KVLQT1* causes the Jervell and Lange-Nielsen cardioauditory syndrome. *Nat. Genet.* 15, 186-189.
- Romano, C., Gemme, G., and Pongiglione, R. (1963). Artimie cardiach rare dell'eta pediatrica. II. Accessi sincopali per fibrillazione ventricolare parossitica. *Clin. Pediatr.* 45, 656-683.
- Sanguinetti, M. C., Curran, M. E., Spector, P. S., and Keating, M. T. (1996). Spectrum of HERG K<sup>+</sup> channel dysfunction in an inherited cardiac arrhythmia. *Proc. Natl. Acad. Sci., USA* 93, 2208-2212.
- Sanguinetti, M. C., Curran, M. E., Zou, A., Shen, J., Spector, P. S., Atkinson, D. L., and Keating, M. T. (1996). Coassembly of KvLQT1 and minK (IsK) proteins to form cardiac I<sub>Ks</sub> potassium channel. *Nature* 384, 80-83.
- Sanguinetti, M. C., Jiang, C., Curran, M. E., and Keating, M. T. (1995). A mechanistic link between an inherited and an acquired cardiac arrhythmia: HERG encodes the I<sub>Kr</sub> potassium channel. *Cell* 81, 299-307.
- Schott, J., Charpentier, F., Peltier, S., Foley, P., Drouin, E., Bouhour, J., Donnelly, P., Vergnaud, G., Bachner, L., Moisan, J., Le Marec, H., and Pascal, O. (1995). Mapping of a gene for long QT syndrome to chromosome 4q25-27. *Am. J. Hum. Genet.* 57, 1114-1122.

- Schulze-Bahr, E., Wang, Q., Wedekind, H., Haverkamp, W., Chen, Q., Sun, Y., Rubie, C., Hordt, M., Towbin, J., Borggreffe, M., Assmann, G., Qu, X., Somberg, J. C., Breithardt, G., Oberti, C., and Funke, H. (1997). *KCNE1* mutations cause Jervell and Lange-Nielsen syndrome. *Nat. Genet.* 17, 267-268.
- Schwartz, P. J., Periti, M., and Malliani, A. (1975). The long Q-T syndrome. *Am. Heart J.* 89, 378-390.
- Shalaby, F. Y., Levesque, P. C., Yang, W. P., Little, W. A., Conder, M. L., Jenkins-West, T., and Blonar, M. A. (1997). Dominant-negative KvLQT1 mutations underlie the LQT1 form of long QT syndrome. *Circulation* 96, 1733-1736.
- Splawski, I., Timothy, K. W., Vincent, G. M., Atkinson, D. L., and Keating, M. T. (1997). Molecular basis of the long-QT syndrome associated with deafness. *N. Engl. J. Med.* 336, 1562-1567.
- Splawski, I., Tristani-Firouzi, M., Lehmann, M. H., Sanguinetti, M. C., and Keating, M. T. (1997). Mutations in the hminK gene cause long QT syndrome and suppress  $I_{Ks}$  function. *Nat. Genet.* 17, 338-340.
- Tesson, F., Donger, C., Denjoy, I., Berthet, M., Bennaceur, M., Petit, C., Coumel, P., Schwartz, K., and Guicheney, P. (1996). Exclusion of *KCNE1* (IsK) as a candidate gene for Jervell and Lange-Nielsen Syndrome. *J. Mol. Cell. Cardiol.* 28, 2051-2055.
- Trudeau, M. C., Warmke, J. W., Ganetzky, B., and Robertson, G. A. (1995). *HERG*, a human inward rectifier in the voltage-gated potassium channel family. *Science* 269, 92-95.
- Tyson, J., Tranebjaerg, L., Bellman, S., Wren, C., Taylor, J. F. N., Bathen, J., Aslaksen, B., Sorland, S. J., Lund, O., Malcolm, S., Pembrey, M., Bhattacharya, S., and Bitner-Glindzicz, M. (1997). IsK and KvLQT1: mutation in either of the two subunits of the slow component of the delayed rectifier potassium channel can cause Jervell and Lange-Nielsen syndrome. *Hum. Mol. Genet.* 6, 2179-2185.
- Vetter, D. E., Mann, J. R., Wangemann, P., Liu, J., McLaughlin, K. J., Lesage, F., Marcus, D. C., Lazdunski, M., Heinemann, S. F., and Barhanin, J. (1996). Inner ear defects induced by null mutation of the *isk* gene. *Neuron* 17, 1251-1264.
- Vincent, G. M., Timothy, K., Leppert, M., and Keating, M. (1992). The spectrum of symptoms and QT intervals in carriers of the gene for the long QT syndrome. *N. Engl. J. Med.* 327, 846-852.
- Wang, Q., Zhizhong, L., Shen, J., and Keating, M. T. (1996). Genomic organization of the human *SCN5A* gene encoding the cardiac sodium channel. *Genomics* 34, 9-16.

Ward, O. C. (1964). A new familial cardiac syndrome in children. *J. Ir. Med. Assoc.* 54, 103-106.

West, J., Patton, D., Scheuer, T., Wang, Y., Goldin, A., and Catterall, W. (1992). A cluster of hydrophobic amino acid residues required for fast Na<sup>+</sup> channel inactivation. *Proc. Natl. Acad. Sci. USA* 89, 10910-10914.

Willich, S. N., Levy, D., Rocco, M. B., Tofler, G. H., Stone, P. H., and Muller, J. O. E. (1987). Circadian variation in the incidence of sudden cardiac death in the Framingham heart study population. *Am. J. Cardiol.* 60, 801-806.

Wollnik, B., Schroeder, B. C., Kubisch, C., Esperer, H. D., Wieacker, P., and Jentsch, T. J. (1997). Pathophysiological mechanisms of dominant and recessive KVLQT1 K<sup>+</sup> channel mutations found in inherited cardiac arrhythmias. *Hum. Mol. Genet.* 6, 1943-1949.



## CHAPTER 2

### TWO LONG QT SYNDROME LOCI MAP TO CHROMOSOMES 3 AND 7 WITH EVIDENCE FOR FURTHER HETEROGENEITY

The following chapter is a reprint from an article coauthored by Jiang, C., Atkinson, D., Towbin, J. A., Lehmann, M. H., Li, H., Timothy, K. W., Taggart, R. T., Schwartz, P. J., Vincent, G. M., Moss, A. J., Keating, M. T., and me. It was originally published in *Nature Genetics*, volume 8, pages 141-147, October 1994 (Copyright Nature America Inc.). It is reprinted here with the permission of the coauthors and Nature America Inc.

# Two long QT syndrome loci map to chromosomes 3 and 7 with evidence for further heterogeneity

Changan Jiang<sup>1,2,3</sup>, Donald Atkinson<sup>1,2,3</sup>, Jeffrey A. Towbin<sup>4,5</sup>, Igor Splawski<sup>1,2,3</sup>, Michael H. Lehmann<sup>6</sup>, Hua Li<sup>4</sup>, Katherine Timothy<sup>7</sup>, R. Thomas Taggart<sup>8</sup>, Peter J. Schwartz<sup>9</sup>, G. Michael Vincent<sup>1,7</sup>, Arthur J. Moss<sup>10</sup> & Mark T. Keating<sup>1,2,3</sup>

<sup>1</sup>Division of Cardiology,  
<sup>2</sup>Department of Human Genetics,  
<sup>3</sup>Eccles Program in Human Molecular Biology and Genetics, University of Utah Health Science Center, Salt Lake City, Utah 84112, USA

<sup>4</sup>Department of Pediatrics,

<sup>5</sup>Department of Molecular and Human Genetics, Baylor College of Medicine, Houston, Texas 77030, USA

<sup>6</sup>Division of Cardiology, Department of Medicine, Wayne State University, Detroit, Michigan 48235, USA

<sup>7</sup>Department of Medicine, LDS Hospital, Salt Lake City, Utah 84037, USA

<sup>8</sup>Molecular Biology, Department of Obstetrics and Gynecology, Carolinas Medical Center, Charlotte, North Carolina 28203, USA

<sup>9</sup>Department of Cardiology, University of Pavia, 20122, Italy

<sup>10</sup>Department of Medicine, University of Rochester Medical Center, Rochester, New York 14627, USA

Correspondence should be addressed to M.T.K.

Cardiac arrhythmias cause sudden death in 300,000 United States citizens every year. In this study, we describe two new loci for an inherited cardiac arrhythmia, long QT syndrome (LQT). In 1991 we reported linkage of LQT to chromosome 11p15.5. In this study we demonstrate further linkage to *D7S483* in nine families with a combined lod score of 19.41 and to *D3S1100* in three families with a combined score of 6.72. These findings localize major LQT genes to chromosomes 7q35–36 and 3p21–24, respectively. Linkage to any known locus was excluded in three families indicating that additional heterogeneity exists. Proteins encoded by different LQT genes may interact to modulate cardiac repolarization and arrhythmia risk.

Sudden death accounts for 11% of all natural deaths<sup>1,2</sup>. In most cases, the underlying causes are cardiac arrhythmias, usually ventricular tachyarrhythmias. Despite their importance, the mechanisms underlying ventricular arrhythmias are poorly understood. Considerable effort has been made to predict and prevent additional ventricular tachyarrhythmias in patients who have already experienced an episode, but the success rate is low and the cost enormous<sup>3–5</sup>. Presymptomatic diagnosis and prevention are clearly preferable, but in most cases not possible.

Abnormal cardiac repolarization may be an important mechanism of ventricular tachyarrhythmias. In animal models, ischaemia-induced ventricular fibrillation has been associated with the onset of abnormal cardiac repolarization<sup>6–8</sup>. In humans, prolongation of the electrocardiographic QT intervals, a temporal measure of cardiac repolarization, predicts sudden death in patients with coronary artery disease<sup>9</sup>. Dispersion of repolarization, as measured by QT intervals on the 12-lead electrocardiogram, is associated with an increased risk of cardiac arrhythmias in patients with congestive heart failure<sup>10</sup>. Finally, prolongation of the QT interval and other repolarization abnormalities have been associated with a syndrome of episodic cardiac arrhythmias in the long QT syndrome (LQT)<sup>11</sup>.

LQT causes episodic and abrupt loss of consciousness (syncope), seizures and sudden death from ventricular tachyarrhythmias<sup>12,13</sup>. Autosomal dominant and recessive patterns of inheritance have been reported<sup>14–16</sup>. Autosomal recessive LQT (Jervell Lange-Nielsen syndrome) has been associated with congenital neural deafness; this form of LQT is rare<sup>14</sup>. Autosomal dominant LQT (Romano-Ward

syndrome) is more common and has not been associated with other phenotypic abnormalities<sup>15,16</sup>. LQT can also be acquired, usually as a result of pharmacological therapy<sup>13,17</sup>.

The incidence of LQT and its relative importance for sudden death are unknown. Identification of relevant genes might provide insight into repolarization-related arrhythmias. In 1991 we reported complete linkage between autosomal dominant LQT and a polymorphism at *HRAS*<sup>8</sup>. This localized an LQT gene to chromosome 11p15.5 and made presymptomatic diagnosis possible in some families. In early experiments we found no evidence of recombination between *HRAS* and LQT<sup>18,19</sup> suggesting that *HRAS* might be a candidate for LQT. This hypothesis was supported by physiologic data. Others had shown that p21 ras proteins modulate cardiac muscarinic potassium channels, and an abnormality of potassium homeostasis could cause LQT<sup>20,21</sup>. We eliminated *HRAS* as a candidate, however, by direct DNA sequencing and refined linkage analysis (Keating, unpublished observations and Curran, M.E. *et al.*, manuscript submitted). These studies also confined this LQT gene to a 1 Mb region and excluded several candidate genes, including *Harveyras-1*, two potassium channels (*KCNA4*, *KCNK1*) and a dopamine receptor (*DRD4*)<sup>22–24</sup>.

The first seven families that we studied with autosomal dominant LQT were linked to chromosome 11p15.5 (*LQT1*, refs 18,19). In 1992, several groups, including our laboratory, identified locus heterogeneity for LQT<sup>25–28</sup>. Here we describe a genetic linkage analysis to localize two new autosomal dominant LQT loci. Nine families were completely linked to markers on chromosome 7q35–36 (*LQT2*) and three families were completely linked to 3p21–24 (*LQT3*). Three families failed to show linkage to

any of the known loci, indicating that at least a fourth LQT locus exists.

#### Phenotypic analysis of LQT families

To identify new LQT loci, we studied 15 multigenerational families with autosomal dominant LQT (Figs 1–3). These families were not related and were North American of varying descent, including Polish, Italian, English, German, Swiss, Finnish, Norwegian and Russian. Segregation analyses indicated an autosomal dominant pattern of LQT gene inheritance with incomplete penetrance in all families (data not shown). Some LQT gene carriers appeared unaffected by the disorder. To avoid misclassifying individuals, we used the same conservative approach to phenotypic assignment that was successful in previous linkage studies<sup>18,19,29–31</sup>. Symptomatic individuals with a corrected QT interval (QTc) of 0.45 seconds or greater and asymptomatic individuals with a QTc of 0.47 seconds or greater were classified as affected. Asymptomatic individuals with a QTc of 0.41 seconds or less were classified as unaffected. Asymptomatic individuals with QTc between 0.41 and 0.47 seconds and

symptomatic individuals with QTc of 0.44 seconds or less were classified as uncertain.

#### A second LQT locus maps to chromosome 7

We initiated linkage analysis in kindreds 1756 and 1977, families that are not linked to chromosome 11p15.5 (ref. 27). Genotypic analyses were performed with 110 short tandem repeat (STR) markers that span the genome<sup>32–35</sup>, including markers mapping near genes that were candidates for the disease based on a physiologic rationale. Seventy markers were successfully scored and 35% of the genome was excluded before linkage was identified. Evidence for linkage was identified with marker *D7S483* (Table 1, refs 33,34). In kindred 1756, the maximum lod score was 1.54 at a recombination fraction ( $\theta$ ) of 0.001. The lod score for kindred 1977 was 2.71, also at  $\theta = 0.001$ . The combined lod score for both families was 4.25, suggesting that a gene for LQT was located near *D7S483*.

To test the hypothesis that a gene for LQT maps to the long arm of chromosome 7, we performed linkage analysis on 13 other families. Seven (K2544, K2547, K2548, K2550, K2551, K2553 and K2556) showed positive LOD scores

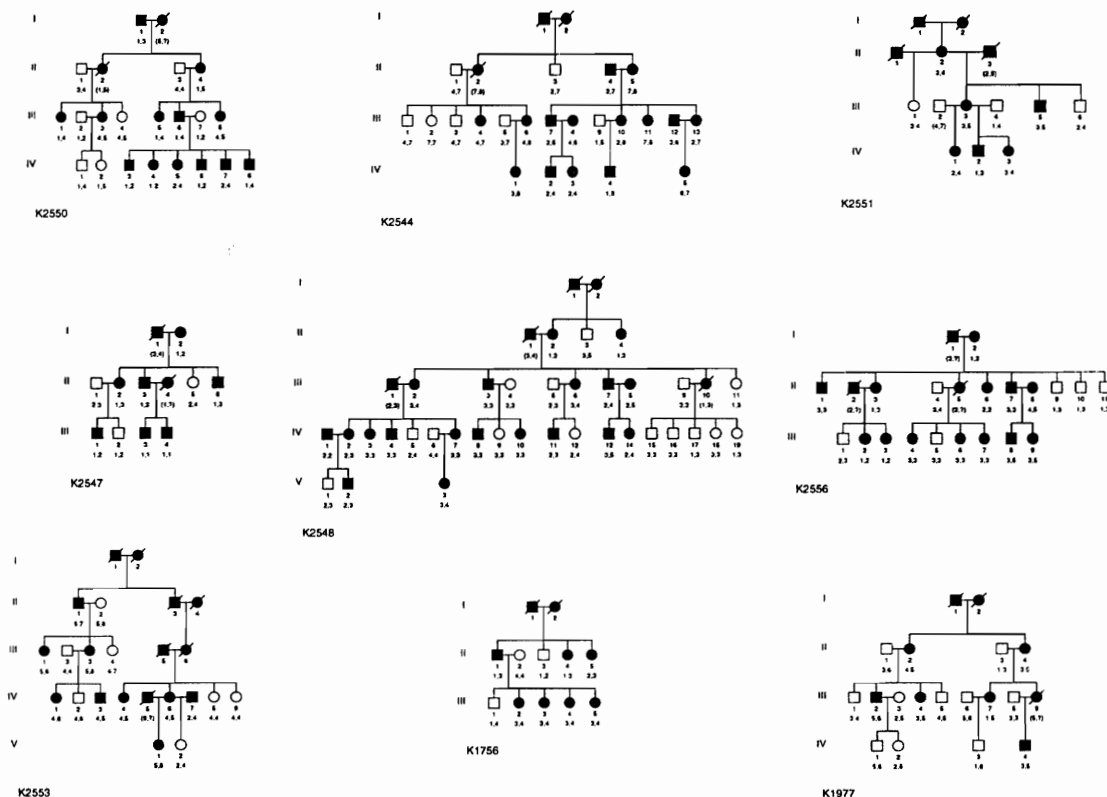


Fig. 1 Pedigree structure and *D7S483* genotype for nine autosomal dominant LQT families linked to chromosome 7. Affected individuals having the characteristic features of LQT are indicated by filled symbols, unaffected individuals by empty symbols. Family members who had an equivocal phenotype or for whom no phenotypic data were available are stippled. The disease phenotype cosegregated with a *D7S483* allele in all families. Alleles shown in parentheses are inferred.

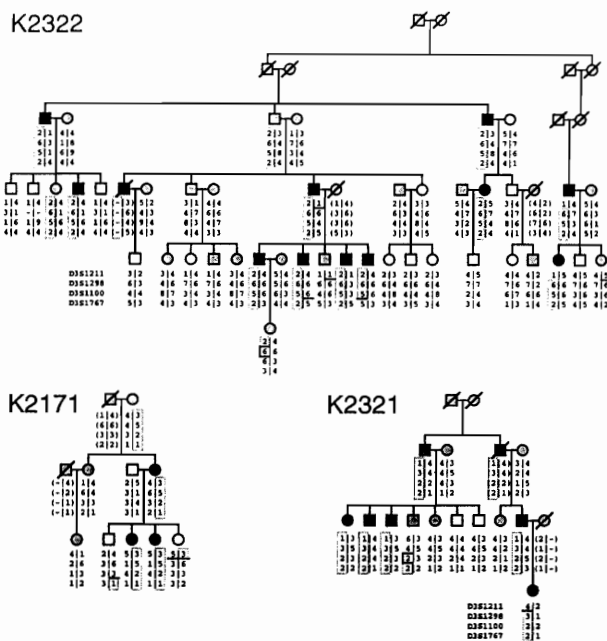


Fig. 2 Pedigree structure for three autosomal dominant LQT families linked to chromosome 3p21-24. Symbols are as described in Fig. 1. The alleles for markers at *D3S1211*, *D3S1298*, *D3S1100* and *D3S1767* are shown for each individual. Horizontal bars indicate recombination breakpoints and dashed bars indicate breakpoints where phase could not be set. The disease chromosome is boxed on each pedigree. The LQT phenotype is completely linked to *D3S1298* and *D3S1100* in each family.

with *D7S483* (Table 1). The lod score was greater than 3 in two families (K2548 and K2553) and the maximum combined lod score for nine families was 19.41. This score corresponds to odds in favour of linkage of greater than  $10^{19}$  to 1. The maximum lod score was identified at a recombination fraction of 0.001, indicating that all affected individuals carried the disease allele. Two possible recombinants were identified. In K2547, individual III 2 was classified as unaffected (no symptoms and QTc = 0.40 seconds) but carried the disease genotype (Fig. 1, allele 1). In K2548, individual V 1 had no symptoms and a QTc of 0.41 seconds, but also carried the disease allele (Fig. 1, allele 3). These patients, therefore, represent incomplete penetrance, phenotypic misclassification or recombination events between the disease gene and

*D7S483*. Taken together, however, these data indicate tight linkage between *D7S483* and an LQT disease locus, *LQT2*.

### A third LQT locus maps to chromosome 3

The LQT phenotype was not linked to *D7S483* in six families; significant negative lod scores were identified in K2109, K2320, K2321, K2322 and K2546 (Fig. 2, Fig. 3 and Table 1). Genotypic analyses with a neighbouring polymorphic marker, *D7S505* (refs 33,34), confirmed the negative lod scores in all six families (data not shown). None of the 15 families in this study demonstrated linkage to markers on chromosome 11p15.5 (data not shown). These data indicate that LQT is not linked to *LQT1* or *LQT2* in six families and that another LQT locus exists. To

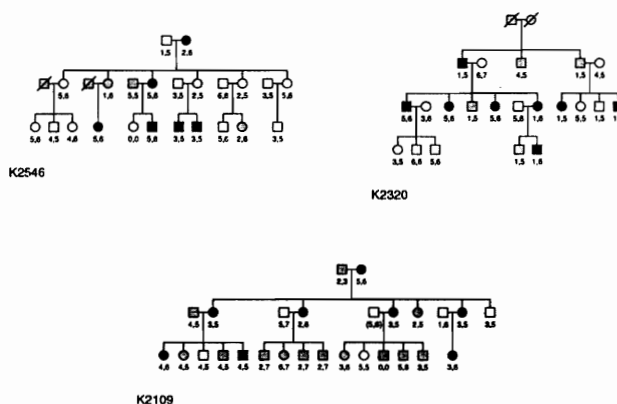


Fig. 3 Pedigree structure for three unlinked LQT families. Symbols are as described in the legend of Fig. 1. *D3S1100* genotypes are shown for each individual. These data indicate that these families are not linked to *LQT3*.

Table 1 Lod scores for *D7S483*, by family

Kindred	Lod score at recombination fraction of						
	0.001	0.01	0.05	0.10	0.20	0.30	0.40
K1756	1.54	1.52	1.39	1.22	0.87	0.50	0.16
K1977	2.71	2.67	2.47	2.21	1.66	1.06	0.46
K2544	2.25	2.22	2.04	1.82	1.33	0.81	0.30
K2547	1.02	1.03	1.03	0.98	0.80	0.54	0.24
K2548	3.07	3.06	2.97	2.79	2.28	1.61	0.80
K2550	2.55	2.51	2.33	2.11	1.64	1.14	0.60
K2551	1.46	1.43	1.33	1.19	0.90	0.59	0.28
K2553	3.09	3.04	2.80	2.50	1.85	1.17	0.50
K2556	1.72	1.69	1.57	1.41	1.07	0.67	0.25
Total	19.41	19.15	17.92	16.23	12.40	8.09	3.59
$Z_{\max}=19.41$ , $\theta=0.001$ , 90% confidence limits: (0–0.035)							
Kindred	Lod score at recombination fraction of						
	0.001	0.01	0.05	0.10	0.20	0.30	0.40
K2109	-2.54	-2.46	-1.88	-1.31	-0.67	-0.35	-0.16
K2171	-2.83	-1.85	-1.06	-0.69	-0.31	-0.12	-0.03
K2320	-4.80	-3.13	-1.65	-0.99	-0.40	-0.15	-0.03
K2321	-5.45	-3.98	-2.44	-1.65	-0.83	-0.39	-0.14
K2322	-4.90	-4.55	-3.14	-2.00	-0.84	-0.34	-0.10
K2546	-3.65	-1.93	-0.67	-0.21	0.09	0.12	0.05

Top panel, linked families; bottom panel, unlinked families. We assumed a disease allele frequency of 0.001 and that female and male recombination frequencies were equal. Lod scores have been calculated assuming autosomal dominant inheritance with a penetrance of 0.90 for all kindreds, as indicated by segregation analysis of these and other LQT Kindreds. When penetrance was varied from 0.60 to 0.95, maximum positive lod scores for all linked families at  $\theta=0.001$  ranged from 17.81–19.32. The *D7S483* data were tested for locus heterogeneity using HOMOG Ver. 3.3 (ref. 55). The null hypothesis of locus homogeneity (that is, the same gene caused LQT in all families) was rejected ( $p<0.0001$ ).

localize a third LQT gene, we began genotypic analysis in K2322. Significant linkage was first obtained on chromosome 3 with a microsatellite at *THRB*<sup>35</sup> which gave a maximum lod score of 2.75 ( $\theta=0.05$ ). Distant positive linkage was also seen at *D3S1217* which maps approximately 48 cM centromeric of *THRB*. To confirm the linkage, markers from seven other loci (*D3S1211*, *D3S1298*, *D3S1260*, *D3S1100*, *D3S1767*, *D3S1289* and *GCT4B10*) which map to the interval between *THRB* and *D3S1217* were analysed (Table 2 and data not shown)<sup>33–35</sup>. Markers at *D3S1100* and *D3S1298* were completely linked, with lod scores of 5.35 and 3.61 respectively ( $\theta=0.001$ ). The marker at *D3S1260* was also completely linked but poorly informative (data not shown).

To determine if additional LQT families were linked to chromosome 3p, linkage analysis was performed in other families. Two families, K2171 and K2321 showed complete linkage to markers at *D3S1100* and *D3S1298* (Fig. 2). The combined pairwise lod scores of the three linked families were 6.72 and 6.39 respectively, at  $\theta=0.001$  (Table 2). To refine the position of this locus, haplotype analysis was performed in families K2171, K2321 and K2322. Obligate recombinants were identified at *D3S1211* and *D3S1767*, defining the telomeric and centromeric flanking markers respectively (Fig. 2). The interval between these flanking loci is estimated to be 17.6 cM.

Three families, K2109, K2320 and K2546 were also analysed at *D3S1298* and *D3S1100* (Fig. 3). Significant negative lod scores were obtained at both loci (Table 2). These data indicate the existence of further locus heterogeneity for autosomal dominant LQT.

## Discussion

A first locus, designated *LQT1*, was mapped near *HRAS* on chromosome 11p15.5 in 1991 (ref. 18). In this report, we used genetic linkage analysis to map two new LQT loci. We demonstrate that *LQT2* is linked to a marker on chromosome 7 while a third locus, *LQT3*, is located on chromosome 3.

*LQT2* was identified with the chromosome 7q marker *D7S483*. *D7S483* is linked to *D7S505* which has been physically mapped to chromosome 7q35–36 (ref. 36, Fig. 4). Two possible candidate genes for *LQT2*, a chloride channel (*CLCN1*)<sup>37,38</sup> and a muscarinic receptor (*CHRM2*)<sup>39–41</sup> have been mapped to this region. Reduced myocellular chloride currents could prolong action potential duration, leading to secondary depolarization and arrhythmia. Point mutations in *CLCN1*, which is expressed in skeletal and cardiac muscle, are reported to cause Thomsen's disease, an inherited myotonia<sup>37,38</sup>. Myotonia was not present in affected members of the families described here, but we have identified patients with both

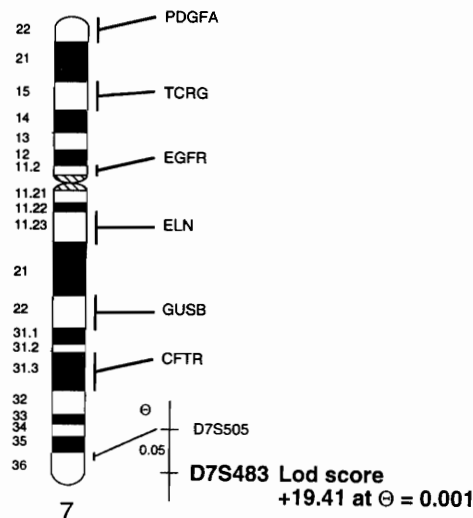


Fig. 4 Ideogram of chromosome 7 showing approximate location of *LQT2*. The map shows sex-averaged recombination fractions between adjacent markers drawn to scale. The order and the distance are based on data from G  n  thon<sup>35</sup> and the Human Genome/NIH/CEPH Collaborative Mapping Group<sup>36</sup>. PDGFA, Platelet derived growth factor Alpha polypeptide; TCRG, T-cell receptor  $\gamma$ -cluster; EGFR, epidermal growth factor receptor; ELN, elastin; GUSB,  $\beta$ -glucuronidase; and CFTR, cystic fibrosis transmembrane conductance regulator.

Table 2 Lod scores for chromosome 3 markers, by family

Marker	Kindred	0.001	0.01	0.05	0.10	0.20	0.30	0.40
D3S1211	K2171	-0.18	-0.15	-0.08	-0.03	0.01	0.02	0.01
	K2321	-0.76	-0.06	0.47	0.60	0.54	0.34	0.10
	K2322	2.56	2.84	3.03	2.87	2.25	1.47	0.64
	Total	1.63	2.62	3.42	3.44	2.81	1.83	0.74
	$Z_{\max}=3.56$ , $\theta=0.07$ , 90% confidence limits: (0.01–0.23)							
D3S1298	K2171	0.82	0.80	0.74	0.65	0.46	0.26	0.08
	K2321	1.96	1.92	1.77	1.58	1.16	0.72	0.28
	K2322	3.61	3.56	3.29	2.94	2.19	1.40	0.61
	Total	6.39	6.28	5.79	5.16	3.81	2.38	0.97
	$Z_{\max}=6.39$ , $\theta=0.001$ , 90% confidence limits: (0–0.07)							
D3S1100	K2171	0.82	0.80	0.74	0.65	0.46	0.26	0.08
	K2321	0.55	0.54	0.49	0.42	0.30	0.19	0.09
	K2322	5.35	5.26	4.88	4.38	3.33	2.20	1.04
	Total	6.72	6.61	6.10	5.45	4.09	2.65	1.20
	$Z_{\max}=6.72$ , $\theta=0.001$ , 90% confidence limits: (0–0.08)							
D3S1767	K2171	-0.18	-0.15	-0.08	-0.03	0.01	0.02	0.01
	K2321	1.29	1.27	1.15	1.01	0.71	0.41	0.15
	K2322	1.99	2.66	2.96	2.80	2.16	1.37	0.56
	Total	3.11	3.77	4.03	3.78	2.88	1.80	0.71
	$Z_{\max}=4.14$ , $\theta=0.03$ , 90% confidence limits: (0.001–0.170)							
D3S1298	K2109	-4.96	-3.93	-2.56	-1.75	-0.88	-0.39	-0.12
	K2320	-3.37	-3.10	-1.93	-1.25	-0.59	-0.27	-0.10
	K2546	-6.49	-4.94	-2.65	-1.60	-0.68	-0.26	-0.06
D3S1100	K2109	-4.87	-3.98	-2.82	-1.94	-0.95	-0.42	-0.13
	K2320	-3.38	-3.13	-1.99	-1.30	-0.62	-0.29	-0.10
	K2546	-4.13	-3.67	-1.94	-1.16	-0.51	-0.25	-0.13

Top panel, linked families; bottom panel, unlinked families. Calculations were performed as described in Table 1. When penetrance was varied from 0.60–0.95, maximum combined lod scores at  $\theta=0.001$  ranged from 5.45–6.56 for D3S1298 and from 5.70–6.90 for D3S1100. The D3S1100 data were tested for locus heterogeneity using HOMOG Ver. 3.3 (ref. 55). The null hypothesis of locus homogeneity was rejected ( $p<0.0001$ ).

disorders, suggesting that they might have common mechanisms (Keating, M.T., unpublished data). A rationale for the involvement of muscarinic receptors in LQT can also be made; *CHRM2* is primarily expressed in the heart and regulates cardiac-specific ion channels, particularly potassium channels<sup>39–41</sup>. Mutations in these receptors might affect cardiac repolarization and increase susceptibility to ventricular tachyarrhythmias. Refined linkage and mutational analyses will determine if either gene causes LQT.

A gene for polysyndactyly has been mapped to chromosome 7q35–36 (refs 42,43). Recently, we identified patients with LQT, malignant tachyarrhythmias and simple syndactyly<sup>44</sup>. These patients were isolated cases, so linkage analysis was not possible. It is possible, however, that the association of LQT and syndactyly results from deletion of two adjacent genes on chromosome 7. If so, these patients will be critical for identification of both genes.

Haplotype analysis of *LQT3* has localized this gene between D3S1211 and D3S1767, which were physically mapped to chromosome 3p21–24 (ref. 45, Fig. 5). The gene encoding an L-type calcium channel  $\alpha$ -1 subunit, *CCHLA2*, has been mapped to chromosome 3p21–23 (refs 46–49) and now becomes a candidate. A physiologic

rationale for involvement of L-type calcium channels in this disease exists, supporting the candidacy of this gene (refs 50,51). Detailed linkage and mutational analyses will determine if *CCHLA2* is an LQT gene.

The relative importance of the four or more LQT loci is not yet known. We have mapped ten families to *LQT1* (refs 18,19,28), nine families to *LQT2* and three families to *LQT3*. Three families are not linked to any of the known loci. Examination of additional LQT families using the markers described in this report will help determine the relative importance of the different LQT loci.

Identification of linked polymorphic markers for *LQT1*, *LQT2* and *LQT3* makes determination of LQT gene-carrier status possible in linked families. We have shown that some LQT gene-carriers with unremarkable QTc intervals may still be at risk of ventricular tachyarrhythmias<sup>52</sup>. Genetic markers may be useful for presymptomatic diagnosis and therapeutic decision making in some cases. Unfortunately, these markers will neither be useful in unlinked families nor in very small families or sporadic cases.

The phenotypes of patients with different forms of LQT are surprisingly similar. With the benefit of these genotypic data we may now find subtle phenotypic difference between the distinct forms of LQT. It seems likely, however, that

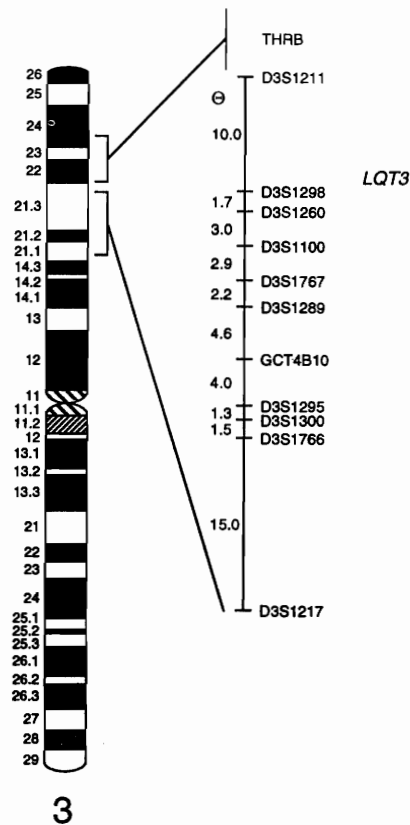


Fig. 5 Ideogram and genetic map of chromosome 3 showing the location of *LQT3*. *THR8* was mapped to a 10 cM interval (black bar). Physical localizations of *THR8* and *D3S1217* are shown by brackets. *LQT3* is genetically mapped between *D3S1211* and *D3S1767*. The order and the distance are based on data from Génethon<sup>35</sup>, the Cooperative Human Linkage Center (CHLC Ver. 2.5) and the Human Genome/NIH/CEPH Collaborative Mapping Group<sup>39</sup>.

onset of symptoms and the occurrence of sudden death. Symptoms such as palpitation and light-headedness were not included in this study. We took a conservative approach to phenotypic assignment that has been successful in our previous linkage studies<sup>18,19,27</sup>. This method errs on the side of avoiding misclassifications but may result in reduced statistical power. All phenotypic data were interpreted without knowledge of genotype.

**Genotypic analysis.** PCR typing was performed as described by Weber and May with the following modifications<sup>32</sup>. PCR was carried out with 50 ng DNA in a final volume of 10  $\mu$ l using a Perkin-Elmer Cetus 9600 thermocycler. Amplification conditions were 94 °C for 5 min followed by 30 cycles of 94 °C for 10 s, 58 °C for 20 s and 72 °C for 20 s. Ten  $\mu$ l of formamide loading dye was added to each reaction, samples were denatured at 94 °C for 10 min and held on ice. 2  $\mu$ l of each sample was separated by electrophoresis on 6% denaturing polyacrylamide gels (Sequagel, National Diagnostics) which were dried and exposed to X-ray film overnight at -70 °C. The sequences of completely linked markers are listed. Sequences of other primers used in this study and PCR conditions are available from the authors. *D7S483*: Forward-AGT GGT CAT TAG CCT TGG CAA AAT C; Reverse-AAC CAG AGT TGT AAG CCA TGA AAG T. *D3S1100*: Forward-GGT TTC ATA TAC CAT CAA TCC CAC; Reverse-GTA CAC CAT CAT GAG GAG TCT GG. *D3S1298*: Forward-AGC TCT CAG TGC CAC CCC; Reverse-GAA AAA TCC CCT GTG AAG CG.

**Linkage analysis.** To avoid bias, all polymorphisms were scored without knowledge of phenotypic data. The LINKAGE Ver. 5.1 software package was used to perform pairwise (MLINK) linkage analysis<sup>33</sup>. Penetrance was set at 0.90 and the LQT gene frequency was assumed to be equal between males and females<sup>18,19,27</sup>. Microsatellite allele frequencies were set to equal (1/n). The approximate 90% confidence limits were calculated using the "1 lod down" method<sup>34</sup>. The HOMOG program (Ver. 3.3) was used to test genetic homogeneity<sup>35</sup>.

#### Acknowledgements

We thank M. Curran, Q. Wang, L. Ptacek, J. Mason, M. Leppert and D. Frankovich for their help and advice. This work was supported by National Institutes of Health Grants RO1 HL48074, RO1 HL33843, and RO1 HL51618, Public Health Service Research Grant MO1-RR00064 from the National Center for Research Resources, the Technology Access Section of Utah genome Center and American Heart Association.

the repolarization abnormalities underlying different form of LQT are the same. LQT genes, therefore, may encode elements of a common physiologic mechanism of arrhythmia. If so, characterization of this mechanism may simplify efforts to improve prediction, prevention and treatment of cardiac arrhythmias.

#### Methodology

**Family studies.** Kindreds were ascertained through medical clinics across North America. Informed consent was obtained from all study participants or their guardians. Evidence of LQT was obtained via historical data and electrocardiograms from each individual, before genotypic analysis. We evaluated the presence of syncope, the number of syncopal episodes, the presence of seizures, the age of

Received 10 August; accepted 5 September 1994.

1. Kannel, W.B., Cupples, A. & D'Agostino, R.B. Sudden death risk in overt coronary heart diseases: The Framingham study. *Am. Heart J.* 113, 799-804 (1987).
2. Willich, S.N. *et al.* Circadian variation in the incidence of sudden cardiac death in the Framingham heart study population. *Am. J. Cardiol.* 60, 801-806 (1987).
3. Mason, J. A comparison of electrophysiologic testing with holter monitoring to predict antiarrhythmic-drug efficacy for ventricular tachyarrhythmias. *New Engl. J. Med.* 329, 445-450 (1993).
4. Mason, J. A comparison of seven antiarrhythmic drugs in patients with ventricular tachyarrhythmias. *New Engl. J. Med.* 329, 452-458 (1993).
5. Myerburg, R.J., Kessler, K.M. & Castellanos, A. Sudden cardiac death: epidemiology, transient risk and intervention assessment. *Ann. Intern. Med.* 119, 1187-1197 (1993).
6. Brooks, C.M., Gilbert, J.L., Greenspan, M.E., Lange, G. & Mazzella, H.M. Excitability and electrical response of ischemic heart muscle. *Am. J. Physiol.* 196, 1143-1147 (1960).
7. Downar, E., Michiel, J.J. & Durrer, D. The effect of acute coronary artery occlusion on subepicardial transmembrane potentials in the intact porcine heart. *Circulation* 56, 217-224 (1977).
8. Penkoske, P.A., Sobel, B.E. & Corr, P.B. Disparate electrophysiological alterations accompanying dysrhythmia due to coronary occlusion and reperfusion in the cat. *Circulation* 58, 1023-1035 (1978).
9. Schwartz, P.J. & Wolf, S. QT interval prolongation as predictor of sudden death in patients with myocardial infarction. *Circulation* 57, 1074-1077 (1978).
10. Barr, C.S., Naas, A., Freeman, M., Lang, C.C. & Struthers, A.D. QT dispersion and sudden unexpected death in chronic heart failure. *Lancet* 343, 327-329 (1994).
11. Day, C.P., McComb, J.M. & Campbell, R.W.F. QT dispersion: an indication of arrhythmia risk in patients with long QT intervals. *Br. Heart J.* 63, 342-344 (1990).
12. Vincent, G.M., Abildskov, J.A. & Burgess, M.J. Q-T interval syndromes. *Prog. Cardiovasc. Dis.* 16, 523-529 (1974).
13. Schwartz, P.J., Periti, M. & Malliani, A. The long Q-T syndrome. *Am. Heart J.* 109, 378-390 (1975).
14. Jervell, A. & Lange-Nielsen, F. Congenital deaf mutism, functional heart disease with prolongation of the QT interval, and sudden death. *Am. Heart J.* 54, 59-78 (1957).
15. Romano, C., Gemme, G. & Pongiglione, R. Aritmie cardiache rare dell'età pediatrica. II. Accessi sinocapali per fibrillazione ventricolare parossistica. *Clin. Pediatr. (Bologna)* 45, 656-663 (1963).
16. Ward, O.C. A new familial cardiac syndrome in children. *J. Ir. Med. Assoc.* 54, 103-106 (1964).
17. Zipes, D.P. Proarrhythmic effects of antiarrhythmic drugs. *Am. J. Cardiol.* 59, 26E-31E (1987).
18. Keating, M. *et al.* Linkage of a cardiac arrhythmia, the long QT syndrome, and the *Harvey ras-1* gene. *Science* 252, 704-706 (1991).
19. Keating, M.T. *et al.* Consistent linkage of the long-QT syndrome to the *Harvey Ras-1* locus on chromosome 11. *Am. J. Hum. Genet.* 49, 1335-1339 (1991).
20. Yatani, A. *et al.* ras p21 and GAP inhibit coupling of muscarinic receptors to atrial potassium channels. *Cell* 61, 769-776 (1990).
21. Davidenko, J.M., Cohen, L., Goodrow, R. & Antzelevitch, C. Quinidine-induced action potential prolongation, early afterdepolarizations, and triggered activity in canine Purkinje fibers. *Circulation* 79, 674-686 (1989).
22. Philipson, L.H., Eddy, R.L., Shows, T.B. & Bell, G.I. Assignment of human potassium channel gene *KCN4A4* (Kv1.4, *PCN2*) to chromosome 11q13.4-q14.1. *Genomics* 15, 463-464 (1993).
23. Ried, T. *et al.* Localization of a highly conserved human potassium channel gene (*NGK2-KV4; KCNC1*) to chromosome 11p15. *Genomics* 15, 405-411 (1993).
24. Petronis, A., Van Tol, H.H.M., Lichter, J.B., Livak, K.J. & Kennedy, J.L. The D4 dopamine receptor gene maps on 11p proximal to *HRA5*. *Genomics* 18, 161-163 (1993).
25. Benhorin, J. *et al.* Evidence of genetic heterogeneity in the long QT syndrome. *Science* 260, 1960-1962 (1993).
26. Keating, M. Evidence of genetic heterogeneity in the long QT syndrome. *Science* 260, 1960-1962 (1993).
27. Curran, M. *et al.* Locus heterogeneity of autosomal dominant long QT syndrome. *J. Clin. Invest.* 92, 799-803 (1993).
28. Towbin, J.A. *et al.* Evidence of genetic heterogeneity in Romano-Ward long QT syndrome (LQTS): Analysis of 23 families. *Circulation* (in the press).
29. Keating, M. Linkage analysis and the long QT syndrome: Using genetics to study cardiovascular disease. *Circulation* 85, 1973-1986 (1992).
30. Keating, M. Genetics of the long QT syndromes. *J. cardiovascular Electrophysiology* 5, 146-153 (1994).
31. Lehmann, M. T wave humps as an electrocardiographic marker of the long QT syndrome. *J. Am. Coll. Cardiol.* (in the press).
32. Weber, J.L. & May, P.E. Abundant class of human DNA polymorphisms which can be typed using polymerase chain reaction. *Am. J. Hum. Genet.* 44, 388-396 (1989).
33. Kramer, P. *et al.* A comprehensive genetic linkage map of the Human Genome/NIH/CEPH collaborative Mapping Group. *Science* 258, 67-86 (1992).
34. Weissensbach, J. *et al.* A second-generation linkage map of the human genome. *Nature* 359, 794-801 (1992).
35. Gyapay, G. *et al.* The 1993-94 Génethon human genetic linkage map. *Nature Genet.* 7, 246-339 (1994).
36. Green, E.D. *et al.* Integration of physical, genetic and cytogenetic maps of human chromosome 7: isolation and analysis of yeast artificial chromosome clones for 117 mapped genetic markers. *Hum. molec. Genet.* 3, 489-501 (1994).
37. George, A.L., Jr., Crackower, M.A., Abdalla, J.A., Hudson, A.J. & Ebers, G.C. Molecular basis of Thomsen's disease (autosomal dominant myotonia congenita). *Nature Genet.* 3, 305-309 (1993).
38. Koch, M.C. *et al.* The skeletal muscle chloride channel in dominant and recessive human myotonia. *Science* 257, 797-800 (1992).
39. Bonner, T.I., Modi, W.S., Sevarius, H.N. & O'Brien, S. Chromosomal mapping of five human genes encoding muscarinic acetylcholine receptors. *Cytogenet. cell Genet.* 58, 1850-1867 (1991).
40. Bonner, T.I., Buckley, N.J., Young, A.C. & Brann, M.R. Identification of a family of muscarinic acetylcholine receptor genes. *Science* 237, 527-532 (1987).
41. Goyal, R.K. Muscarinic receptors subtypes: Physiology and clinical implications. *New Engl. J. Med.* 321, 1022-1029 (1989).
42. Tsukurov, O. *et al.* A complex bilateral polysyndactyly disease locus maps to chromosome 7q36. *Nature Genet.* 6, 282-288 (1994).
43. Heutink, P. *et al.* The gene for triphalangeal thumb maps to the subtelomeric region of chromosome 7q. *Nature Genet.* 6, 287-292 (1994).
44. Marks, M.L., Whisler, S.L., Clericuzio, C. & Keating, M. A new form of long QT syndrome associated with syndactyly. *J. Am. Coll. Cardiol.* (in the press).
45. Garcia, D.K. *et al.* CA repeat polymorphisms for human chromosome 3. *Cytogenet. cell Genet.* 58, 1877 (1993).
46. Chin, H., Kozak, G.A., Kim, H., Mock, B. & McBride, O.W. A brain L-type calcium channel  $\alpha 1$  subunit gene (*CCHL1A2*) maps to mouse chromosome 14 and human chromosome 3. *Genomics* 11, 814-819 (1991).
47. Seino, S., Yamada, Y., Espinosa III, R., Le Beau, M.M. & Bell, G.I. Assignments of the gene encoding the  $\alpha 1$  subunit of the neuroendocrine/brain-type calcium channel (*CACNL1A2*) to human chromosome 3, band p14.3. *Genomics* 13, 1375-1377 (1992).
48. Seino, S. *et al.* Cloning of the  $\alpha 1$  subunit of a voltage-dependent calcium channel expressed in pancreatic  $\beta$  cells. *Proc. natn. Acad. Sci. U.S.A.* 89, 584-588 (1992).
49. Williams, M.E. *et al.* Structure and functional expression of  $\alpha 1$ ,  $\alpha 2$  and  $\beta$  subunit of a novel human neuronal calcium channel subtype. *Neuron* 8, 71-84 (1992).
50. January, C.T., Riddle, J.M., & Salata, J.J. A model for early afterdepolarization: induction with the  $Ca^{2+}$  channel agonist Bay K8644. *Circ. Res.* 62, 563-571 (1988).
51. January, C.T. & Riddle, J.M. Early afterdepolarizations: mechanism of induction and block, A role for L-type  $Ca^{2+}$  current. *Circ. Res.* 64, 977-990 (1989).
52. Vincent, G.M., Timothy, K.W., Leppert, M. & Keating, M. The spectrum of symptoms and QT intervals in carriers of the gene for the long-QT syndrome. *New Engl. J. Med.* 327, 846-852 (1992).
53. Lathrop, G.M., Lalouel, J.M., Julier, C. & Ott, J. Multilocus linkage analysis in humans: detection of linkage and estimation of recombination. *Am. J. Hum. Genet.* 37, 482-498 (1985).
54. Conneally, P.M. *et al.* Report of the committee on methods of linkage analysis and reporting. *Cytogenet. cell Genet.* 40, 356-358 (1985).
55. Ott, J. Linkage analysis and family classification under heterogeneity. *Annals hum. Genet.* 47, 311-320 (1983).



## CHAPTER 3

### A MOLECULAR BASIS FOR CARDIAC ARRHYTHMIA: *HERG* MUTATIONS CAUSE LONG QT SYNDROME

The following chapter is a reprint from an article coauthored by Curran, M., Timothy, K. W., Vincent, G. M., Green, E., Keating, M. T., and me. It was originally published in *Cell*, volume 80, pages 795-803, March 10, 1995 (Copyright Cell Press). It is reprinted here with the permission of the coauthors and Cell Press.

# A Molecular Basis for Cardiac Arrhythmia: HERG Mutations Cause Long QT Syndrome

Mark E. Curran,\*† Igor Splawski,\*†  
Katherine W. Timothy,\* G. Michael Vincent,\*§  
Eric D. Green,\* and Mark T. Keating\*†‡

\*Department of Human Genetics

†Eccles Program in Human Molecular Biology  
and Genetics

‡Cardiology Division

§Howard Hughes Medical Institute  
University of Utah Health Sciences Center  
Salt Lake City, Utah 84112

¶Department of Medicine  
Latter Day Saints Hospital  
Salt Lake City, Utah 84037

#National Center for Human Genome Research  
National Institutes of Health  
Bethesda, Maryland 20892

## Summary

To identify genes involved in cardiac arrhythmia, we investigated patients with long QT syndrome (LQT), an inherited disorder causing sudden death from a ventricular tachyarrhythmia, torsade de pointes. We previously mapped LQT loci on chromosomes 11 (LQT1), 7 (LQT2), and 3 (LQT3). Here, linkage and physical mapping place LQT2 and a putative potassium channel gene, *HERG*, on chromosome 7q35-36. Single strand conformation polymorphism and DNA sequence analyses reveal *HERG* mutations in six LQT families, including two intragenic deletions, one splice-donor mutation, and three missense mutations. In one kindred, the mutation arose de novo. Northern blot analyses show that *HERG* is strongly expressed in the heart. These data indicate that *HERG* is LQT2 and suggest a likely cellular mechanism for torsade de pointes.

## Introduction

Long QT syndrome (LQT) is an inherited cardiac disorder that causes syncope, seizures, and sudden death, usually in young, otherwise healthy individuals (Ward, 1964; Romano, 1965; Schwartz et al., 1975). Most LQT gene carriers manifest prolongation of the QT interval on electrocardiograms, a sign of abnormal cardiac repolarization (Vincent et al., 1992). The clinical features of LQT result from episodic cardiac arrhythmias, specifically torsade de pointes, named for the characteristic undulating nature of the electrocardiogram in this arrhythmia. Torsade de pointes may degenerate into ventricular fibrillation, a particularly lethal arrhythmia. Although LQT is not a common diagnosis, ventricular arrhythmias are very common; more than 300,000 Americans die suddenly every year (Kannel et al., 1987; Willich et al., 1987), and in many cases the underlying mechanism may be aberrant cardiac repolarization. LQT,

therefore, provides a unique opportunity to study life-threatening cardiac arrhythmias at the molecular level.

A molecular basis for LQT was not previously known. In 1991, we discovered tight linkage between autosomal dominant LQT and a polymorphism at H-RAS (Keating et al., 1991a). This discovery localized an LQT gene (*LQT1*) to chromosome 11p15.5 and made genetic testing possible in some families. Autosomal dominant LQT was previously thought to be genetically homogeneous, and the first seven families that we studied were linked to 11p15.5 (Keating et al., 1991b). In 1993, however, several laboratories, including our group, identified families that were not linked to chromosome 11p15.5 (Benhorin et al., 1993; Curran et al., 1993a; Towbin et al., 1994). In 1994, we identified two additional LQT loci, *LQT2* on chromosome 7q35-36 (nine families) and *LQT3* on chromosome 3p21-24 (three families) (Jiang et al., 1994). Since three families in our study remained unlinked, at least one more LQT locus exists. This degree of heterogeneity suggests that distinct LQT genes may encode proteins that interact to modulate cardiac repolarization and arrhythmia risk.

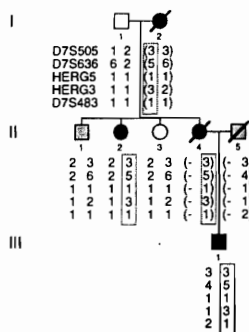
Since LQT is associated with abnormal cardiac repolarization, genes that encode ion channels (or their modulators) are reasonable candidates. H-RAS, which was localized to chromosome 11p15.5, was excluded as a candidate for *LQT1* based on direct DNA sequence analyses (unpublished data) and by linkage analyses (Roy et al., 1994). A skeletal muscle chloride channel (*CLCN1*; Koch et al., 1992) and a cardiac muscarinic-acetylcholine receptor (*CHRM2*; Bonner et al., 1987) became candidates for *LQT2* based on their chromosome 7q35-36 location, but subsequent linkage analyses have excluded these genes (Wang et al., submitted).

Warmke and Ganetzky (1994) identified a novel human cDNA, the human *ether-a-go-go*-related gene (*HERG*). *HERG* was localized to human chromosome 7 by polymerase chain reaction (PCR) analysis of a somatic cell hybrid panel (Warmke and Ganetzky, 1994). The function of the protein encoded by *HERG* is not known, but it has predicted amino acid sequence homology to potassium channels. *HERG* was isolated from a hippocampal cDNA library by homology to the *Drosophila ether-a-go-go* (*eag*) gene, which encodes a Ca<sup>2+</sup>-modulated potassium channel (Bruggeman et al., 1993). *HERG* is not the human homolog of *eag*, however, their products sharing only ~50% amino acid sequence homology.

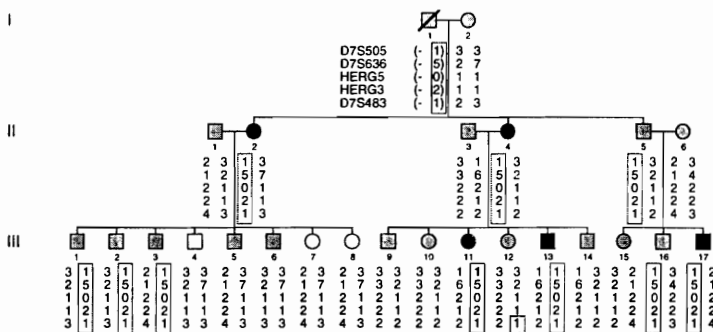
In this study, we provide evidence indicating that *HERG* is *LQT2*. First, we identified and characterized new LQT families and showed that all were linked to markers on chromosome 7q35-36, confirming the location of *LQT2*. Second, we mapped *HERG* to chromosome 7q35-36, making *HERG* a candidate gene for *LQT2*. Third, we demonstrated that *HERG* is strongly expressed in the heart. Finally, we identified six *HERG* mutations associated with LQT; one of these mutations arose de novo.

Cell  
796

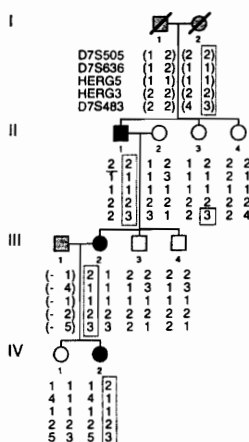
K1956



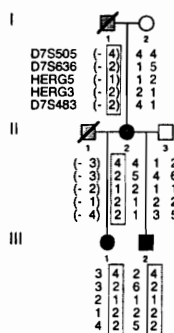
K2287



K2595



K2596



K2600

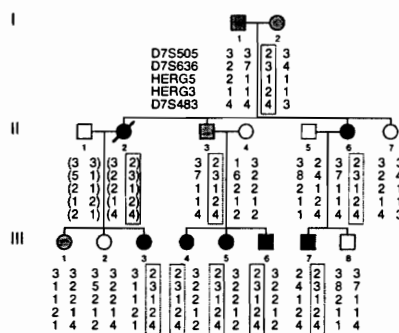


Figure 1. Pedigree Structure and Genotypic Analyses of Five LQT Families

Individuals showing the characteristic features of LQT, including prolongation of the QT interval and history of syncope, seizures, or aborted sudden death, are indicated by closed circles (females) or closed squares (males). Unaffected individuals are indicated by open circles or open squares. Individuals with an equivocal phenotype or those for whom phenotypic data are unavailable are shown as stippled. Circles or squares with a slash denote deceased individuals. Haplotypes for polymorphic markers linked to *LQT2* are shown under each individual. These markers include (centromere to telomere) *D7S505*, *D7S636*, *HERG 5-11*, *HERG 3-8*, and *D7S483* (Gyapay et al., 1994; Wang et al., submitted). Haplotypes cosegregating with the disease phenotype are indicated by a box. Recombination events are indicated with a horizontal black line. Informed consent was obtained from all individuals or from their guardians in accordance with local institutional review board guidelines. Haplotype analyses indicate that the LQT phenotype in these kindreds is linked to markers on chromosome 7q35-36.

## Results

### *LQT2* Is Linked to Markers on Chromosome 7q35-36

To determine the relative frequency of the three known LQT loci (*LQT1*, *LQT2*, and *LQT3*), we performed linkage analyses in families with this disorder. Five LQT families were identified and phenotypically characterized (Figure 1). These families were unrelated and of varying descent, including Mexican (Spanish), German, English, and Danish. In each case, an autosomal dominant pattern of inheritance was suggested by inspection of the pedigree. Af-

ected individuals were identified by the presence of QT prolongation on electrocardiograms and, in some cases, a history of syncope or aborted sudden death. No patients had signs of congenital neural hearing loss, a finding associated with the rare autosomal recessive form of LQT, or other phenotypic abnormalities. Genotype analyses with polymorphic markers linked to the known LQT loci suggested that the disease phenotype in these families was linked to polymorphic markers on chromosome 7q35-36 (Figure 1). The maximum combined two-point lod score for these five families was 5.13 at *D7S636* ( $\theta = 0.0$ ; Table 1). When combined with our previous studies (Jiang et al.,

Table 1. Maximum Pairwise Lod Scores, Recombination Fractions for Linkage of *LQT2* with *HERG*, and Polymorphic Markers on Chromosome 7

Locus	Families from Present Study		Families Studied to Date	
	Z <sub>max</sub>	θ	Z <sub>max</sub>	θ
<i>D7S505</i>	4.40	0.0	22.91	0.009
<i>D7S636</i>	5.13	0.0	26.14	0.00
<i>HERG 3-8</i>	0.11	0.0	6.34	0.00
<i>HERG 5-11</i>	3.55	0.0	9.64	0.00
<i>D7S483</i>	2.48	0.0	22.42	0.00

Markers are shown in chromosomal order (centromere to telomere) (Gyapay et al., 1994). The first column (families from present study) indicates combined lod scores for the five families described in this study. The second column (families studied to date) indicates combined lod scores from the five families studied here, as well as the nine families from our previous study (Jiang et al., 1994). Z<sub>max</sub> indicates maximum lod score; θ indicates estimated recombination fraction at Z<sub>max</sub>.

1994; Wang et al., submitted), the maximum combined two-point lod score for the 14 chromosome 7-linked families was 26.14, also at *D7S636* (θ = 0.0; Table 1). Haplotype analyses were consistent with our previous studies, placing *LQT2* between *D7S505* and *D7S483* (Figure 1; Wang et al., submitted), localizing this gene to chromosome 7q35-36.

#### *HERG* Maps to Chromosome 7q35-36

*HERG* was previously mapped to chromosome 7 (Warmke and Ganetzky, 1994). To test the candidacy of this gene, we refined the localization of *HERG* using two physical mapping techniques. First, we mapped *HERG* on a set of yeast artificial chromosome (YAC) contigs constructed for chromosome 7 (Green et al., 1994). *HERG* was localized to the same YAC as *D7S505*, a polymorphic marker that was tightly linked to *LQT2* (Table 1). Second, we mapped *HERG* to chromosome 7q35-36 using fluorescent in situ hybridization (FISH) with a P1 genomic clone containing *HERG* (data not shown).

To determine whether *HERG* was genetically linked to the LQT locus, we used single strand conformation polymorphism (SSCP) analyses to identify polymorphisms within *HERG* and performed linkage analyses in the chromosome 7-linked families. Two aberrant SSCP conformers were identified in DNA samples from patients and controls using primer pairs 5-11 and 3-8 (Figure 2). These conformers were cloned and sequenced. One abnormal conformer resulted from a C to T substitution at position 3 of codon 489 (cDNA nucleotide 1467; observed heterozygosity of 0.37). The second abnormal conformer resulted from an A to G substitution at position 3 of codon 564 (cDNA nucleotide 1692; observed heterozygosity of 0.44). Neither substitution affected the predicted amino acid sequence of *HERG*. *HERG* polymorphisms were used for genotypic analyses in chromosome 7-linked families (see Figure 1; data not shown). No recombination events between *HERG* and LQT were identified in any of these families. The maximum combined lod score for the 14

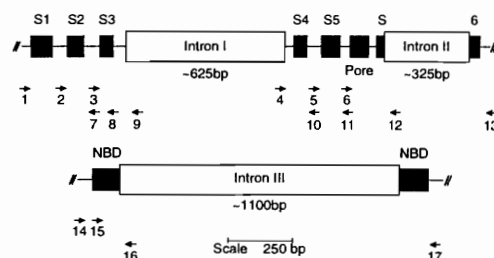


Figure 2. Partial Genomic Structure of *HERG* and Location of PCR Primers Used in This Study

Regions encoding predicted membrane-spanning domains (S1-S6), the pore domain, and the nucleotide-binding domain (NBD) are indicated. The DNA sequences for the intron-exon boundaries are these: intron I, 5'-AGGAGgtggg...ccccagCTGATC-3'; intron II, 5'-TGG-CTgtgagt...ccccagCCCTC-3'; intron III, 5'-CCTGGgtatgg...ctccag-GAAG-3'.

families was 9.64 (θ = 0.0; Table 1). These data indicate that *HERG* is completely linked to *LQT2*.

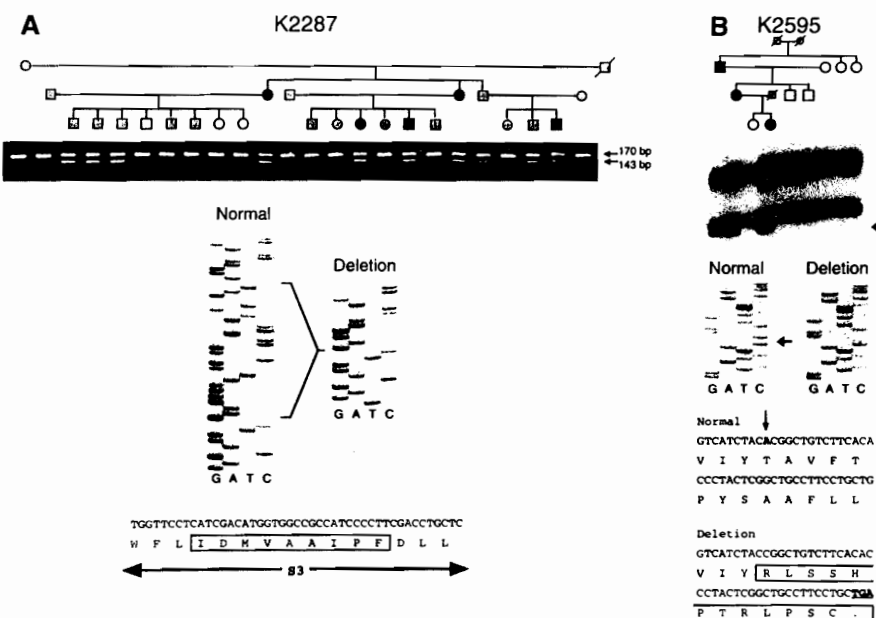
#### *HERG* Intragenic Deletions Associated with LQT in Two Families

To test the hypothesis that *HERG* is *LQT2*, we used SSCP analyses to screen for mutations in affected individuals. Since the genomic structure of *HERG* was unknown, oligonucleotide primer pairs were designed from published (Warmke and Ganetzky, 1994) *HERG* cDNA sequences (Figure 2; Table 2). In most cases, single products of expected size were generated. For primer pairs 1-10, 6-13, and 15-17, however, products of greater than expected size were obtained, suggesting the presence of intronic sequences. To examine this possibility, we cloned and sequenced these larger products. DNA sequence analyses identified three introns at positions 1557/1558, 1945/

Table 2. *HERG* PCR Primers

Name	Position	Sequence
1 L	1147-1166	GACGTGCTGCCTGAGTACAA
2 L	1291-1312	TTCCTGCTGAAGGAGACGGAAG
3 L	1417-1437	ACCACCTACGTCAATGCCAAC
4 L	Intron I	TGCCCCATCAACGGAATGTGC
5 L	1618-1636	GATCGCTACTCAGAGTACG
6 L	1802-1823	GCCTGGGCGGCCCTCCATCAA
7 R	1446-1426	CACCTCCTCGTTGGCATTGAC
8 R	1527-1503	GTCGAAGGGGATGGCGCCACCATG
9 R	Intron I	TACACCCTGCCTCCTTGCTGA
10 R	1643-1623	GCCCGCGCTACTCTGAGTAG
11 R	1758-1736	CAGCCAGCCGATGCGTGAAGTCA
12 R	Intron II	GCCCGCCCTGGGCACACTCA
13 R	2034-2016	CAGCATCTGTGTGTGGTAG
16 R	Intron III	GGCATTTCCAGTCCAGTGC
15 L	2259-2278	CCTGGCCATGAAGTTCAAGA
14 L	2214-2233	GCACTGCAAAACCTTCCGAG
17 R	2550-2529	GTCGGAGAAGTACAGGTACATG

All primers are shown in 5' to 3' direction. Sense strand oligonucleotides are indicated with an L and antisense oligonucleotides are indicated with an R. cDNA sequence was obtained from the GenBank data base; nucleotide numbering begins with the initiator methionine.



(A) Pedigree structure of K2287, results of PCR amplification using primer pair 3-9, and the effect of the deletion on the predicted structure of HERG protein are shown. Note that an aberrant fragment of 143 bp is observed in affected members of this kindred, indicating the presence of a disease-associated intragenic deletion. DNA sequence of normal and aberrant PCR products defines a 27 bp deletion ( $\Delta$ 1500-F508). This mutation causes an in-frame deletion of nine amino acids in the third membrane-spanning domain (S3). Deleted sequences are indicated.

(B) Pedigree structure of K2595 is shown. Deceased individuals are indicated by a slash. The results of SSCP analyses using primer pair 1-9 are shown beneath each individual. Note that an aberrant SSCP conformer cosegregates with the disease in this family. DNA sequence shows a single base pair deletion ( $\Delta$ 1261). This deletion results in a frameshift followed by a stop codon 12 amino acids downstream. The deleted nucleotide is indicated with an arrow.

As indicated previously, SSCP analyses using primer pair 3-8 identified an A to G polymorphism within *HERG* (cDNA nucleotide 1692). Analysis of kindred 2287 (K2287) using this SSCP defined a pattern of genotypes consistent with a null allele (see Figure 1). Possible explanations for these findings included multiple misinheritances, a possibility not supported by our previous genotypic analyses, DNA sample errors, base pair substitutions, or a deletion. To test the hypothesis that the genotypic data were due to a small deletion, we repeated PCR analyses of K2287 using a new primer pair (3-9) flanking the previous set of primers. These experiments identified two products of 170 bp and 143 bp in affected members of K2287 (Figure 3A). By contrast, only a single product of 170 bp was observed in unaffected members of this kindred. Furthermore, only the 170 bp band was seen in DNA samples from more than 200 unaffected individuals (data not shown). The 143 bp and 170 bp products were cloned from affected individual II-2. Direct sequence analyses of the aberrant PCR product revealed the presence of a 27 bp deletion begin-

To test further the hypothesis that *HERG* is *LQT2*, we continued SSCP analyses in additional kindreds. SSCP using the primer pair 1-9 identified an aberrant conformer in affected individuals of K2595 (Figure 3B). Analyses of more than 200 unaffected individuals failed to show this anomaly (data not shown). The normal and aberrant conformers were cloned and sequenced, revealing a single base deletion at position 1261 ( $\Delta$ 1261). This deletion results in a frameshift in sequences encoding the first membrane-spanning domain (S1), leading to a new stop codon within 12 amino acids. The identification of intragenic deletions of *HERG* in two LQT families suggests that *HERG* mutations can cause LQT.

To identify additional *HERG* mutations in *LQT2*, we continued SSCP analyses in linked kindreds and sporadic cases. Three aberrant SSCP conformers were identified in affected members of K1956, K2596, and K2015 (Figure 4). In each case, the normal and aberrant conformers were cloned and sequenced. In K1956, a C to T substitution at position 1682 was identified. This mutation results in substitution of valine for a highly conserved alanine at

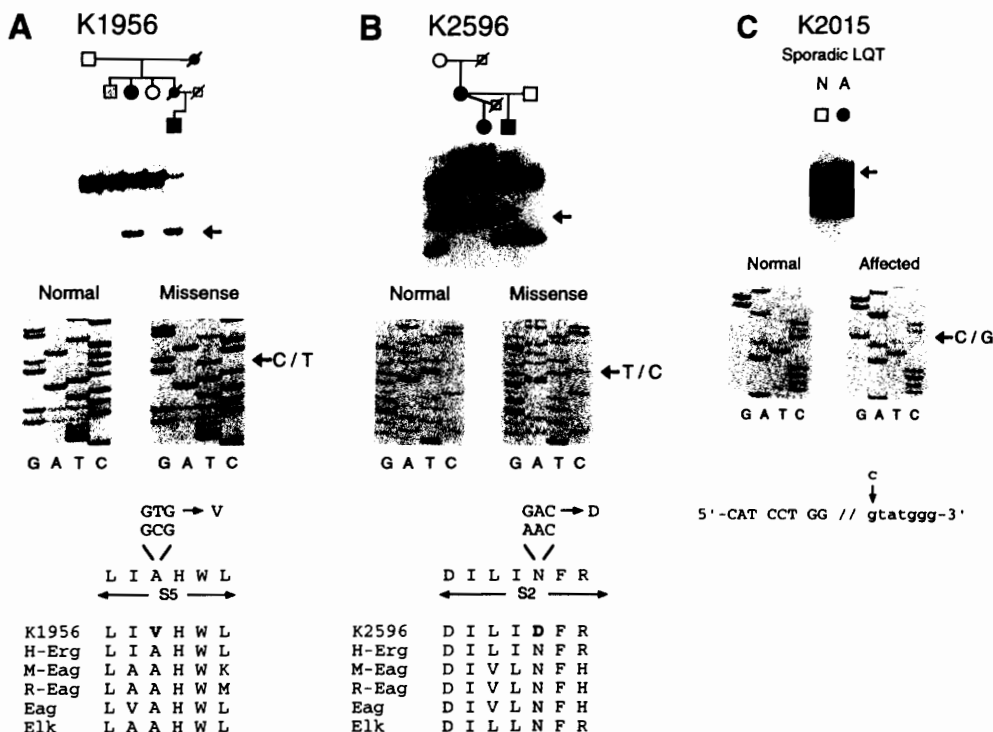


Figure 4. *HERG* Point Mutations Identified in Three LQT Kinreds

Pedigree structure of K1956 (A), K2596 (B), and K2015 (C) are shown. Below each pedigree, the results of SSCP analyses with primer pair 5-11 (K1956), primer pair 1-9 (K2596), and primer pair 14-16 (K2015) are shown. Aberrant SSCP conformers cosegregate with the disease in each kindred. DNA sequence analyses of the normal and aberrant conformers reveals a C to T substitution at position 1882 in K1956. This mutation results in substitution of valine for a highly conserved alanine residue at codon 561 (A561V). Analyses of K2596 reveals an A to G substitution at position 1408 (T to C substitution on the antisense strand is shown). This mutation results in substitution of aspartic acid for a conserved asparagine in the second transmembrane domain (N470D). Analyses of K2015 reveals a G to C substitution (C to G substitution on the antisense strand is shown). This mutation occurs in the splice-donor sequence of intron III. Coding sequences are shown in uppercase and intronic sequences are lowercase. Note that the G to C substitution disrupts the splice-donor site (*HERG*, *M-eag*, *elk* [Warmke and Ganetzky, 1994]; *R-eag* [Ludwig et al., 1994]).

codon 561 (A561V), altering the fifth membrane-spanning domain (S5) of the *HERG* protein (Figure 4A). In K2596, an A to G substitution was identified at position 1408. This mutation results in substitution of aspartic acid for a conserved asparagine at codon 470 (N470D), located in the second membrane-spanning domain (S2) (Figure 4B). In K2015, a G to C substitution was identified. This substitution disrupts the splice-donor sequence of intron III, affecting the cyclic nucleotide-binding domain (Figure 4C). None of the aberrant conformers were identified in DNA samples from more than 200 unaffected individuals (data not shown).

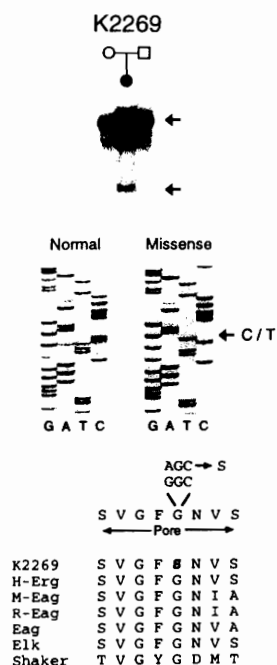
#### De Novo Mutation of *HERG* in a Sporadic Case of LQT

To substantiate that *HERG* mutations cause LQT, we used SSCP analysis to screen for mutations in sporadic cases. Primer pair 4-12 identified an aberrant conformer in affected individual II-1 of K2269 (Figure 5). This conformer was not identified in either parent or in more than 200

unaffected individuals. Direct DNA sequencing of the aberrant conformer identified a G to A substitution at position 1882. This mutation results in substitution of serine for a highly conserved glycine at codon 628 (G628S), altering the pore-forming domain. Genotype analysis of this kindred using nine informative short tandem repeat polymorphisms confirmed maternity and paternity. The identification of a de novo mutation in a sporadic case demonstrates that *HERG* is LQT2.

#### *HERG* Is Expressed in the Heart

*HERG* was originally identified from a hippocampal cDNA library [Warmke and Ganetzky, 1994]. To determine the tissue distribution of *HERG* mRNA, we isolated partial cDNA clones and used them in Northern blot analyses. Northern blot analyses showed strongest hybridization to heart mRNAs, with faint signals in brain, liver, and pancreas (Figure 6). Nonspecific hybridization was also seen in lung, possibly due to genomic DNA contamination. The size of the bands observed in cardiac mRNA was consis-

Cell  
800

**Figure 5. De Novo Mutation of *HERG* in a Sporadic Case of LQT**  
Pedigree structure of K2269 and SSCP analyses (primer pair 14-16) showing an aberrant conformer in a sporadic case of LQT. DNA sequence analyses identified a G to A substitution at position 1882 of the cDNA sequence (C to T substitution on the antisense strand is shown). Note that this mutation results in the substitution of a serine for a highly conserved glycine residue at codon 628 (G628S). This amino acid sequence is known to be critical for potassium ion selectivity.

tent with the predicted size of *HERG*. Two bands of ~4.1 and 4.4 kb were identified, possibly due to alternative splicing or the presence of a second related mRNA. These data indicate that *HERG* is strongly expressed in the heart, consistent with its involvement in LQT.

#### Discussion

We conclude that mutations in *HERG* cause the chromosome 7-linked form of LQT. Several lines of evidence support this conclusion. First, we used linkage analyses to map an LQT locus (*LQT2*) to chromosome 7q35-36 in 14 families. Second, we used physical and genetic mapping to place *HERG* in the same chromosomal region as *LQT2*. Third, we demonstrated that *HERG* is expressed in the heart. Fourth, we identified intragenic deletions of *HERG* associated with LQT in two families. Fifth, we identified four *HERG* point mutations in LQT patients. Finally, one of the point mutations arose de novo and occurs within a highly conserved region encoding the potassium-selective pore domain.

Our data suggest a likely molecular mechanism for chromosome 7-linked LQT. Although the function of *HERG* is

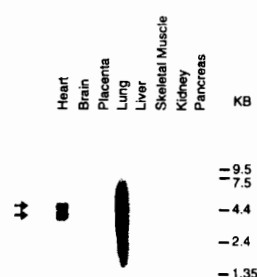


**Figure 6. Northern Blot Analysis of *HERG* mRNA Showing Strong Expression in the Heart**

A Northern blot (poly[A]<sup>+</sup> RNA, 2 μg/lane; Clontech) was probed using an *HERG* cDNA containing nucleotides 679-2239 of the coding sequence. Two cardiac mRNAs of ~4.1 and 4.4 kb are indicated. Background in mRNA extracted from lung was high, but no specific bands were identified.

not yet known, analyses of its predicted amino acid sequence indicates that it encodes a potassium channel  $\alpha$  subunit. Potassium channels are formed from four  $\alpha$  subunits (MacKinnon, 1991), either as homo- or heterotetramers (Covarrubias et al., 1991). These biophysical observations suggest that combination of normal and mutant *HERG*  $\alpha$  subunits could form abnormal *HERG* channels. This raises the possibility that *HERG* mutations have a dominant negative effect on potassium channel function.

The mutations that we identified are consistent with a dominant negative mechanism (Figure 7). Two mutations result in premature stop codons and truncated proteins ( $\Delta 1261$  and the splice-donor mutation). In the first case, only the amino terminus and a portion of the first membrane-spanning domain (S1) remain. In the second, the carboxyl end of the protein is truncated, leaving all membrane-spanning domains intact. *HERG* contains a cyclic nucleotide-binding domain near the carboxyl terminus, and in both mutations this domain is deleted. In another mutation, an in-frame deletion of nine amino acids disrupts the third membrane-spanning domain ( $\Delta 1500$ -F508). Two missense mutations also affect membrane-spanning domains, A561V in the S5 domain and N470D in S2. Both mutations affect amino acids conserved in the eag family of potassium channels and likely alter the secondary structure of the protein. The de novo missense mutation G628S occurs in the pore-forming domain. This domain is highly conserved in all potassium channel  $\alpha$  subunits. This mutation affects a conserved amino acid that is of known importance for ion selectivity. When this substitution was introduced into *Shaker* H4, potassium ion selectivity was lost (Heginbotham et al., 1994). As discussed above, these mutations could induce the loss of *HERG* function.

Our data have implications for the mechanism of arrhythmias in LQT. Two hypotheses for LQT have previously been proposed (Schwartz et al., 1995). One suggests that a predominance of left autonomic innervation causes abnormal cardiac repolarization and arrhythmias. This hypothesis is supported by the finding that arrhythmias

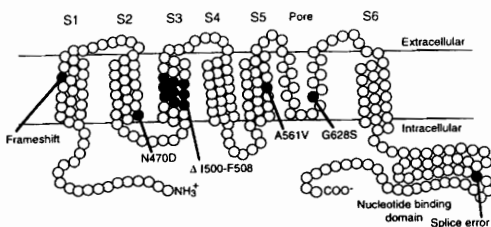


Figure 7. Schematic Representation of the Predicted Topology of the Protein Encoded by *HERG* and the Location of LQT-Associated Mutations

For simplicity, not all amino acids are shown. SSCP analyses identified *HERG* mutations in 4 of the 14 chromosome 7-linked kindreds.

mias can be induced in dogs by removal of the right stellate ganglion. In addition, anecdotal evidence suggests that some LQT patients are effectively treated by  $\beta$ -adrenergic blocking agents and by left stellate ganglionectomy (Schwartz et al., 1995). The second hypothesis for LQT-related arrhythmias suggests that mutations in cardiac-specific ion channel genes (or genes that modulate cardiac ion channels) cause delayed myocellular repolarization. Delayed myocellular repolarization could promote reactivation of L-type  $\text{Ca}^{2+}$  channels, resulting in secondary depolarizations (January and Riddle, 1989). These secondary depolarizations are the likely cellular mechanism of torsade de pointes arrhythmias (Surawicz, 1989). This hypothesis is supported by the observation that pharmacologic block of potassium channels can induce QT prolongation and repolarization-related arrhythmias in human and animal models (Antzelevitch and Sicouri, 1994). The discovery that one form of LQT results from mutations in a cardiac potassium channel gene supports the myocellular hypothesis.

The presence of a cyclic nucleotide-binding domain in *HERG* suggests a mechanism for the link between altered autonomic nervous activity and arrhythmias in LQT.  $\beta$ -Adrenergic receptor activation increases intracellular cAMP and enhances L-type  $\text{Ca}^{2+}$  channel function. Cyclic AMP may also activate *HERG*, thereby increasing net outward current and accelerating the rate of myocellular repolarization. Dominant negative mutations of *HERG* might interrupt the normal modulation of *HERG* function by cAMP, thereby permitting a predominant effect on L-type  $\text{Ca}^{2+}$  channel function. The resulting imbalance would increase the likelihood that enhanced sympathetic tone could induce  $\text{Ca}^{2+}$  channel-dependent secondary depolarizations, the probable cellular mechanism of torsades de pointes.  $\beta$ -Adrenergic blocking agents could act by interrupting the effect of cAMP on L-type  $\text{Ca}^{2+}$  channels, possibly explaining the beneficial effects of  $\beta$  blockers in some LQT patients.

The relative frequency of the three LQT loci is not yet known. In this study, we identified five new families with autosomal dominant LQT, and all were linked to chromosome 7. This brings the total number of chromosome 7-linked families to 14. To date, we have linked seven

families to chromosome 11 (*LQT1*), 14 families to chromosome 7 (*LQT2*), and three families to chromosome 3 (*LQT3*), and three families remain unlinked (Keating et al., 1991a, 1991b; Jiang et al., 1994). Although preliminary, these data suggest that *LQT2* is a common form of inherited LQT.

This work may have important clinical implications. Recently, presymptomatic diagnosis has been possible in large families using linkage analysis. Most cases of LQT are sporadic, and therefore genetic testing using linkage analysis is not feasible. Continued mutational analyses of *LQT2* will facilitate genetic testing for this form of LQT. Identification and characterization of genes responsible for other forms of LQT will be necessary for the development of generalized diagnostic tests. Improved diagnostic capacity may enable rational therapy. For example, chromosome 7-linked LQT patients may respond to potassium channel activators, like pinacidil.

In summary, our results provide the molecular mechanism of a life-threatening cardiac arrhythmia. Future experiments will define the specific function of *HERG* and its role in LQT. In addition, we will continue to search for LQT genes; these genes will provide further insight into cardiac repolarization and repolarization-related arrhythmias.

#### Experimental Procedures

##### Identification and Phenotyping of LQT Kindreds

LQT kindreds were ascertained from medical clinics throughout North America. Phenotypic criteria were identical to those used in our previous studies (Keating et al., 1991a, 1991b; Keating, 1992; Curran et al., 1993a; Jiang et al., 1994). Individuals were evaluated for LQT based on the QT interval corrected for heart rate (QTc; Bazette, 1920) and for the presence of syncope, presence of seizures, and aborted sudden death. Informed consent was obtained from all individuals or from their guardians in accordance with local institutional review board guidelines. Phenotypic data were interpreted without knowledge of genotype.

##### Genotypic and Linkage Analyses

Amplification and detection of microsatellite markers were performed as described previously (Curran et al., 1993a; Jiang et al., 1994). Polymorphic markers used in this study were *D7S483*, *D7S636*, and *D7S505* (Gyapay et al., 1994). Pairwise linkage analysis was performed using the MLINK program of the LINKAGE software package (Lathrop et al., 1985). In accordance with our previous studies, we assumed a penetrance of 0.90 and a disease gene frequency of 0.001. Gene frequency between males and females was assumed to be equal.

##### Isolation of *HERG* Genomic and cDNA Clones

*HERG* probes were generated using the products of PCRs with human genomic DNA and primer pairs 1-10, 6-13, and 15-17. These products were cloned, radiolabeled to high specific activity, and used to screen a human genomic P1 library (Sternberg, 1990). Positive clones were purified, characterized, and used for FISH and DNA sequence analyses. To isolate *HERG* cDNA clones, genomic probes containing *HERG* coding sequences were used to probe  $10^6$  recombinants of a human hippocampal cDNA library (Stratagene). A single clone containing ~2.2 kb of *HERG* coding sequence was isolated and characterized.

##### YAC-Based Mapping of *HERG*

APCR assay specific for the 3' untranslated region of *HERG* (employing primers 5'-GCTGGGCGCTCCCTTGA-3' and 5'-GCATCTTCATTAATTATTCA-3' and yielding a 309 bp product) was used to screen a collection of YAC clones highly enriched for human chromosome 7 (Green et al., 1995). Two positive YAC clones were identified (yWSS2193 and yWSS1759), both contained within a larger contig that



Cell  
802

includes YACs positive for the genetic marker *D7S505* (Green et al., 1994).

#### FISH

Metaphase chromosome spreads were prepared from normal cultured lymphocytes (46 X,Y) by standard procedures of colcemid arrest, hypotonic treatment, and acetic acid-methanol fixation. *HERG* P1 clone 16B4 was labeled by incorporation of biotin-14-dATP (BioNick System, GIBCO BRL), hybridized to metaphase spreads, and detected with streptavidin-Cy3 according to standard methods (Lichter et al., 1988). A digoxigenin-labeled centromere-specific  $\alpha$ -satellite probe (Oncor) was cohybridized and detected with antidigoxigenin-FITC to identify chromosome 7. Chromosomes were counterstained with DAPI and visualized directly on the photomicroscope.

#### SSCP and DNA Sequence Analyses

Genomic DNA samples were amplified by PCR and used in SSCP analyses as described (Orita et al., 1989; Ptacek et al., 1991). Primer pairs used for this study are shown in Table 2. Annealing temperature was 58°C for all PCRs. Reactions (10  $\mu$ l) were diluted with 40  $\mu$ l of 0.1% SDS and 1 mM EDTA and with 30  $\mu$ l of 95% formamide dye. Diluted products were denatured by heating at 100°C for 5 min, and 3  $\mu$ l of each sample was electrophoresed on 7.5% nondenaturing polyacrylamide gels (49:1 polyacrylamide:bisacrylamide) at 4°C. Electrophoresis was carried out at 40 W for 2–5 hr. Gels were transferred to filter paper, dried, and exposed to X-ray film at –80°C for 12–36 hr.

Normal and aberrant SSCP conformers were cut directly from dried gels and eluted in 75  $\mu$ l of distilled water at 37°C for 30 min. The eluted DNA (10  $\mu$ l) was used as template for a second PCR using the original primer pair. Products were fractionated in 2% low melting temperature agarose gels (FMC Corporation), and bands were cloned directly into pBluescript II SK(+) (Stratagene) using the T vector method as described (Marchuk et al., 1990). Plasmid DNA samples were purified and sequenced as previously described (Curran et al., 1993b).

#### Northern Blot Analysis

A multiple tissue Northern blot containing ~2  $\mu$ g/lane of poly(A)<sup>+</sup> mRNA was purchased from Clontech (human MTN blot 1). A high specific activity (>1.5  $\times$  10<sup>6</sup> cpm/ $\mu$ g DNA) and radiolabeled *HERG* cDNA fragment containing nucleotides 679–2239 of the coding sequence was prepared by random hexamer priming as described (Feinberg and Vogelstein, 1983). Probe was added to the hybridization solution at a final concentration of 5  $\times$  10<sup>6</sup> cpm/ml. Hybridization was carried out at 42°C for 24 hr in 20 ml of Quickhyb solution (Stratagene). Final washes were carried out at 65°C for 30 min in a solution of 0.1% SDS, 0.1  $\times$  SSC.

#### Acknowledgments

We thank M. Katoch, K. Kuehl, D. Wolfe, and members of the Sudden Arrhythmia Death Syndrome Foundation for their assistance in identifying and collecting LQT families. We thank D. Atkinson, C. Jiang, Q. Wang, B. Boak, and M. Ewart for their assistance. The authors appreciate helpful discussions with M. Sanguinetti, R. White, M. Leppert, S. Prescott, J. Mason, L. Ptacek, S. Odeberg, L. Bartlett, J. Dudson, and D. Li. FISH analyses were carried out in the University of Utah core facility. This work was supported by National Institutes of Health grant RO1-HL48074, Public Health Service research grant MO1-RR00064 from the National Center for Research Resources, the Technology Access Section of the Utah Genome Center, and the American Heart Association.

Received January 20, 1995; revised February 1, 1995.

#### References

Antzelevitch, C., and Sicouri, S. (1994). Clinical relevance of cardiac arrhythmias generated by afterdepolarizations: role of M cells in the generation of U waves, triggered activity and *torsade de pointes*. *J. Am. Coll. Cardiol.* 23, 259–277.  
Bazette, H. C. (1920). An analysis of the time-relationships of electrocardiograms. *Heart* 7, 353–370.

Benhorin, J., Kalman, Y. M., Madina, A., Towbin, J., Rave-Harel, N., Dyer, T. D., Blangero, J., MacCluer, J. W., and Kerem, B. (1993). Evidence of genetic heterogeneity in the long QT syndrome. *Science* 260, 1960–1962.  
Bonner, T. I., Buckley, N. J., Young, A. C., and Brann, M. R. (1987). Identification of a family of muscarinic acetylcholine receptor genes. *Science* 237, 527–532.  
Bruggeman, A., Pardo, L. A., Struhmer, W., and Pongs, O. (1993). *ether-a-go-go* encodes a voltage-gated channel permeable to K<sup>+</sup> and Ca<sup>2+</sup> and modulated by cAMP. *Nature* 365, 445–448.  
Covarrubias, M., Wei, A., and Salkoff, L. (1991). *Shaker, shal, shab*, and *shaw* express independent K<sup>+</sup> current systems. *Neuron* 7, 763–773.  
Curran, M. E., Atkinson, D., Timothy, K., Vincent, G. M., Moss, A. J., Leppert, M., and Keating, M. T. (1993a). Locus heterogeneity of autosomal dominant long QT syndrome. *J. Clin. Invest.* 92, 799–803.  
Curran, M. E., Atkinson, D. L., Ewart, A. K., Morris, C. A., Leppert, M. F., and Keating, M. T. (1993b). The elastin gene is disrupted by a translocation associated with supravalvular aortic stenosis. *Cell* 73, 159–168.  
Feinberg, A. P., and Vogelstein, B. A. (1983). Techniques for radiolabeling DNA to high specific activity. *Anal. Biochem.* 132, 6–13.  
Green, E. D., Idol, J. R., Mohr-Tidwell, R. M., Branden, V. V., Peluso, D. C., Fulton, R. S., Massa, H. F., Magness, C. L., Wilson, A. M., Kimura, J., Weissenbach, J., and Trask, B. J. (1994). Integration of physical, genetic and cytogenetic maps of human chromosome 7: isolation and analysis of yeast artificial chromosomes for 117 mapped genetic markers. *Hum. Mol. Genet.* 3, 489–501.  
Green, E. D., Branden, V. V., Fulton, R. S., Lim, R., Ueltzen, M. S., Peluso, D. C., Mohr-Tidwell, R. M., Idol, J. R., Smith, L. M., Chumakov, I., LePaslier, D., Cohen, D., Featherstone, T., and Green, P. (1995). A human chromosome 7 yeast artificial chromosome (YAC) resource: construction, characterization, and screening. *Genomics*, in press.  
Gyapay, G., Morissette, J., Vignal, A., Dib, C., Fizames, C., Millasseau, P., Marc, S., Bernardi, G., Lathrop, M., and Weissenbach, J. (1994). The 1993–1994 Genethon human genetic linkage map. *Nature Genet.* 7, 246–339.  
Heginbotham, L., Lu, Z., Abramson, T., and MacKinnon, R. (1994). Mutations in the K<sup>+</sup> channel signature sequence. *Biophys. J.* 66, 1061–1067.  
January, C. T., and Riddle, J. M. (1989). Early afterdepolarizations: mechanism of induction and block. *Circ. Res.* 64, 977–990.  
Jiang, C., Atkinson, D., Towbin, J. A., Splawski, I., Lehmann, M. H., Li, H., Timothy, K., Taggart, R. T., Schwartz, P. J., Vincent, G. M., Moss, A. J., and Keating, M. T. (1994). Two long QT syndrome loci map to chromosomes 3 and 7 with evidence for further heterogeneity. *Nature Genet.* 8, 141–147.  
Kannel, W. B., Cupples, A., and D'Agostino, R. B. (1987). Sudden death risk in overt coronary heart diseases: the Framingham study. *Am. Heart J.* 113, 799–804.  
Keating, M. T. (1992). Linkage analysis and long QT syndrome: using genetics to study cardiovascular disease. *Circulation* 85, 1973–1986.  
Keating, M. T., Atkinson, D., Dunn, C., Timothy, K., Vincent, G. M., and Leppert, M. (1991a). Linkage of a cardiac arrhythmia, the long QT syndrome, and the Harvey *ras-1* gene. *Science* 252, 704–706.  
Keating, M. T., Atkinson, D., Dunn, C., Timothy, K., Vincent, G. M., and Leppert, M. (1991b). Consistent linkage of the long QT syndrome to the Harvey *ras-1* locus on chromosome 11. *Am. J. Hum. Genet.* 49, 1335–1339.  
Koch, M. C., Steinmeyer, K., Lorenz, C., Ricker, K., Wolf, F., Otto, M., Zoll, B., Lehmann-Horn, F., Grzeschik, K.-H., and Jentsch, T. J. (1992). The skeletal muscle chloride channel in dominant and recessive human myotonia. *Science* 257, 797–800.  
Lathrop, G. M., Lalouel, J.-M., Julier, C., and Ott, J. (1985). Multilocus linkage analysis in humans: detection of linkage and estimation of recombination. *Am. J. Hum. Genet.* 37, 482–498.  
Lichter, P., Cremer, T., Borden, J., Manuelidis, L., and Ward, D. C. (1988). Delineation of individual human chromosomes in metaphase and interphase cells by *in situ* suppression hybridization using recom-

- binant DNA libraries. *Hum. Genet.* 80, 224-234.
- Ludwig, J., Terlau, H., Wunder, F., Bruggeman, A., Pardo, L. A., Marquardt, A., Strüder, W., and Pongs, O. (1994). Functional expression of a rat homologue of the voltage gated *ether a go-go* potassium channel reveals differences in selectivity and activation kinetics between the *Drosophila* channel and its mammalian counterpart. *EMBO J.* 13, 4451-4458.
- MacKinnon, R. (1991). Determination of the subunit stoichiometry of a voltage-activated potassium channel. *Nature* 350, 232-235.
- Marchuk, D., Drumm, M., Saulino, A., and Collins, F. S. (1990). Construction of T-vectors, a rapid and general system for direct cloning of unmodified PCR products. *Nucl. Acids Res.* 19, 1154.
- Orita, M., Iwahana, H., Kanazawa, H., and Sekiya, T. (1989). Detection of polymorphisms of human DNA by gel electrophoresis as single strand conformation polymorphisms. *Proc. Natl. Acad. Sci. USA* 86, 2766-2770.
- Ptacek, L. J., George, A. L., Griggs, R. C., Tawil, R., Kallen, R. G., Barchi, R. L., Robertson, M., and Leppert, M. F. (1991). Identification of a mutation in the gene causing hyperkalemic periodic paralysis. *Cell* 67, 1021-1027.
- Romano, C. (1965). Congenital cardiac arrhythmia. *Lancet* 1, 658-659.
- Roy, N., Kahlem, P., Dausse, E., Bennaceur, M., Faure, S., Weissenbach, J., Komajda, M., Denjoy, I., Coumel, P., Schwartz, K., and Guicheney, P. (1994). Exclusion of HRAS from long QT locus. *Nature Genet.* 8, 113-114.
- Schwartz, P. J., Periti, M., and Malliani, A. (1975). The long QT syndrome. *Am. Heart J.* 109, 378-390.
- Schwartz, P. J., Locati, E. H., Napolitano, C., and Priori, S. G. (1995). The long QT syndrome. In *Cardiac Electrophysiology: From Cell to Bedside*, D. P. Zipes and J. Jalife, eds. (Philadelphia: W. B. Saunders Company), pp. 788-811.
- Sternberg, N. (1990). Bacteriophage P1 cloning system for the isolation, amplification, and recovery of DNA fragments as large as 100 kilobase pairs. *Proc. Natl. Acad. Sci. USA* 87, 103-107.
- Surawicz, B. (1989). Electrophysiologic substrate of *torsade de pointes*: dispersion of repolarization or early afterdepolarizations? *J. Am. Coll. Cardiol.* 14, 172-184.
- Towbin, J. A., Li, H., Taggart, T., Lehmann, M. H., Schwartz, P. J., Satter, C. A., Ayyagari, R., Robinson, J. L., Moss, A., and Hejtmancik, F. (1994). Evidence of genetic heterogeneity in Romano-Ward long QT syndrome (LQTS): analysis of 23 families. *Circulation* 90, 2635-2644.
- Vincent, G. M., Timothy, K. W., Leppert, M. F., and Keating, M. T. (1992). The spectrum of symptoms and QT intervals in carriers of the gene for the long QT syndrome. *N. Engl. J. Med.* 327, 846-852.
- Ward, O. C. (1964). A new familial cardiac syndrome in children. *J. Ir. Med. Assoc.* 54, 103-106.
- Warmke, J. E., and Ganetzky, B. (1994). A family of potassium channel genes related to *eag* in *Drosophila* and mammals. *Proc. Natl. Acad. Sci. USA* 91, 3438-3442.
- Willich, S. N., Levy, D., Rocco, M. B., Tofler, G. H., Stone, P. H., and Muller, J. O. E. (1987). Circadian variation in the incidence of sudden cardiac death in the Framingham heart study population. *Am. J. Cardiol.* 60, 801-806.

## CHAPTER 4

### *SCN5A* MUTATIONS ASSOCIATED WITH AN INHERITED CARDIAC ARRHYTHMIA, LONG QT SYNDROME

The following chapter is a reprint from an article coauthored by Wang, Q., Shen, J., Atkinson, D., Li, Z., Robinson, J., Moss, A. J., Towbin, J. A., Keating, M. T. and me. It was originally published in *Cell*, volume 80, pages 805-811, March 10, 1995 (Copyright Cell Press). It is reprinted here with the permission of the coauthors and Cell Press.

## SCN5A Mutations Associated with an Inherited Cardiac Arrhythmia, Long QT Syndrome

Qing Wang,<sup>1,2,3</sup> Jiaxiang Shen,<sup>1,2,3</sup> Igor Splawski,<sup>2,3</sup>

Donald Atkinson,<sup>1,2,3</sup> Zhizhong Li,<sup>2,3</sup>

Jennifer L. Robinson,<sup>4</sup> Arthur J. Moss,<sup>5</sup>

Jeffrey A. Towbin,<sup>6</sup> and Mark T. Keating<sup>1,2,3,7</sup>

<sup>1</sup>Howard Hughes Medical Institute

<sup>2</sup>Department of Human Genetics

<sup>3</sup>Eccles Program in Human Molecular Biology and Genetics

<sup>7</sup>Cardiology Division

University of Utah Health Sciences Center

Salt Lake City, Utah 84112

<sup>4</sup>Department of Community and Preventive Medicine

<sup>5</sup>Department of Medicine

University of Rochester Medical Center

Rochester, New York 14627

<sup>6</sup>Department of Pediatrics

and Department of Molecular and Human Genetics

Baylor College of Medicine

Houston, Texas 77030

### Summary

Long QT syndrome (LQT) is an inherited disorder that causes sudden death from cardiac arrhythmias, specifically torsade de pointes and ventricular fibrillation. We previously mapped three LQT loci: *LQT1* on chromosome 11p15.5, *LQT2* on 7q35-36, and *LQT3* on 3p21-24. Here we report genetic linkage between *LQT3* and polymorphisms within *SCN5A*, the cardiac sodium channel gene. Single strand conformation polymorphism and DNA sequence analyses reveal identical intragenic deletions of *SCN5A* in affected members of two unrelated LQT families. The deleted sequences reside in a region that is important for channel inactivation. These data suggest that mutations in *SCN5A* cause chromosome 3-linked LQT and indicate a likely cellular mechanism for this disorder.

### Introduction

Although sudden death from cardiac arrhythmias is thought to account for 11% of all natural deaths, the mechanisms underlying arrhythmias are poorly understood (Kannel et al., 1987; Willich et al., 1987). Long QT syndrome (LQT) is an inherited cardiac arrhythmia that causes abrupt loss of consciousness, seizures, and sudden death from ventricular tachyarrhythmias, specifically torsade de pointes and ventricular fibrillation (Ward, 1964; Romano, 1965; Schwartz et al., 1975; Moss et al., 1991). Autosomal dominant and autosomal recessive forms of this disorder have been reported. Autosomal recessive LQT (also known as Jervell-Lange-Nielsen syndrome) has been associated with congenital neural deafness; this form of LQT is rare (Jervell and Lange-Nielsen, 1957). Autosomal dominant

LQT (Romano-Ward syndrome) is more common and is not associated with other phenotypic abnormalities. A disorder very similar to inherited LQT can also be acquired, usually as a result of pharmacologic therapy (Schwartz et al., 1975; Zipes, 1987).

We have used two strategies to identify LQT genes, a candidate gene approach and positional cloning. Positional information is now available for three LQT loci, as we have mapped *LQT1* to chromosome 11p15.5 (Keating et al., 1991a, 1991b), *LQT2* to 7q35-36, and *LQT3* to 3p21-24 (Jiang et al., 1994). The candidate gene approach relies on likely mechanistic hypotheses based on physiology. Although little is known about the physiology of LQT, the disorder is associated with prolongation of the QT interval on electrocardiograms, a sign of abnormal cardiac repolarization. This association suggests that genes encoding ion channels (or their modulators) are reasonable candidates for LQT. This hypothesis is now supported by our recent discovery that chromosome 7-linked LQT results from mutations in the human *ether-a-go-go*-related gene (*HERG*), a putative cardiac potassium channel gene (Curran et al., 1995 [this issue of *Cell*]). A neuroendocrine calcium channel gene (*CACNL1A2*; Chin et al., 1991; Seino et al., 1992) and a gene encoding a GTP-binding protein that modulates potassium channels (*GNAI2*; Weinstein et al., 1988; Magovcevic et al., 1992) became candidates for *LQT3* based on their chromosomal location. Subsequent linkage analyses, however, have excluded these genes (Q. W. and M. T. K., unpublished data).

In theory, mutations in a cardiac sodium channel gene could cause LQT. Voltage-gated sodium channels mediate rapid depolarization in ventricular myocytes and also conduct a small current during the plateau phase of the action potential (Attwell et al., 1979). Subtle abnormalities of sodium channel function (e.g., delayed sodium channel inactivation or altered voltage dependence of channel inactivation) could delay cardiac repolarization, leading to QT prolongation and arrhythmias. A few years ago, Gellens et al. (1992) cloned and characterized a cardiac sodium channel gene, *SCN5A*. The structure of this gene was similar to previously characterized sodium channels, encoding a large protein of 2016 amino acids. These channel proteins contain four homologous domains (DI-DIV), each of which contains six putative membrane-spanning segments (S1-S6). *SCN5A* was recently mapped to chromosome 3p21, making it an excellent candidate gene for *LQT3* (George et al., 1995).

In this study, we provide evidence suggesting that *SCN5A* is *LQT3*. We used genotypic analyses to show that *SCN5A* was tightly linked to *LQT3* in three unrelated families. We then identified the same intragenic deletion of *SCN5A* in affected members of two of these families. These deletions disrupted sequences within a region of known importance for sodium channel inactivation, suggesting a likely cellular mechanism for chromosome 3-linked LQT.

Table 1. PCR Primers Used to Define *SCN5A* Polymorphisms and Mutations

Primer	Sequence	Region Amplified	Exon
1L	GCCTGTCTGATCTCCCTGTGTGA	DIII/S6; IDIII-IV	21
2R	ACCCAGCCAGTGGGAGCTGGT		
3L	CCATGCTGGGCTCTGAGAAC	IDIII-IV	22
4R	GGCTCTGATGGCTGGCCATGTG		
5L	CCCAGCGAGCACTTTCCATTTG	IDIII-IV; DIV/S1-S3	23
6R	GCTTCTCCGTCCAGCTGACTTGTA		
7L	GAGCCAGCCGTGGGCATCCT	DIV/S6	24
8R	GTCCCACTCACCATGGGAG		

All primers are shown in 5' to 3' direction. Sense strand oligonucleotides are indicated with an L and antisense oligonucleotides are indicated with an R. D, domain; ID, interdomain; S, membrane-spanning segment.

## Results

### Genetic Linkage of *SCN5A* and *LQT3*

In 1995, *SCN5A* was mapped to chromosome 3p21 (George et al., 1995). To test the candidacy of *SCN5A* for *LQT*, we used single strand conformation polymorphism (SSCP) analyses to identify polymorphisms within this gene and then performed linkage analyses in chromosome 3-linked families. Since the genomic structure of *SCN5A* was unknown, we designed oligonucleotide primer pairs from published *SCN5A* cDNA sequences (Gellens et al., 1992), based on the assumption that the genomic structure of *SCN5A* would be similar to the known structure of *SCN4A*, the skeletal muscle sodium channel gene (McClatchey et al., 1992a). Primer pairs that gave appropriately sized products from genomic DNA were used to

screen DNA samples from patients. An aberrant SSCP conformer was identified using primer pair 7-8 (Table 1). The normal and aberrant bands were cloned and sequenced. The aberrant conformer resulted from a C to T substitution at position 3 of codon 1819 (cDNA nucleotide 5607; Gellens et al., 1992). This substitution did not affect the predicted amino acid sequence of the product of *SCN5A*. The observed heterozygosity for this polymorphism was <0.50. The *SCN5A* polymorphism was used for genotypic analyses in chromosome 3-linked families (Figure 1). No recombination events between *SCN5A* and *LQT* were identified in any of these families. The maximum combined two-point lod score for all chromosome 3-linked families was 2.74 at a recombination fraction of 0.0 (Table 2).

No additional SSCP anomalies were identified using

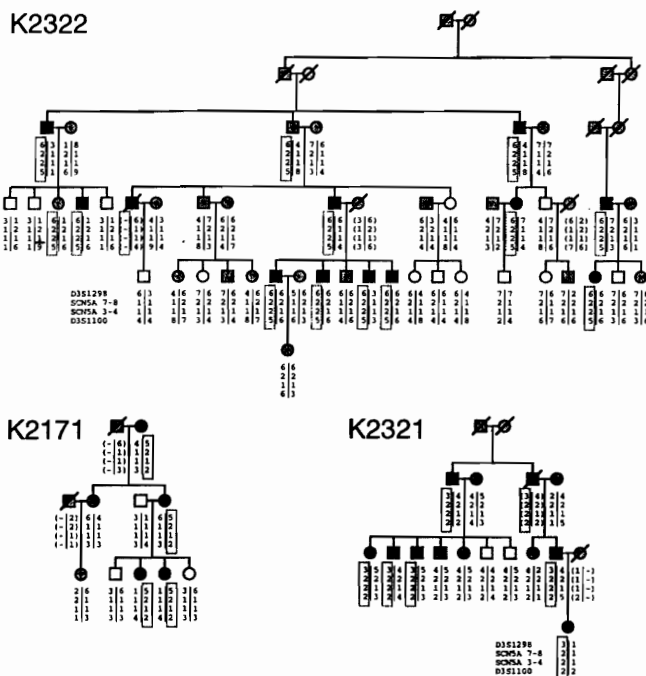


Figure 1. Genetic Linkage of *SCN5A* and *LQT3*

Pedigree structure and genotypic analyses of *LQT* kindreds 2171, 2321, and 2322. Individuals with the characteristic features of *LQT*, including prolongation of the QT interval on electrocardiogram and a history of syncope or aborted sudden death, are indicated by closed circles (females) or closed squares (males). Unaffected individuals are indicated by open symbols, and individuals with an equivocal phenotype are shown as stippled. Deceased individuals are indicated by a slash. The results of genotypic analyses are shown below each symbol. Genotypes for the following *LQT3*-linked polymorphic markers are shown (telomere to centromere): *D3S1298*, *SCN5A* 7-8, *SCN5A* 3-4, and *D3S1100*. Haplotypes cosegregating with the disease are indicated by a box. Recombination events are indicated by a horizontal black line. Haplotype analyses indicate that *LQT3* and *SCN5A* are tightly linked in all chromosome 3-linked families.

Table 2. Pairwise Lod Scores and Recombination Fractions for Linkage of LQT3 with SCN5A

Marker	Kindred	Recombination Fractions						
		0.001	0.01	0.05	0.10	0.20	0.30	0.40
SCN5A 3-4	K2171	0.00	0.00	0.00	0.00	0.00	0.00	0.00
	K2321	1.50	1.47	1.35	1.20	0.87	0.53	0.18
	K2322	4.03	3.95	3.62	3.20	2.34	1.47	0.61
	Total <sup>a</sup>	5.53	5.43	4.97	4.40	3.22	2.00	0.79
SCN5A 7-8	K2171	0.82	0.80	0.74	0.65	0.46	0.26	0.08
	K2321	0.12	0.12	0.10	0.08	0.04	0.02	0.00
	K2322	1.80	1.78	1.66	1.48	1.05	0.60	0.20
	Total <sup>b</sup>	2.74	2.70	2.50	2.20	1.55	0.87	0.28

Lod scores were calculated assuming autosomal dominant inheritance with a penetrance of 0.90 for all kindreds, as indicated by segregation analysis of these and other LQT kindreds. We assumed a disease allele frequency of 0.001 and that female and male recombination frequencies were equal. When penetrance was varied from 70%–100%, the maximum combined two-point lod score for linkage between SCN5A 3–4 and LQT3 ranged from 4.85 to 5.91, respectively. The results for SCN5A 7–8 varied from 2.26 (70%) to 3.01 (100%).

<sup>a</sup>  $Z_{\max} = 5.54$ ,  $\theta = 0.00$ ;  $Z_{\max}$  indicates maximum lod score.  $\theta$  indicates estimated recombination fraction at  $Z_{\max}$ .

<sup>b</sup>  $Z_{\max} = 2.74$ ,  $\theta = 0.00$ .

cDNA sequences. To facilitate this work, we isolated and partially characterized two genomic P1 clones. These clones spanned the entire gene and were used to begin determining the genomic structure of SCN5A. We hypothesized that LQT-causing mutations would be subtle (e.g., missense mutations or small in-frame deletions) and might affect delayed inactivation of encoded sodium channels or alter the voltage dependence of channel inactivation. We focused, therefore, on regions of known importance for channel inactivation. Primers based on sequences predicted to encode the cytoplasmic region between DIII and DIV were synthesized. This region corresponds to exons 21–23 of SCN4A and is known to be critical for channel inactivation. These primers were used to characterize the flanking introns by cycle sequencing. Additional primers were designed to these intronic sequences (see Table 1).

When primer pair 3–4 was used in SSCP analyses, an

anomalous conformer was identified in DNA samples from affected members of kindreds 2321 and 2322 (Figure 1). By contrast, only the normal conformer was seen in DNA samples from unaffected members of these families. The combined two-point lod score for linkage between this anomaly and LQT3 was 5.54 (Table 2). Again, no recombination was observed between SCN5A and LQT3, indicating that these loci are tightly linked.

#### Identical SCN5A Intragenic Deletions Associated with LQT in Two Unrelated Families

The mobility shift between the aberrant and normal SSCP conformers identified in kindreds 2321 and 2322 was large, suggesting the possibility of a small deletion. To test this hypothesis, the conformers were separated by electrophoresis on denaturing polyacrylamide gels (Figures 2 and 3). These data demonstrated the presence of two products of 235 bp and 244 bp. The 235 bp product was only seen in affected individuals. Furthermore, this aberrant conformer was not observed in more than 500 control individuals (data not shown). These data indicate that an intragenic deletion of SCN5A is the likely cause of LQT in these families.

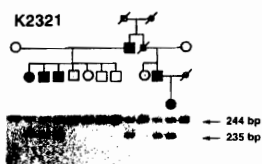


Figure 2. SCN5A Intragenic Deletion Cosegregates with the Disease in Kindred 2321

The pedigree structure for kindred 2321 is shown. The results of polymerase chain reaction (PCR) analyses using primer pair 3–4 and denaturing polyacrylamide gel electrophoresis are shown below each symbol. Note that the 235 bp allele cosegregates with the disease in this family, indicating the presence of a disease-associated intragenic deletion of SCN5A. To avoid phenotypic misclassification, the phenotypic criteria used in this study were stringent, and many individuals were classified as having an uncertain phenotype. Individuals with a QTc of 0.47 s or greater were classified as affected, whereas individuals with a QTc of 0.41 s or less were considered unaffected. All other individuals were classified as uncertain. If typical criteria were used (individuals with a QTc of 0.44 s or greater considered affected and individuals with a QTc less than 0.44 s classified as normal), all affected members of kindreds 2321 and 2322 would carry the SCN5A deletion and all unaffected individuals would carry only the normal allele.

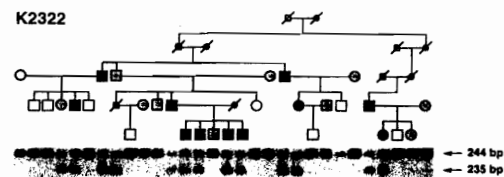
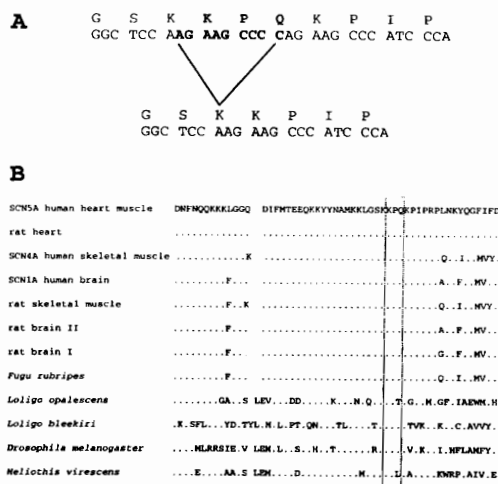


Figure 3. SCN5A Intragenic Deletion in Kindred 2322

The results of PCR analyses using primer pair 3–4 and denaturing polyacrylamide gel electrophoresis are shown below each symbol. Note that the 235 bp allele cosegregates with the disease in this family, indicating the presence of a disease-associated intragenic deletion. The individuals represented in lanes 4 and 8 carried the deletion but were phenotypically classified as uncertain. These individuals had a QTc of 0.46 s and with less stringent phenotypic criteria would be considered affected.

Cell  
808

**Figure 4.** DNA and Amino Acid Sequence of the *SCN5A* Intragenic Deletion Associated with LQT

(A) DNA sequence analysis of the *SCN5A* intragenic deletion identified in kindred 2322. DNA sequence of normal and aberrant PCR products defines a 9 bp deletion. This mutation causes a deletion of three amino acids (KPQ) in the cytoplasmic region between DIII and DIV. Deleted sequences are indicated.

(B) Amino acid sequence homology of the cytoplasmic region between DIII and DIV of sodium channels. Sequences were obtained from GenBank.

To determine the effect of the LQT-associated deletion on *SCN5A* structure, we amplified the normal and aberrant SSCP conformers and performed cycle sequencing. These experiments revealed the presence of a 9 bp deletion beginning at nucleotide 4661 of the cDNA (Figure 4A). We also cloned and sequenced the aberrant and normal SSCP conformers. These experiments confirmed the size and location of the deletion. This deletion disrupts the coding sequence, resulting in a deletion of three conserved amino acids, Lys-1505–Pro-1506–Gln-1507 (KPQ), in the cytoplasmic linker between DIII and DIV (Figures 4B and 5).

DNA sequence analyses of the aberrant conformer in kindred 2321 indicated that the intragenic deletion was identical to that found in kindred 2322 (data not shown). One possible explanation for the identical deletions in these two kindreds is that they are distantly related. Both families were North American of European descent, one German and the other English. Examination of a genealogy data base failed to reveal a relationship between these families for more than eight generations. Furthermore, genotypic analyses of these kindreds indicated different haplotypes on the disease chromosome (see Figure 1). The presence of identical deletions in two apparently unrelated LQT families strongly suggests that *SCN5A* is *LQT3*.

## Discussion

We conclude that mutations in the cardiac sodium channel gene *SCN5A* are the likely cause of chromosome 3–linked

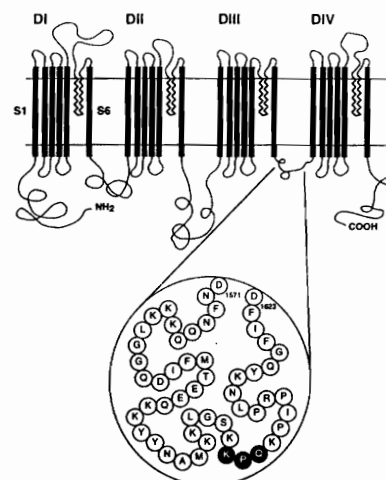


**Figure 5.** Schematic Representation of the Predicted Topology of the Protein Encoded by *SCN5A* and of the Location of the LQT-Associated Deletion

LQT. Several lines of evidence support this conclusion. First, we identified genetic linkage between *SCN5A* and *LQT3* in three unrelated families. No recombination was identified between these loci. Second, we identified identical intragenic deletions of *SCN5A* in affected members of two LQT families. This deletion was not identified in more than 500 control individuals. Third, *SCN5A* is the cardiac sodium channel gene. Subtle mutations of this gene would be expected to cause an LQT phenotype. Finally, the type (an in-frame deletion of three amino acids) and location (a region of known importance for sodium channel inactivation) of the deletions support the conclusion that *SCN5A* is *LQT3*.

Additional evidence supports a role for *SCN5A* in the pathogenesis of LQT. Pharmacologic data, for example, suggest that abnormal cardiac sodium channel function could cause LQT. Toxins and drugs that slow the rate of sodium channel inactivation or that shift the voltage dependence of channel activation or inactivation can prolong cardiac action potential duration and induce arrhythmias (Honertjager, 1982). Molecular genetic studies also support a link between sodium channel inactivation and clinical electrophysiologic abnormalities. Studies of hyperkalemic periodic paralysis and paramyotonia congenita indicate that missense mutations in the skeletal muscle sodium channel gene (*SCN4A*) cause myotonia (Fontaine et al., 1990; Ptacek et al., 1991, 1992; Rojas et al., 1991; McClatchey et al., 1992b, 1992c; Ebers et al., 1991; Rudolph et al., 1992; Lerche et al., 1993). Physiologic data show that these mutations affect sodium channel inactivation, leading to repetitive depolarizations, consistent with the myotonic phenotype (Yang et al., 1994). By analogy, similar mutations in the cardiac sodium channel gene could cause a phenotype like LQT.

We have also demonstrated that mutations in *HERG*, a

putative cardiac potassium channel gene, cause the chromosome 7-linked form of LQT (Curran et al., 1995). The mutations that we identified in *HERG*, along with the biophysics of potassium channel  $\alpha$  subunits, suggest that chromosome 7-linked LQT results from dominant negative mutations and a resultant reduction in functional channels. In chromosome 3-linked LQT, by contrast, the LQT-associated deletions identified in *SCN5A* are likely to result in functional cardiac sodium channels with altered properties, such as delayed inactivation or altered voltage dependence of channel inactivation. Delayed sodium channel inactivation would increase inward sodium current, depolarizing the membrane. This effect is similar to the altered membrane potential expected from *HERG* mutations, in which outward potassium current is decreased. It is unlikely that more deleterious mutations of *SCN5A* would cause LQT. A reduction of the total number of cardiac sodium channels, for example, would be expected to reduce action potential duration, a phenotype opposite that of LQT. The mutations described in this study cause the deletion of three amino acids, KPQ, in the cytoplasmic linker between DIII and DIV. The KPQ sequence is highly conserved, suggesting the presence of genetic pressure for its conservation during evolution (Figure 4B). The cytoplasmic peptide segment that links DIII and DIV is the region responsible for fast inactivation (West et al., 1992). Heterologous expression of neural sodium channels in the form of two polypeptides lacking this DIII-DIV linker results in a sodium current with greatly slowed inactivation (Stuhmer et al., 1989). Site-directed mutagenesis studies of this region in *SCN4A* have focused on another amino acid triplet, Ile-1488-Phe-1489-Met-1490 (IFM). Mutations of these amino acids to glutamine residues eliminate sodium channel fast inactivation, but leave slow inactivation intact (West et al., 1992). It will be of interest to determine whether the KPQ deletion has a similar functional effect on cardiac sodium channel inactivation.

Our data predict a likely cellular mechanism for chromosome 3-linked LQT. Delayed myocellular sodium channel inactivation would prolong action potential duration and the QT interval. Excessive prolongation could result in reactivation of L-type calcium or sodium channels, thereby leading to secondary depolarizations, a likely mechanism of torsades de pointes (Antzelevitch and Sicouri, 1994).

We have not yet identified a mutation in *SCN5A* in kindred 2171, the third chromosome 3-linked LQT family. Although the disease phenotype in this kindred appears to be linked to *SCN5A*, SSCP analyses of sequences encoding the putative inactivation region failed to show a deletion or other anomalies. Presumably, the disease in this family results from *SCN5A* mutations in another region of this approximately 35 kb gene. Mutational analyses of hyperkalemic periodic paralysis and paramyotonia congenita families have demonstrated several other regions of *SCN4A* that are important for channel inactivation (Fontaine et al., 1990; Ptacek et al., 1991, 1992; Rojas et al., 1991; McClatchey et al., 1992b, 1992c; Ebers et al., 1991; Rudolph et al., 1992; Lerche et al., 1993). Once we have determined the genomic structure of *SCN5A*, we will screen for additional LQT-causing mutations.

Although LQT kindreds 2321 and 2322 appear unrelated, both had the same KPQ deletion. The haplotype of the affected chromosome in each family was distinct, but this does not exclude the possibility of a distant relationship. Continued genotypic analysis of sequences near *SCN5A* may help determine whether these deletions are distinct.

Presymptomatic diagnosis of LQT has depended on identification of QT prolongation on electrocardiograms. Unfortunately, electrocardiograms are rarely performed in young, healthy individuals. In addition, many LQT gene carriers have relatively normal QT intervals, and the first sign of disease can be a fatal cardiac arrhythmia (Vincent et al., 1992). Now that two LQT genes have been identified, we can begin to contemplate genetic testing for this disorder. This will require continued mutational analyses and identification of additional LQT genes. With more detailed phenotypic analyses, we may also discover phenotypic differences among the varied forms of LQT. These differences may be useful for diagnosis and treatment.

In summary, we have identified a gene, *SCN5A*, that is likely to cause LQT. Along with our finding that mutations in *HERG* cause the chromosome 7-linked form of LQT, this discovery further supports the hypothesis that LQT results from mutations in cardiac ion channels.

#### Experimental Procedures

##### LQT Kindreds

This investigation was performed on three previously described LQT kindreds (Jiang et al., 1994). Phenotypic criteria were identical to those used in our previous studies (Keating et al., 1991a, 1991b; Keating, 1992). Individuals were evaluated for LQT based on the QT interval corrected for heart rate (QTc; Bazette, 1920) and on the presence of syncope, seizures, and aborted sudden death. Informed consent was obtained from individuals or their guardians, in accordance with local institutional review board guidelines. Phenotypic data were interpreted without knowledge of genotype.

##### Linkage Analyses

Pairwise linkage analysis was performed using MLINK in LINKAGE version 5.1 (Lathrop et al., 1985). As in our previous studies, we assumed a penetrance of 0.90 and an LQT gene frequency of 0.001 (Keating et al., 1991a, 1991b). Gene frequency was assumed to be equal between males and females.

##### Isolation of *SCN5A* Genomic Clones and Partial Characterization of Genomic Structure

*SCN5A* probes were generated using the products of PCRs with human genomic DNA and primer pairs based on *SCN5A* cDNA sequences. One primer pair, 5'-ACTTTCATCGTACTGAATAAGGCAA-3' and 5'-GAGTGAACAGAACTCTTCACAGC-3', was designed from 5' coding sequences and yielded the predicted product of 118 bp. The second primer pair, 5'-GGACCGTGAGTCCATCGTGTGA-3' and 5'-AGCCCATCACAACATATACAGTCT-3', was derived from the 3' noncoding sequences and yielded a product of 336 bp. The third primer pair, 5'-AGCAACTTCATCCAGCTGCTGAG-3' and 5'-CTCCAGCATCTCAGGTCAAGTG-3', was based on 3' noncoding sequences and yielded a product of 297 bp. These PCR products were purified from 2% agarose gels, radiolabeled to high specific activity, and used to screen a human genomic P1 library (Sternberg, 1990).

To characterize the genomic structure of *SCN5A* exons encoding the cytoplasmic linker between DIII-DIV, we designed sequencing primers based on cDNA sequences and predicted genomic structure (McClatchey et al., 1992a; Gellens et al., 1992). The primer pair for presumed exon 21 (based on the structure of *SCN4A*) was 5'-TATG-AAGAGCAGCTCAGTGGGAA-3' and 5'-CTTTTCTCTCTGTGGTT-



GAAGTTG-3'. Primers for presumed exon 22 were 5'-TTAGGGG-GCCAGGACATCTTC-3' and 5'-CAGGGGCGGTGGGATGGGCTTC-TGG-3'. Primers for presumed exon 23 were 5'-CACCATATTCAGCA-GATCAG-3' and 5'-CTGCGCCACTACTTCCAC-3'. These primers were used to determine intronic sequences from *SCN5A* clones as described previously (Wang and Keating, 1994).

#### SSCP Analyses

Genomic DNA samples were amplified by PCR and used in SSCP analyses as described previously (Orita et al., 1989). Primer pairs used for this study are shown in Table 1. Annealing temperature was 62°C for all PCRs. Reactions (10 µl) were diluted with 50 µl of 0.1% SDS and 1 mM EDTA and 50 µl of 95% formamide dye. Diluted products were denatured by heating at 94°C for 10 min, and 5 µl of each sample was separated by electrophoresis on 10% nondenaturing polyacrylamide gels (50:1 acrylamide:bisacrylamide) at 4°C. Electrophoresis was carried out at 50 W for 2–5 hr. Gels were transferred to 3MM filter paper, dried, and exposed to X-ray film at –80°C for 12 hr.

#### Sequence Analyses of SSCP Conformers

Normal and aberrant SSCP conformers were cut directly from dried gels and eluted in 100 µl of distilled water at 65°C for 30 min. The eluted DNA (10 µl) was used as template for a second PCR using the original primer pair. Products were fractionated in 2% low melting temperature agarose gels (FMC Corporation), and DNA fragments were purified and sequenced directly by cycle sequencing (Wang and Keating, 1994). Alternatively, purified PCR products were cloned into pBluescript II SK(+) (Stratagene) using the T-vector method as described previously (Marchuk et al., 1990). Plasmid DNA samples were purified and sequenced by the dideoxy chain termination method using SequiTherm polymerase (Epicentre Technologies).

#### Acknowledgments

We thank M. Sanguinetti, T. Olson, M. Curran, and L. Jorde for their help and advice. We thank C. Jiang, B. Boak, M. Ewart, J. Stevens, H. Li, L. Bartlett, and K. Timothy for their assistance. The authors appreciate helpful discussions with R. White, M. Leppert, L. Ptacek, S. Odeberg, D. Li, and M. Frangiskakis. This work was supported by National Institutes of Health grants RO1-HL48074, RO1-HL33843, and RO1-HL51618, by Public Health Service research grant MO1-RR00064 from the National Center for Research Resources, by the Technology Access Section of the Utah Genome Center, and by the American Heart Association.

Received February 6, 1995; revised February 16, 1995.

#### References

- Antzelevitch, C., and Sicouri, S. (1994). Clinical relevance of cardiac arrhythmias generated by afterdepolarizations: role of M cells in the generation of U waves, triggered activity and *torsade de pointes*. *J. Am. Coll. Cardiol.* 23, 259–277.
- Attwell, D., Cohen, I., Eisner, D., Ohba, M., and Ojeda, C. (1979). Steady-state TTX-sensitive ("window") current in cardiac Purkinje fibres. *Pflügers Arch.* 379, 137–142.
- Bazette, H. C. (1920). An analysis of the time-relationships of electrocardiograms. *Heart* 7, 353–370.
- Chin, H., Kozak, C., Kim, H.-L., Mock, B., and McBride, O. W. (1991). A brain L-type calcium channel  $\alpha 1$  subunit gene (*CCHL1A2*) maps to mouse chromosome 14 and human chromosome 3. *Genomics* 11, 914–919.
- Curran, M. E., Splawski, I., Timothy, K. W., Vincent, G. M., Green, E. D., and Keating, M. T. (1995). A molecular basis for cardiac arrhythmia: *HERG* mutations cause long QT syndrome. *Cell* 80, this issue.
- Ebers, G. C., George, A. L., Barchi, R. L., Ting-Passador, S. S., Kallen, R. G., Lathrop, G. M., Beckman, J. S., Hahn, A. F., Brown, W. F., Campbell, R. D., and Hudson, A. J. (1991). Paramyotonia congenita and hyperkalemic periodic paralysis are linked to the adult muscle sodium channel gene. *Ann. Neurol.* 30, 810–816.
- Fontaine, B., Khurana, T. S., Hoffman, E. P., Bruns, G., Haines, J. L., Trofatter, J. A., Hanson, M. P., Rich, J., McFarlane, H., Yasek, D. M., Romano, D., Gusella, J., and Brown, R. (1990). Hyperkalemic periodic paralysis and the adult skeletal muscle sodium channel gene. *Science* 250, 1000–1002.
- Gellens, M., George, A., Chen, L., Chahine, M., Horn, R., Barchi, R., and Kallen, R. (1992). Primary structure and functional expression of the human cardiac tetrodotoxin-insensitive voltage-dependent sodium channel. *Proc. Natl. Acad. Sci. USA* 89, 554–558.
- George, A. L., Varkony, T. A., Drabkin, H. A., Han, J., Knops, J. F., Finley, W. H., Brown, G. B., Ward, D. C., and Hass, M. (1995). Assignment of the human heart tetrodotoxin-resistant voltage-gated  $\text{Na}^+$  channel  $\alpha$ -subunit gene (*SCN5A*) to band 3p21. *Cytogenet. Cell Genet.* 68, 67–70.
- Honerjager, P. (1982). Cardioactive substances that prolong the open state of sodium channels. *Rev. Physiol. Biochem. Pharmacol.* 92, 1–74.
- Jervell, A., and Lange-Nielsen, F. (1957). Congenital deaf mutism, functional heart disease with prolongation of the QT interval, and sudden death. *Am. Heart J.* 54, 59–78.
- Jiang, C., Atkinson, D., Towbin, J. A., Splawski, I., Lehmann, M. H., Li, H., Timothy, K., Taggart, R. T., Schwartz, P. J., Vincent, G. M., Moss, A. J., and Keating, M. T. (1994). Two long QT syndrome loci map to chromosomes 3 and 7 with evidence for further heterogeneity. *Nature Genet.* 8, 141–147.
- Kannel, W. B., Cupples, A., and D'Agostino, R. B. (1987). Sudden death risk in overt coronary heart diseases: the Framingham study. *Am. Heart J.* 113, 799–804.
- Keating, M. T. (1992). Linkage analysis and long QT syndrome: using genetics to study cardiovascular disease. *Circulation* 85, 1973–1986.
- Keating, M. T., Atkinson, D., Dunn, C., Timothy, K., Vincent, G. M., and Leppert, M. (1991a). Linkage of a cardiac arrhythmia, the long QT syndrome, and the Harvey *ras-1* gene. *Science* 252, 704–706.
- Keating, M. T., Atkinson, D., Dunn, C., Timothy, K., Vincent, G. M., and Leppert, M. (1991b). Consistent linkage of the long QT syndrome to the Harvey *ras-1* locus on chromosome 11. *Am. J. Hum. Genet.* 49, 1335–1339.
- Lathrop, G. M., Lalouel, J.-M., Julier, C., and Ott, J. (1985). Multilocus linkage analysis in humans: detection of linkage and estimation of recombination. *Am. J. Hum. Genet.* 37, 482–498.
- Lerche, H., Heine, R., Plika, U., George, A. L., Mitrovic, N., Browatzki, M., Weiss, T., River-Bastide, M., Franke, C., Lomonaco, M., Ricker, K., and Lehmann-Horn, F. (1993). Human sodium channel myotonia: slowed channel inactivation due to substitutions for a glycine within the III–IV linker. *J. Physiol.* 470, 13–22.
- Magovcevic, I., Ang, S.-L., Seidman, J. G., Tolman, C., Neer, E., and Mortons, C. (1992). Regional localization of the human G protein  $\alpha_2$  (*GNAI2*) gene: assignment to 3021 and a related sequence (*GNAI2L*) to 12p12-p13. *Genomics* 12, 125–129.
- Marchuk, D., Drumm, M., Saulino, A., and Collins, F. S. (1990). Construction of T-vectors, a rapid and general system for direct cloning of unmodified PCR products. *Nucl. Acids Res.* 19, 1154.
- McClatchey, A., Lin, C., Wang, J., Hoffman, E., Rojas, C., and Gusella, J. (1992a). The genomic structure of the human skeletal muscle sodium channel gene. *Hum. Mol. Genet.* 1, 521–527.
- McClatchey, A., Van den Bergh, P., Pericak-Vance, M., Raskind, W., Verellen, C., McKenna-Yasek, D., Rao, K., Haines, J. L., Bird, T., Brown, R. H., and Gusella, J. F. (1992b). Temperature-sensitive mutations in the III–IV cytoplasmic loop region of the skeletal muscle sodium channel gene in paramyotonia congenita. *Cell* 68, 769–774.
- McClatchey, A., McKenna-Yasek, D., Cros, D., Worthens, H. G., Kuncil, R. W., DeSilva, S. M., Cornblath, D. R., Guesella, J. F., and Brown, R. H. (1992c). Novel mutations in families with unusual and variable disorders of the skeletal muscle sodium channel. *Nature Genet.* 2, 148–152.
- Moss, A. J., Schwartz, P. J., Crampton, R. S., Tzivoni, D., Locati, E. H., MacCluer, J., Hall, W. J., Weitkamp, L., Vincent, G. M., Garson, A., Robinson, J. L., Benhorin, J., and Choi, S. (1991). The long QT syndrome: prospective longitudinal study of 328 families. *Circulation* 84, 1136–1144.

- Orita, M., Iwahana, H., Kanazawa, H., and Sekiya, T. (1989). Detection of polymorphisms of human DNA by gel electrophoresis as single strand conformation polymorphisms. *Proc. Natl. Acad. Sci. USA* 86, 2766-2770.
- Ptacek, L. J., George, A. L., Griggs, R. C., Tawil, R., Kallen, R. G., Barchi, R. L., Robertson, M., and Leppert, M. F. (1991). Identification of a mutation in the gene causing hyperkalemic periodic paralysis. *Cell* 67, 1021-1027.
- Ptacek, L. J., George, A. L., Barchi, R., Griggs, R., Riggs, J., Robertson, M., and Leppert, M. (1992). Mutations in an S4 segment of the adult skeletal muscle sodium channel cause paramyotonia congenita. *Neuron* 8, 891-897.
- Rojas, C., Wang, J., Schwartz, L. S., Hoffman, E. P., Powell, B. R., and Brown, R. H. (1991). A Met-to-Val mutation in the skeletal muscle Na<sup>+</sup> channel  $\alpha$ -subunit in hyperkalemic periodic paralysis. *Nature* 354, 387-389.
- Romano, C. (1965). Congenital cardiac arrhythmia. *Lancet* 1, 658-659.
- Rudolph, J. A., Spier, S. J., Byrns, G., Rojas, C. V., Bernoco, D., and Hoffman, E. P. (1992). Periodic paralysis in quarter horses: a sodium channel mutation disseminated by selective breeding. *Nature Genet.* 2, 144-147.
- Schwartz, P. J., Periti, M., and Malliani, A. (1975). The long QT syndrome. *Am. Heart J.* 109, 378-390.
- Seino, S., Yamada, Y., Espinosa, R., III, LeBeau, M., and Bell, G. (1992). Assignment of the gene encoding the  $\alpha$  subunit of the neuroendocrine/brain-type calcium channel (CACNL1A2) to human chromosome 3, band p14.3. *Genomics* 13, 1375-1377.
- Sternberg, N. (1990). Bacteriophage P1 cloning system for the isolation, amplification, and recovery of DNA fragments as large as 100 kilobase pairs. *Proc. Natl. Acad. Sci. USA* 87, 103-107.
- Stuhmer, W., Conti, F., Suzuki, H., Wang, X., Noda, M., Yahagi, N., Kubo, H., and Numa, S. (1989). Structural parts involved in activation and inactivation of the sodium channel. *Nature* 339, 597-603.
- Vincent, G. M., Timothy, K. W., Leppert, M. F., and Keating, M. T. (1992). The spectrum of symptoms and QT intervals in carriers of the gene for the long QT syndrome. *N. Engl. J. Med.* 327, 846-852.
- Wang, Q., and Keating, M. T. (1994). Isolation of P1 insert ends by direct sequencing. *Biotechniques* 17, 282-284.
- Ward, O. C. (1964). A new familial cardiac syndrome in children. *J. Ir. Med. Assoc.* 54, 103-106.
- Weinstein, L. S., Speigel, A. M., and Carter, A. D. (1988). Cloning and characterization of the human gene for the  $\alpha$ -subunit of G<sub>s</sub>, a GTP-binding signal transduction protein. *FEBS Lett.* 232, 333-340.
- West, J., Patton, D., Scheuer, T., Wang, Y., Goldin, A., and Catterall, W. (1992). A cluster of hydrophobic amino acid residues required for fast Na<sup>+</sup>-channel inactivation. *Proc. Natl. Acad. Sci. USA* 89, 10910-10914.
- Willich, S. N., Levy, D., Rocco, M. B., Toffler, G. H., Stone, P. H., and Muller, J. O. E. (1987). Circadian variation in the incidence of sudden cardiac death in the Framingham heart study population. *Am. J. Cardiol.* 60, 801-806.
- Yang, N., Ji, S., Shou, M., Ptacek, L., Barchi, R., Horn, R., and George, A. (1994). Sodium channel mutations in paramyotonia congenita exhibit similar biophysical phenotypes *in vitro*. *Proc. Natl. Acad. Sci. USA* 91, 12785-12789.
- Zipes, D. P. (1987). Proarrhythmic effects of antiarrhythmic drugs. *Am. J. Cardiol.* 59, 26E-31E.

## CHAPTER 5

### POSITIONAL CLONING OF A NOVEL POTASSIUM CHANNEL GENE: *KVLQT1* MUTATIONS CAUSE CARDIAC ARRHYTHMIAS

The following chapter is a reprint from an article coauthored by Wang, Q., Curran, M. E., Burn, T. C., Millholland, J. M., VanRaay, T. J., Shen, J., Timothy, K. W., Vincent, G. M., de Jager, T. Schwartz, P. J., Towbin, J. A., Moss, A. J., Atkinson, D. L., Landes, G. M. Connors, T. D., Keating, M. T. and me. It was originally published in Nature Genetics, volume 12, pages 17-23, January 1996 (Copyright Nature America Inc.). It is reprinted here with the permission of the coauthors and Nature America Inc.

# Positional cloning of a novel potassium channel gene: *KVLQT1* mutations cause cardiac arrhythmias

Q. Wang<sup>1,2,3,4</sup>, M.E. Curran<sup>2,3,4</sup>, I. Splawski<sup>2,3,4</sup>, T.C. Burn<sup>5</sup>, J.M. Millholland<sup>5</sup>, T.J. VanRaay<sup>5</sup>, J. Shen<sup>1,2,3,4</sup>, K.W. Timothy<sup>6</sup>, G.M. Vincent<sup>3,6</sup>, T. de Jager<sup>2,3,4,7</sup>, P.J. Schwartz<sup>8</sup>, J.A. Towbin<sup>9</sup>, A.J. Moss<sup>10</sup>, D.L. Atkinson<sup>1,2,3,4</sup>, G.M. Landes<sup>5</sup>, T.D. Connors<sup>5</sup> & M.T. Keating<sup>1,2,3,4</sup>

<sup>1</sup>Howard Hughes Medical Institute,

<sup>2</sup>Department of Human Genetics,

<sup>3</sup>Cardiology Division, and

<sup>4</sup>Eccles Institute of Human Genetics, University of Utah, Salt Lake City, Utah 84112, USA

<sup>5</sup>Department of Human Genetics, Integrated Genetics, Framingham, Massachusetts 01701, USA

<sup>6</sup>Department of Medicine, LDS Hospital, Salt Lake City, Utah 84037, USA

<sup>7</sup>US/MRC Center for Molecular and Cellular Biology, Department of Medical Physiology and Biochemistry, University of Stellenbosch Medical School, Tygerberg 7505, Republic of South Africa.

<sup>8</sup>Department of Cardiology, University of Pavia, and Policlinico S. Matteo, IFCCS, 27100 Pavia, Italy

<sup>9</sup>Department of Pediatrics and Department of Molecular and Human Genetics, Baylor College of Medicine, Houston, Texas 77030, USA

<sup>10</sup>Department of Medicine, University of Rochester Medical Center, Rochester, New York 14627, USA

Correspondence should be addressed to M.T.K.

Genetic factors contribute to the risk of sudden death from cardiac arrhythmias. Here, positional cloning methods establish *KVLQT1* as the chromosome 11-linked *LQT1* gene responsible for the most common inherited cardiac arrhythmia. *KVLQT1* is strongly expressed in the heart and encodes a protein with structural features of a voltage-gated potassium channel. *KVLQT1* mutations are present in affected members of 16 arrhythmia families, including one intragenic deletion and ten different missense mutations. These data define *KVLQT1* as a novel cardiac potassium channel gene and show that mutations in this gene cause susceptibility to ventricular tachyarrhythmias and sudden death.

Cardiac arrhythmias are a common cause of morbidity and mortality, accounting for approximately 11% of all natural deaths<sup>1,2</sup>. In general, presymptomatic diagnosis and treatment of individuals with life-threatening ventricular tachyarrhythmias is poor, and in some cases medical management actually increases the risk of arrhythmia and death<sup>3</sup>. These factors make early detection of individuals at risk for cardiac arrhythmias and arrhythmia prevention high priorities.

Both genetic and acquired factors contribute to the risk of developing cardiac arrhythmias. Long QT syndrome (LQT) is a cardiac disorder that causes abrupt loss of consciousness (syncope), seizures and sudden death, often in young, otherwise healthy people<sup>4-6</sup>. Many individuals with LQT have prolongation of the QT interval on electrocardiograms, an indication of abnormal cardiac repolarization. The clinical features of LQT result from episodic cardiac arrhythmias, specifically repolarization-related ventricular tachyarrhythmias like *torsade de pointes* and ventricular fibrillation<sup>7,8</sup>. Both inherited and acquired forms of LQT have been defined. Acquired LQT and secondary arrhythmias can result from cardiac ischemia, bradycardia and metabolic abnormalities such as low serum potassium or calcium concentrations<sup>9</sup>. LQT can also result from treatment with certain medications, including antibiotics, antihistamines, general anesthetics and, most commonly, antiarrhythmic medications<sup>9</sup>. Inherited forms of LQT can result from mutations in at least four different genes. In previous studies, we mapped LQT loci to chromosome 11p15.5 (*LQT1*)<sup>10,11</sup>, 7q35-36 (*LQT2*), and 3p21-24 (*LQT3*)<sup>12</sup>. Recently, the fourth LQT locus (*LQT4*) was mapped to

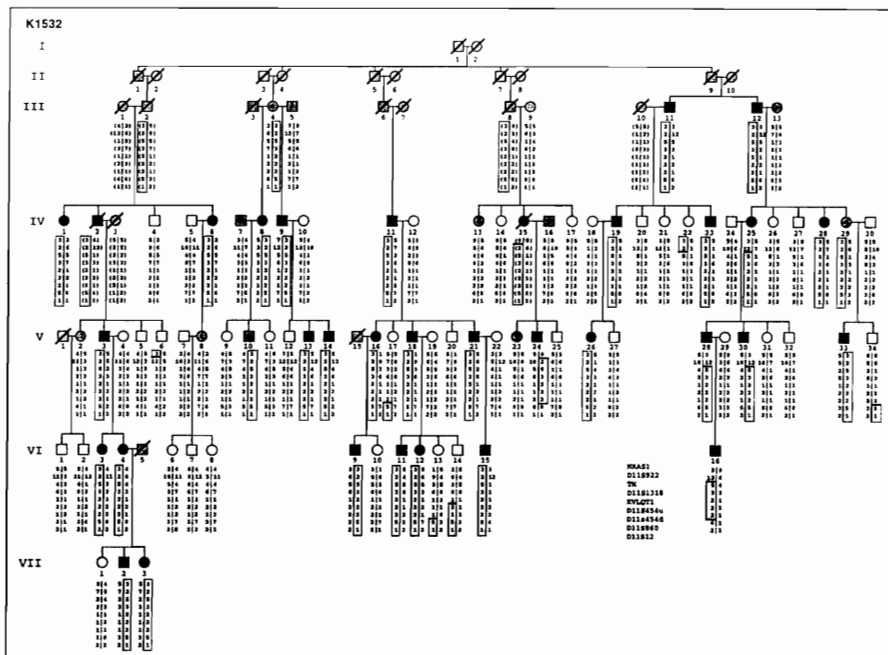
4q25-27 (ref. 13). Of these, the most common cause of inherited LQT is *LQT1*. Our data indicate that mutations in this gene are responsible for more than 50% of inherited LQT (unpublished observations).

We have used two approaches to identify genes responsible for LQT, a candidate gene approach and positional cloning. The candidate gene approach relies on mechanistic hypotheses based on physiology. Since LQT is associated with abnormal cardiac repolarization, we proposed that mutations in genes encoding cardiac ion channels, or genes that modulate ion channel function, could cause this disorder. Using the candidate gene approach, we recently discovered that mutations in a cardiac potassium channel gene (*HERG*) cause chromosome 7-linked LQT and that mutations in the cardiac sodium channel gene (*SCN5A*) cause the chromosome 3-linked form of this disorder<sup>14-18</sup>. Despite considerable effort, however, a candidate gene approach to chromosome 11-linked LQT has not been successful. Two potassium channel genes (*KCNA4* and *KCNC1*) were mapped to the short arm of chromosome 11 (ref. 19), but both were excluded as candidates for *LQT1* by linkage analyses (ref. 20; this study). All other previously characterized cardiac potassium, chloride, sodium and calcium channel genes were similarly excluded based on their chromosomal locations. In this study we used positional cloning and mutational analyses to identify *LQT1*.

## Refined genetic and physical localization of *LQT1*

To determine the precise location of *LQT1*, we performed genotypic analyses in kindred 1532 (K1532), a large Utah family of northern European descent (Fig.

Fig. 1 Pedigree structure for a portion of LQT kindred 1532. Affected individuals are shown as filled circles (females) or squares (males), unaffected individuals as empty symbols and individuals with equivocal phenotypes are stippled. Genotypes for chromosome 11 markers are indicated beneath each symbol and are shown as haplotypes. Marker order (top to bottom) is: *TEL-HRAS-D11S922-TH-D11S1318-D11S454-D11S860-D11S12*-*Cen*. The accuracy of haplotypes was ensured using genotypes from additional chromosome 11p15.5 markers (data not shown). Inferred genotypes are shown in brackets. Disease chromosomes are indicated by boxes and recombination events are indicated with solid horizontal lines. Recombination events affecting disease chromosomes occur in individuals: IV-22, IV-25, V-6, V-17, V-24, V-34, VI-13, VI-14, and VI-16. Recombination events occurring in non-disease chromosomes are not indicated. *KVLQT1* is an SSCP conformer within *KVLQT1* identified by primers 5 and 6; this conformer was only identified in K1532 and represents a disease-associated mutation (allele 2 is the mutant allele). Haplotype analyses indicate that *KVLQT1* is located between flanking markers *D11S922* and *D11S454*.



1). This kindred was used in our initial study linking the first LQT gene, *LQT1*, to chromosome 11p15.5 (refs 10, 11). Additional family members were identified and phenotyped for a total sample size of 217 individuals. We performed phenotypic determination as previously described<sup>10-12</sup>. Preliminary genotypic analyses using markers at *HRAS*, *TH*, *D11S454*, and *D11S12* included all ascertained members of K1532. These experiments identified informative branches of this family. Additional genotypic analyses were performed using three highly polymorphic markers from chromosome 11p15.5: *D11S922*, *D11S1318*, and *D11S860* (ref. 21). Genotypes and pairwise lod scores for each marker are shown in Fig. 1 and Table 1. Of these markers, *TH* and *D11S1318* were completely linked. Recombination was identified with all other

markers tested, including *HRAS*, but in each case a statistically significant positive lod score (+3 or greater) was identified. These data indicate that *LQT1* is completely linked to *TH* and *D11S1318* in this kindred and that the disease gene is located centromeric of *HRAS*.

To refine localization of *LQT1*, we performed haplotype analyses of K1532 (Fig. 1). Nine chromosomes bearing informative recombination events were identified. Telomeric recombination events were observed in unaffected individual IV-22 (between *D11S922* and *TH*), affected individual IV-25 (between *D11S922* and *TH*), unaffected individual V-6 (between *HRAS* and *D11S922*), and affected individual V-24 (between *HRAS* and *D11S922*). Centromeric recombination events were identified in unaffected individual V-17 (between *D11S860* and *D11S454*), affected individual V-24 (between *D11S860* and *D11S454*), unaffected individual V-34 (between *D11S860* and *D11S454*), unaffected individual VI-13 (between *D11S860* and *D11S454*), unaffected individual VI-14 (between *D11S454* and *D11S1318*), and affected individual VI-16 (between *D11S860* and *D11S454*). These data indicate that *LQT1* is located between *D11S922* and *D11S454*. Together with recent studies placing *LQT1* centromeric of *TH*<sup>20</sup>, these data place *LQT1* in the interval between *TH* and *D11S454*.

The size of the region containing *LQT1* was estimated using pulsed-field gel analyses with genomic probes from chromosome 11p15.5. Probes from *TH*, *D11S551*, and *D11S454* hybridized to a 700-kb *MluI* restriction fragment (Fig. 2). These data suggested that

Table 1 Pairwise lod scores between *LQT1* and 11p15.5 markers

	0.0	0.001	0.01	0.05	0.1	0.2	$Z_{max}^a$	$\theta_{max}^b$
<i>HRAS</i>	9.67	9.94	10.50	10.38	9.62	7.57	10.59	0.021
<i>D11S922</i>	10.05	13.05	13.85	13.59	12.59	10.01	13.92	0.019
<i>TH</i>	11.01	10.99	10.82	10.06	9.07	6.96	11.01	0.0
<i>D11S1318</i>	10.30	10.29	10.13	9.40	8.47	6.50	10.30	0.0
<i>KVLQT1</i>	14.19	14.17	13.94	12.89	11.54	8.68	14.19	0.0
<i>D11S454</i>	11.06	11.05	10.89	10.16	9.17	7.01	11.06	0.0
<i>D11S860</i>	5.77	6.92	8.32	9.14	8.92	7.46	9.15	0.058
<i>D11S12</i>	1.50	2.26	3.12	3.46	3.27	2.49	3.46	0.047

Lod scores were computed with the assumption of 90% penetrance and gene frequency of 0.001 (ref. 31).

<sup>a</sup> $Z_{max}$  indicates maximum lod score.

<sup>b</sup> $\theta_{max}$  indicates estimated recombination fraction at  $Z_{max}$ .

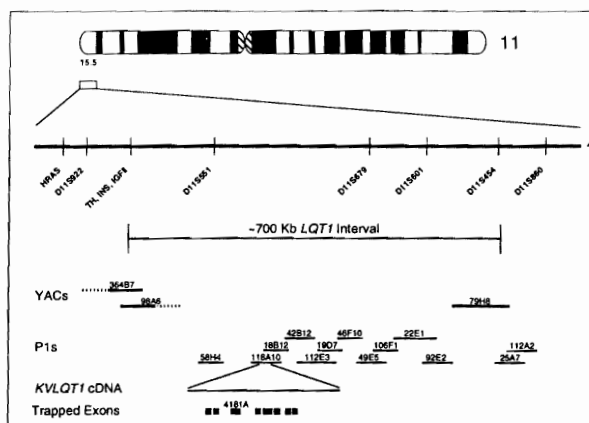


Fig. 2 Physical map of the *LQT1* region. Ideogram of chromosome 11 indicates the approximate location of *LQT1* (11p15.5). The location of polymorphic markers and some cosmids are indicated by vertical lines on the map. Refined genetic mapping places *LQT1* between *TH* and *D11S454*. The distance between *TH* and *D11S454* was estimated by pulsed field gel analyses as <700 kb. A physical map of the minimal set of overlapping YAC and P1 clones is shown. The locations of the *KVLQT1* cDNA and trapped exons are indicated. Dashed lines in YACs indicate chimaerism.

the region containing *LQT1* is less than 700 kb. Physical representation was achieved by screening yeast artificial chromosome (YAC) and P1 libraries with probes from the region<sup>22,23</sup>. The order of these clones was confirmed using fluorescent in situ hybridization

(FISH) analyses as: telomere-*TH*-*D11S551*-*D11S679*-*D11S601*-*D11S454*-centromere. The clones identified in initial experiments were then used for identification of adjacent, overlapping clones. The minimum set of clones from the *LQT1* interval is shown in Fig. 2.

#### Identification and characterization of *KVLQT1*

To identify candidate genes for *LQT1*, we performed exon amplification with clones from the physical map. DNA sequence and database analyses revealed eight possible exons with predicted amino acid sequence similarity to ion channels (Fig. 2). The highest similarity was obtained for a 238-bp trapped exon (4181A), with 53% similarity to potassium channel proteins from multiple species, including similarity to a portion of a putative pore region. PCR analyses were used to map 4181A to the short arm of chromosome 11 and to two P1s from the physical map (118A10, 18B12). These data suggested that 4181A was part of a potassium channel gene on chromosome 11p15.5.

We used two different cDNA library screening methods to determine if trapped exon 4181A was part of a gene. Traditional plaque filter hybridization with an adult human cardiac cDNA library led to the identification of a single positive clone. A variation of cDNA selection was used to screen a second cardiac cDNA library, and twelve independent clones were recovered. DNA sequence analyses revealed complete alignment with the eight trapped exons described above. The composite sequence of these cDNA clones is shown in Fig. 3a. The longest open reading frame spans 1645 bp.

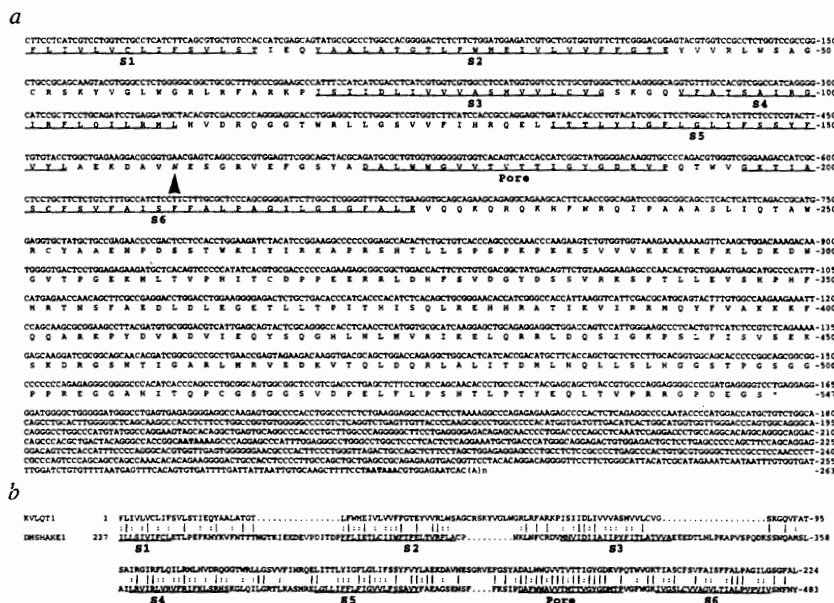


Fig. 3 Nucleotide and deduced amino acid sequences of *KVLQT1*. a, The composite sequence of *KVLQT1* is shown. Six putative transmembrane segments (S1 to S6) and a putative pore region (N160) is italicized (indicated with an arrowhead). Two consensus polyadenylation signals are indicated in bold. Composite cDNA sequences for *KVLQT1* were obtained by end sequencing of overlapping cDNA clones and by primer walking. *KVLQT1* sequences have been assigned GenBank accession number U40990. b, Alignment of the S1-S6 region of *KVLQT1* with *Drosophila* Shaker potassium channel, DMSHAKE1 (SHA; 24). Identity (I) and similarity (S) are indicated.

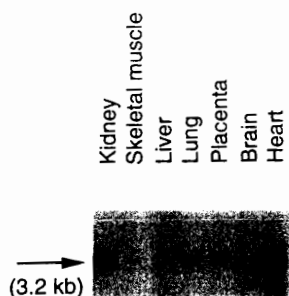


Fig. 4 Tissue expression pattern of *KVLQT1*. Northern analyses revealed a 3.2-kb *KVLQT1* mRNA in human kidney, lung, placenta, and heart, with highest levels in the heart.

Two consensus polyadenylation signals were identified upstream of the poly (A)<sup>+</sup> tail in the 3' untranslated region. The identity of the initiation codon is not yet certain.

This cDNA predicted a protein with structural characteristics of potassium channels. Hydropathy analyses suggested a topology of six major hydrophobic regions that may represent membrane-spanning  $\alpha$ -helices. These regions share sequence similarity with potassium channel transmembrane domains S1–S6. A comparison of the predicted amino acid sequence derived from the identified gene and the Shaker (SHA) potassium channel<sup>24</sup> is shown in Fig. 3b. In the region

containing S1–S6, the amino acid sequence identity was 30% and similarity was 59%. The sequence located 3' of S1–S6 did not have significant similarity to any known protein. Because this gene has high similarity to voltage-gated potassium channel genes and became a strong candidate for *LQT1*, we named it *KVLQT1*.

Northern blot analyses were used to determine the tissue distribution of *KVLQT1* mRNA. *KVLQT1* cDNA probes detected a 3.2-kb transcript in human heart, kidney, lung, and placenta, but not in skeletal muscle, liver, or brain (Fig. 4). The heart showed highest levels of *KVLQT1* mRNA.

Table 2 PCR primers used to define *KVLQT1* mutations

Primer	Sequence	Region amplified
1	GAGATCGTGCTGGTGGTGTCT	S2–S3
2	CTTCTGGTCTGGAAACCTGG	
3	CTCTCCCTGGGGCCCTGGC	S3–S4
4	TGCGGGGAGCTTGTGGCACAG	
5	GGGATCCGCTTCTGTCAGA	S4
6	CTGGGCCCTACCTAACCC	
7	TCCTGGAGCCCGAACTGTGTGT	S5–Pore
8	TGTCTGCCCACTCCTCAGCCT	
9	CCCCAGACCCAGCTGTCCAA	Pore–S6
10	AGGCTGACCACTGTCCCTCT	
11	GCTGGCAGTGGCTGTGTGGA	S6
12	AACAGTGACCAAAATGACAGTGAC	

### *KVLQT1* in six large families

To test the hypothesis that *KVLQT1* is *LQT1*, we used single-strand conformational polymorphism (SSCP) analyses to screen for functional mutations in affected members of K1532, the largest LQT family that showed linkage to chromosome 11. We focused our analyses on the region between S2 and S6 since these regions might be important for *KVLQT1* function. We designed oligonucleotide primers based on cDNA sequences and used these primers for cycle sequencing reactions with the *KVLQT1*-containing P1, 18B12 (ref. 25). These experiments defined intronic sequences flanking exons encoding S2–S6. Additional primers were then generated from these intronic sequences and used for SSCP analyses (Table 2).

SSCP analyses identified an anomalous conformer in the 70 affected members of K1532 (Fig. 5). This aberrant conformer was not observed in the 147 unaffected members of this kindred or in genomic DNA from more than 200 unrelated control individuals (data not shown). The two-point lod score for linkage between this anomaly and LQT was 14.19 at a recombination fraction of 0 (Table 1). No recombination was observed between *KVLQT1* and *LQT1*, indicating that these loci are completely linked. DNA sequence analyses of the normal and aberrant SSCP conformers revealed a single base substitution, a G to A transition, at the first nucleotide of codon Val125 (Fig. 5; Table 3). This mutation results in a valine to methionine substitution in the predicted intracellular domain between S4 and S5.

To further test the hypothesis that mutations in *KVLQT1* cause LQT, DNA samples from affected members of five additional large LQT kindreds were studied. Linkage analyses with polymorphic markers from this region had shown that the disease phenotype was linked to chromosome 11 in these families (data not shown). Aberrant SSCP conformers were

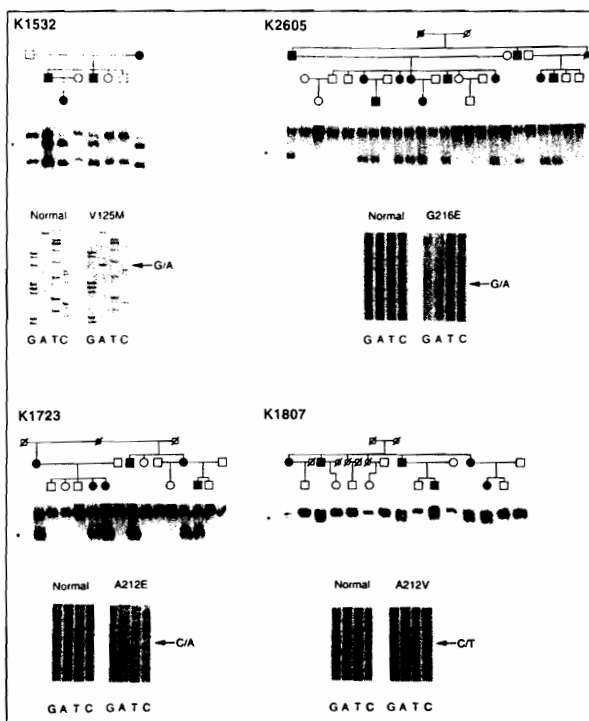


Fig. 5 *KVLQT1* missense mutations cosegregate with LQT in kindreds K1532, K1723, K2605, and K1807. The results of SSCP analyses with primer pair 5–6 (K1532), primer pair 9–10 (K1723, K1807), and primer pair 11–12 (K2605) are shown below each pedigree. Aberrant SSCP conformers (indicated by \*) cosegregate with LQT in each kindred. For K1532, only eight of the 217 individuals are shown; the results of SSCP analyses in additional members of K1532 are shown in Fig. 1 (*KVLQT1* allele 2). Because aberrant SSCP conformers cosegregating with LQT in K161 and K162 were identical to the aberrant conformer defined in K1807, results for these kindreds are not shown. Results of DNA sequence analyses of the normal (left) and aberrant conformers (right) are shown below each pedigree.

Table 3 Summary of *KVLQT1* mutations

Codon	Nucleotide change	Coding effect	Mutation	Region	Kindred	Number of affected
38-39	ΔTCG	Deletion	F38W/G39Δ	S2	K13216	1
49	GCC to CCC	Missense	A49P	S2-S3	K13119	1
60	GGG to AGG	Missense	G60R	S2-S3	K2557	3
61	CGG to CAG	Missense	R61Q	S2-S3	K15019	2
125	GTG to ATG	Missense	V125M	S4-S5	K1532	70
144	CTC to TTC	Missense	L144F	S5	K1777	2
177	GGG to AGG	Missense	G177R	Pore	K20926	1
183	ACC to ATC	Missense	T183I	Pore	K20925	1
212	GCG to GAG	Missense	A212E	S6	K1723	6
212	GCG to GAG	Missense	A212E	S6	K2050	2
212	GCG to GTG	Missense	A212V	S6	K1807	6
212	GCG to GTG	Missense	A212V	S6	K161	18
212	GCG to GTG	Missense	A212V	S6	K162	18
212	GCG to GTG	Missense	A212V	S6	K163	3
212	GCG to GTG	Missense	A212V	S6	K164	2
216	GCG to GAG	Missense	G216E	S6	K2605	11

identified in affected members of K1723, K2605, K1807 (Fig. 5), K161 and K162 (data not shown). The SSCP anomalies identified in K161 and K162 were identical to that observed in K1807. The aberrant SSCP conformer was not seen in unaffected members of these kindreds or in DNA samples from more than 200 unrelated control individuals (Fig. 5; data not shown). The normal and aberrant conformers identified in each family were sequenced. The nucleotide change, coding effect, and location of each mutation are summarized in Table 3.

#### *KVLQT1* mutations in small LQT families

To identify additional LQT-associated mutations in *KVLQT1*, we continued SSCP analyses in small kindreds and sporadic cases. SSCP revealed an aberrant conformer in kindred 13216 (Fig. 6). Analyses of more than 200 unrelated control individuals failed to show this anomaly (data not shown). This aberrant conformer was cloned and sequenced, revealing a three base pair deletion encompassing codons 38 and 39. This mutation results in a phenylalanine to tryptophan

substitution and deletion of a glycine in the putative S2 domain (Table 3).

Aberrant SSCP conformers were identified in affected members of nine additional kindreds: K1777, K20925, K2557, K13119, K20926, K15019 (Fig. 6), K2050, K163, and K164 (data not shown). An aberrant SSCP conformer identified in K2050 was identical to that in K1723, and aberrant conformers identified in K163 and K164 were identical to that observed in K1807. None of the aberrant conformers were identified in DNA samples from more than 200 control individuals (data not shown). In each

case, the normal and aberrant conformers were sequenced (Fig. 6; Table 3). In total, we identified *KVLQT1* mutations associated with LQT in 16 families or sporadic cases (Fig. 7), providing strong molecular genetic evidence that mutations in *KVLQT1* cause the chromosome 11-linked form of LQT.

#### Discussion

In this study we used positional cloning methods to identify a novel gene for chromosome 11-linked LQT, *KVLQT1*. The function of *KVLQT1* protein, however, and the mechanism of chromosome-11 linked LQT, are not yet certain. Our molecular genetic analyses suggest that *KVLQT1* encodes a voltage-gated potassium channel with functional importance in cardiac repolarization. If correct, the mechanism of chromosome 11-linked LQT probably involves reduced repolarizing *KVLQT1* current. Since potassium channels with six transmembrane domains are thought to be formed from homo- or hetero-tetramers<sup>26-28</sup>, it is possible that LQT-associated mutations of *KVLQT1* act through a dominant-negative mechanism. The type and location of *KVLQT1* mutations described here are consistent with this hypothesis. The resultant suppression of potassium channel function, in turn, would likely lead to abnormal cardiac repolarization and increased risk of ventricular tachyarrhythmias.

In recent studies, we used candidate gene approaches to define

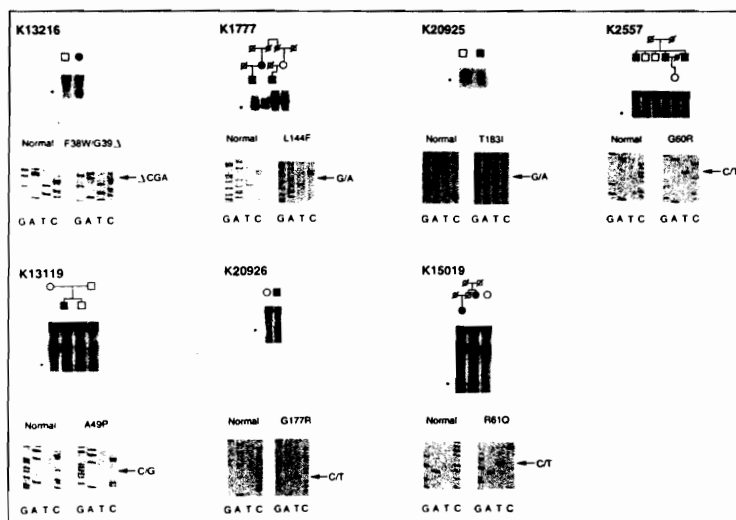


Fig. 6 *KVLQT1* intragenic deletions and missense mutations associated with LQT in kindreds K13216, K1777, K20925, K2557, K13119, K20926, and K15019. The results of SSCP analyses with primer pair 1-2 (K13216, K2557, K13119, K15019), primer pair 7-8 (K1777, K20926), and primer pair 9-10 (K20925) are shown below each pedigree. Because aberrant SSCP conformers cosegregating with LQT in K2050, K163, and K164 were identical to the aberrant conformers defined in K1723 and K1807, results for these kindreds are not shown. Results of DNA sequence analyses of the normal (left) and aberrant (right) conformers are shown below each pedigree. Sequences shown are on the antisense strand.



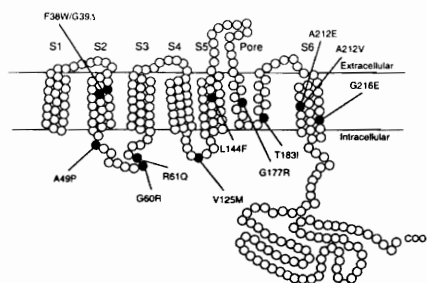


Fig. 7 Schematic representation of the predicted topology of KVLQT1 protein and location of KVLQT1 mutations.

two additional LQT genes. The chromosome 7-linked form of LQT results from mutations in a cardiac potassium channel gene, *HERG*<sup>14-16</sup>, and chromosome 3-linked LQT results from mutations in the cardiac sodium channel gene, *SCN5A*<sup>17,18</sup>. Current data indicate that *LQT1* accounts for more than 50% of inherited LQT, and that these three LQT genes account for most inherited cardiac arrhythmias. Positional cloning of *KVLQT1*, therefore, forms the foundation for genetic testing and presymptomatic diagnosis. Genetic testing and improved mechanistic understanding of LQT provide the opportunity for prevention of life-threatening arrhythmias through rational therapies. It is possible, for example, that potassium channel opening agents will reduce the risk of arrhythmias in patients with *KVLQT1* or *HERG* mutations; sodium channel blocking agents, by contrast, may be a more effective treatment for patients with mutations that alter the function of *SCN5A*<sup>29</sup>. Finally, these studies may provide insight into mechanisms underlying common arrhythmias, as these arrhythmias are often associated with abnormal cardiac repolarization and may result from a combination of inherited and acquired factors.

In summary, we have discovered a novel gene, *KVLQT1*, and conclude that mutations in this gene cause chromosome 11-linked LQT. The data supporting this conclusion are: i) *LQT1* maps to a 700-kb interval of chromosome 11p15.5 between flanking genetic markers *TH* and *D11S454*; ii) *KVLQT1* was cloned from physical reagents that map between these flanking markers; iii) a polymorphism within *KVLQT1* is completely linked to LQT in a large family; iv) mutations of *KVLQT1* cosegregate with the disease in six large families and are associated with LQT in ten small families or sporadic cases; v) *KVLQT1* is expressed at a high level in the heart; and vi) *KVLQT1* encodes a protein with sequence similarity to potassium channels. The function of *KVLQT1* protein, and the consequences of LQT-associated mutations, are not yet known, but these mutations likely cause abnormal ventricular repolarization and susceptibility to arrhythmias. Thus, these data indicate that *KVLQT1* is *LQT1*. Together with our previous discoveries implicating *HERG* and *SCN5A* in the pathogenesis of LQT, our work establishes that mutations in cardiac ion channel genes contribute to the risk of developing life-threatening cardiac arrhythmias.

## Methods

**Identifying and phenotyping LQT patients.** LQT patients were identified from medical clinics throughout North America and Europe. Informed consent was obtained from all participants or their guardians, in accordance with standards established by local institutional review boards. Two factors were considered for phenotyping: 1) historical data (the presence of syncope, the number of syncopal episodes, the presence of seizures, the age of onset of symptoms, and the occurrence of sudden death); and 2) the QT interval on electrocardiograms corrected for heart rate (QTc). To avoid misclassifying individuals, we took the same conservative approach to phenotypic assignment that was successful in our previous studies<sup>10-12</sup>. Individuals without symptoms and with a QTc of 0.41 s or less were classified as unaffected. Symptomatic individuals with QTc of 0.45 s or greater and asymptomatic individuals with a QTc of 0.47 s or greater were considered affected. Symptomatic individuals with QTc of 0.44 s or less and asymptomatic individuals with QTc between 0.41 and 0.47 s were classified as uncertain.

**Genotyping and linkage analyses.** Genomic DNA was prepared from peripheral blood lymphocytes or cell lines derived from Epstein-Barr virus transformed lymphocytes using standard procedures<sup>30</sup>. For genotypic analyses, we used four small tandem repeat (STR) polymorphisms that were previously mapped to chromosome 11p15.5: *D11S922*, *TH*, *D11S1318*, and *D11S860* (ref. 21). Amplification of each STR was carried out as previously described<sup>12</sup>. Genotyping of RFLP markers (*HRAS1*, *D11S454*, and *D11S12*) was performed as previously described<sup>10</sup>.

Pairwise linkage analyses was performed using MLINK in LINKAGE v5.1 (ref. 31). As in our previous studies, penetrance was set at 0.90 and the *LQT1* gene frequency of 0.001 was assumed to be equal between males and females<sup>10-12</sup>. STR allele frequencies were set at 1/n.

**Physical mapping.** Primers were designed based on sequences from *TH-INS-IGFII* and *D11S454* loci and used to identify and isolate clones from CEPH YAC libraries using the PCR based technique<sup>32,33</sup>. YAC terminal sequences were determined by inverse PCR as described<sup>34</sup> and used as STSs.

P1 clones were isolated using single copy probes from previously identified cosmid cosQW22 (this study), cC111-469 (*D11S679*), cC111-385 (*D11S551*), cC111-565 (*D11S601*), cC111-237 (*D11S454*)<sup>22,23,35</sup>. Newly isolated P1s were mapped to chromosome 11p15 by FISH or Southern analyses. End-specific riboprobes were generated from newly isolated P1s and used to identify additional adjacent clones (Riboprobe Gemini Core System Kit; Promega). DNA for P1 and cosmid clones was prepared using alkaline lysis plasmid isolation and purified by equilibrium centrifugation in CsCl-ethidium bromide gradients as described<sup>36</sup>. P1 insert end sequences were determined by cycle sequencing as described<sup>25</sup>. STSs were generated based on these insert end sequences. Overlap between P1s and cosmids was calculated by summing the restriction fragments in common.

**Exon trapping.** Exon trapping was performed using pSPL3B (ref. 37) on genomic P1 clones as previously described<sup>38,39</sup>. A minimum of 128 trapped exons from each P1 clone were initially characterized by sizing the PCR products. From these, 400 clones were further analysed by dideoxy sequencing using an A.L.F. automated sequencer (Pharmacia).

**Isolation and characterization of *KVLQT1* clones.** An adult human cardiac cDNA library (Stratagene) was plated, and  $1 \times 10^6$  plaques were screened using trapped exon 4181A as the probe. Sequences of trapped exon 4181A were used to design oligonucleotide probes for cDNA library screening. The GENETRAPP<sup>TM</sup> cDNA Positive Selection System was used to screen  $1 \times 10^{11}$  clones from a human heart cDNA library (Life

Technologies, Inc.). The sequence of the capture and repair oligonucleotides were 5'-CAGATCCTGAGGATGCT-3' and 5'-GTACCTGGCTGAGAAGG-3'.

Composite cDNA sequences for *KVLQT1* were obtained by end-sequencing of overlapping cDNA clones and by primer walking. Sequencing was performed either automatically, using Pharmacia A.L.F. automated sequencers, or manually, using a Sequenase Version 2.0 DNA Sequencing Kit (United States Biochemical, Inc.). Database analyses and sequence analyses were carried out using the GCG software package, IG software package, and the BLAST network service from the National Center for Biotechnology Information.

The partial genomic structure (from transmembrane domain S2 to S6) of *KVLQT1* was determined by cycle sequencing of P1 18B12 as described<sup>25</sup>. Primers were designed based on *KVLQT1* cDNA sequence and used for cycle sequencing.

**Mutation analyses.** SSCP was carried out as previously described<sup>17,18</sup>. Normal and aberrant SSCP products were isolated sequenced directly as described<sup>25</sup> or subcloned into pBluescript (SK+; Stratagene) using the T-vector method<sup>40</sup>. When the latter method was used, several clones were sequenced by the dideoxy chain termination method using Sequenase™ Version 2.0 (United States Biochemicals, Inc.).

**Northern analyses.** A multiple tissue northern filter (Human MTN blot 1, Clontech) was probed with <sup>32</sup>P-labelled *KVLQT1* cDNA probes as previously described<sup>14</sup>.

## Acknowledgments

We thank the members of LQT families for their participation in this study. We thank P. Brink, V. Corfield, C. Corbett, K. Badenhurst, M. Greenberg, J. Shea, and M. Schaffer for their help with LQT kindreds; M. Sanguinetti, R. White, J. Mason, R. Gesteland, L. Ptacek, T. Olson, S. Odelberg, D. Li, L. Urness, L. Bartlett, R. Weiss, J. Stevens, B. Boak, A. Ewart, P. Arneson, Z. Li, M. Leppert, P. Guicheney, and M. Lehmann for their help and advice; Y. Nakamura for providing cosmid cC111-237, cC111-385, cC111-469, cC111-565; and C. Jones for providing J1-5 and J1-7 hybrids. This work was supported by the NHLBI R01 HL48074, SCOR Grant HL53773, the PHS Grant M01 RR00064, the Technology Access Section of the Utah Genome Center, and the American Heart Association.

Received 31 October; accepted 28 November 1995.

- Kannel, W.B., Cupples, A. & D'Agostino, R.B. Sudden death risk in overt coronary heart diseases: the Framingham study. *Am. Heart J.* 113, 799-804 (1987).
- Willich, S.N. et al. Circadian variation in the incidence of sudden cardiac death in the Framingham heart study population. *Am. J. Cardiol.* 60, 801-806 (1987).
- The Cardiac Arrhythmia Suppression Trial II Investigators. Effect of the antiarrhythmic agent moricizine on survival after myocardial infarction. *N. Engl. J. Med.* 327, 227-233 (1992).
- Jervell, A. & Lange-Nielsen, F. Congenital deaf mutism, functional heart disease with prolongation of the QT interval, and sudden death. *Am. Heart J.* 54, 59-78 (1957).
- Romano, C. Congenital cardiac arrhythmias. *Lancet* 1, 658 (1965).
- Ward, O.C. A new familial cardiac syndrome in children. *J. Ir. Med. Assoc.* 54, 103-106 (1964).
- Schwartz, P.J., Periti, M. & Malliani, A. The long QT syndrome. *Am. Heart J.* 109, 378-390 (1975).
- Moss, A.J. & McDonald, J. Unilateral cervicothoracic sympathetic ganglionectomy for the treatment of long QT interval syndrome. *N. Engl. J. Med.* 285, 903-904 (1970).
- Zipes, D.P. Proarrhythmic effects of antiarrhythmic drugs. *Am. J. Cardiol.* 59, 26E-31E (1987).
- Keating, M.T. et al. Linkage of a cardiac arrhythmia, the long QT syndrome, and the Harvey-ras-1 gene. *Science* 252, 704-706 (1991).
- Keating, M.T. et al. Consistent linkage of the long QT syndrome to the Harvey-ras-1 locus on chromosome 11. *Am. J. Hum. Genet.* 49, 1335-1339 (1991).
- Jiang, C. et al. Two long QT syndrome loci map to chromosomes 3 and 7 with evidence for further heterogeneity. *Nature Genet.* 6, 141-147 (1994).
- Schott, J. et al. Mapping of a gene for long QT syndrome to chromosome 4q25-27. *Am. J. Hum. Genet.* 57, 1114-1122 (1995).
- Curran, M.E. et al. A molecular basis for cardiac arrhythmia: *HERG* mutations cause long QT syndrome. *Cell* 80, 795-803.
- Sanguinetti, M.C., Jiang, C., Curran, M.E. & Keating, M.T. A mechanistic link between an inherited and an acquired cardiac arrhythmia: *HERG* encodes the  $I_{Kr}$  potassium channel. *Cell* 81, 299-307 (1995).
- Trudeau, M.C., Warmke, J., Ganetzky, B. & Robertson, G. *HERG*, a human inward rectifier in the voltage-gated potassium channel family. *Science* 269, 92-95 (1995).
- Wang, Q. et al. *SCN5A* mutations associated with an inherited cardiac arrhythmia, long QT syndrome. *Cell* 80, 805-811 (1995).
- Wang, Q. et al. Cardiac sodium channel mutations in patients with long QT syndrome, an inherited cardiac arrhythmia. *Hum. Mol. Genet.* 4, 1603-1607 (1995).
- Wymore, R.S. et al. Genomic organization, nucleotide sequence, biophysical properties, and localization of the voltage-gated  $K^+$  channel gene *KCNA4/Kv1.4* to mouse chromosome 2/human 11p14 and mapping of *KCNC1/Kv3.1* to mouse 7/human 11p14.3-p15.2 and *KCNA1/Kv1.1* to human 12p13. *Genomics* 20, 191-202 (1994).
- Russell, M.W. et al. Localization of Romano-Ward long QT syndrome gene, *LQT1*, to the interval between tyrosine hydroxylase (*TH*) and *D11S1349*. *Am. J. Hum. Genet.* 57, 503-507 (1995).
- Gyspary, G. et al. The 1993-94 G  n  thon human genetic linkage map. *Nature Genet.* 7, 246-339 (1994).
- Tanigami, A. et al. Mapping of 262 DNA markers into 24 intervals on human chromosome 11. *Am. J. Hum. Genet.* 50, 56-64 (1992).
- Tokino, T. et al. Isolation and mapping of 62 new RFLP markers on human chromosome 11. *Am. J. Hum. Genet.* 48, 258-268 (1991).
- Pongs, O. et al. *Shaker* encodes a family of putative potassium channel proteins in the nervous system of *Drosophila*. *EMBO J.* 7, 1087-1095 (1988).
- Wang, Q. & Keating, M.T. Isolation of P1 insert ends by direct sequencing. *BioTechniques* 17, 282-284 (1994).
- MacKinnon, R. Determination of the subunit stoichiometry of a voltage-activated potassium channel. *Nature* 350, 232-235 (1991).
- MacKinnon, R., Aldrich, R.W. & Lee, A.W. Functional stoichiometry of shaker potassium channel inactivation. *Science* 262, 757-759 (1993).
- Covarrubias, M., Wei, A. & Sakoff, L. *Shaker*, *shal*, *shab*, and *shaw* express independent  $K^+$  current systems. *Neuron* 7, 763-773 (1991).
- Schwartz, P. et al. Long QT syndrome patients with mutations of the *SCN5A* and *HERG* genes have differential responses to  $Na^+$  channel blockade and to increases in heart rate. Implications for gene-specific therapy. *Circulation* (in press).
- Anderson, M.A. & Gusella, J.K. Use of cyclosporin A in establishing Epstein-Barr virus-transformed human lymphoblastoid cell lines. *In Vitro* 20, 656-658 (1984).
- Lathrop, G.M., Lalouel, J.-M., Julier, C. & Ott, J. Multilocus linkage analysis in humans: detection of linkage and estimation of recombination. *Am. J. Hum. Genet.* 37, 482-498 (1985).
- Green, E.D. & Olson, M.V. Systematic screening of yeast artificial-chromosome libraries by use of the polymerase chain reaction. *Proc. Natl. Acad. Sci. USA* 87, 1213-1217 (1990).
- Kwiatkowski, T.J., Zoghbi, H.Y., Ledbetter, S.A., Ellison, K.A. & Chinault, A.C. Rapid identification of yeast artificial chromosome clones by matrix pooling and crude lysate PCR. *Nucl. Acids Res.* 17, 7191-7192 (1990).
- Ochman, H., Gerber, A.S. & Hartl, D.L. Genetic application of an inverse polymerase chain reaction. *Genetics* 120, 621-623 (1988).
- Sternberg, N. Bacteriophage P1 cloning system for the isolation, amplification, and recovery of DNA fragments as large as 100 kilobase pairs. *Proc. Natl. Acad. Sci. USA* 87, 103-107 (1990).
- Sambrook, J., Fritsch, E.F. & Maniatis, T. *Molecular Cloning: A Laboratory Manual*. Second Edition. (Cold Spring Harbor Laboratory Press, New York, 1989).
- Burn, T.C., Connors, T.D., Klinger, K.W. & Landes, G.M. Increased exon trapping efficiencies through modifications to the pSPL3 splicing vector. *Gene* 161, 183-187 (1995).
- Buckler, A.J. et al. Exon amplification: a strategy to isolate mammalian genes based on RNA splicing. *Proc. Natl. Acad. Sci. USA* 88, 4005-4009 (1991).
- Church, D.M. et al. Isolation of genes from complex sources of mammalian genomic DNA using exon amplification. *Nature Genet.* 6, 98-104 (1994).
- Marchuk, D., Drumm, M., Saulino, A. & Collins, F.S. Construction of T-vectors, a rapid and general system for direct cloning of unmodified PCR products. *Nucl. Acids Res.* 19, 1154 (1990).

## CHAPTER 6

### MUTATIONS IN THE HMINK GENE CAUSE LONG QT SYNDROME AND SUPPRESS $I_{Ks}$ FUNCTION

The following chapter is a reprint from an article coauthored by Tristani-Firouzi, M., Lehmann, M. H., Sanguinetti, M. C., Keating, M. T. and me. It was originally published in Nature Genetics, volume 17, pages 338-340, November 1997 (Copyright Nature America Inc.). It is reprinted here with the permission of the coauthors and Nature America Inc.

# Mutations in the hminK gene cause long QT syndrome and suppress $I_{Ks}$ function

Igor Splawski<sup>1</sup>, Martin Tristani-Firouzi<sup>2</sup>, Michael H. Lehmann<sup>6</sup>, Michael C. Sanguinetti<sup>3,4</sup> & Mark T. Keating<sup>1,2,4,5</sup>

Ion-channel  $\beta$ -subunits are ancillary proteins that co-assemble with  $\alpha$ -subunits to modulate the gating kinetics and enhance stability of multimeric channel complexes<sup>1,2</sup>. Despite their functional importance, dysfunction of potassium-channel  $\beta$ -subunits has not been associated with disease. Recent physiological studies suggest that *KCNE1* encodes  $\beta$ -subunits (hminK) that co-assemble with KvLQT1  $\alpha$ -subunits to form the slowly activating delayed rectifier  $K^+$  ( $I_{Ks}$ ) channel<sup>3,4</sup>. Because *KVLQT1* mutations cause arrhythmia susceptibility in the long QT syndrome (LQT)<sup>5-7</sup>, we hypothesized that mutations in *KCNE1* also cause this disorder. Here, we define *KCNE1* missense mutations in affected members of two LQT families. Both mutations (S74L, D76N) reduced  $I_{Ks}$  by shifting the voltage dependence of activation and accelerating channel deactivation. D76N hminK also had a strong dominant-negative effect. The functional consequences of these mutations would be delayed cardiac repolarization and an increased risk of arrhythmia. This is the first description of *KCNE1* as an LQT gene and confirms that hminK is an integral protein of the  $I_{Ks}$  channel.

We ascertained and phenotypically characterized individuals with LQT<sup>8,9</sup>. Single-strand conformation polymorphism (SSCP) analyses using primers that span *KCNE1* led to the identification of an anomalous conformer in affected members of kindred 1789 (Fig. 1a). This conformer was not observed in unaffected family members or in 200 unrelated control individuals (400 chromosomes). DNA sequence analysis revealed a G→A transition at the first nucleotide of codon 76, causing an Asp→Asn substitution (D76N, Fig. 1c).

Further SSCP analyses defined a second anomaly that co-segregated with the disease in kindred 1754 (Fig. 1b). This anomaly was not observed in unaffected members of the family or in 200

controls. DNA sequence analysis revealed a C→T transition in the second nucleotide of codon 74, leading to substitution of Ser for Leu (S74L, Fig. 1c). Analyses of DNA samples obtained from 280 unrelated individuals with LQT failed to reveal additional *KCNE1* mutations.

To determine the functional consequences of these *KCNE1* mutations, we expressed mutant and wild-type proteins in *Xenopus* oocytes. Because the stoichiometry of KvLQT1 and hminK interaction is not known, varying amounts of *KCNE1* cRNA (0.01–2.5 ng/oocyte) were co-injected with a fixed quantity of *KVLQT1* cRNA (6 ng/oocyte) and the resultant currents recorded.  $I_{Ks}$  amplitude increased as a function of injected *KCNE1*, and saturated at *KCNE1* cRNA levels of at least 0.6 ng/oocyte (Fig. 2). Subsequent co-expression experiments were performed with 1.2 ng/oocyte *KCNE1* and 6 ng/oocyte *KVLQT1* cRNA, to ensure that *KCNE1* was not a limiting factor for expression of heteromultimeric channels.

Co-injection of D76N *KCNE1* and *KVLQT1* cRNA failed to induce detectable  $K^+$  currents ( $n=13$ , data not shown). Because LQT is inherited as an autosomal-dominant trait, affected individuals possess one normal and one mutant *KCNE1* allele. Therefore, we co-injected mutant *KCNE1* cRNA with wild-type *KCNE1* and *KVLQT1* cRNA. The current ( $I_{Ks-D76N}$ ) induced by co-injection of D76N *KCNE1* (0.6 ng/oocyte), wild-type *KCNE1* (0.6 ng/oocyte) and *KVLQT1* cRNA (6 ng/oocyte) was 91% smaller than the current ( $I_{Ks-WT}$ ) induced by wild-type *KCNE1* (1.2 ng/oocyte) and *KVLQT1* (6 ng/oocyte) cRNA at +40 mV (Fig. 3a,b). These data indicate that D76N hminK subunits form heteromultimeric channels with wild-type hminK and KvLQT1, and reduce  $I_{Ks}$  by a strong dominant-negative mechanism.

To compare the biophysical properties of wild-type and mutant

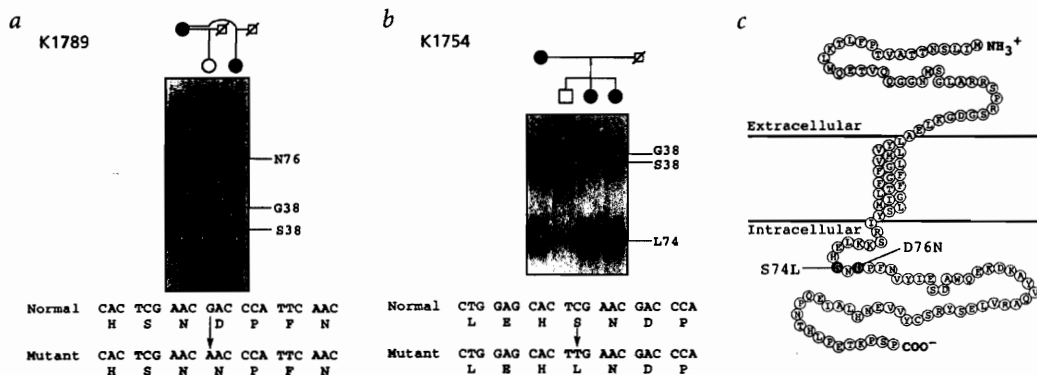


**Fig. 1** *KCNE1* mutations associated with LQT. Pedigree structure for LQT kindreds 1789 (**a**) and 1754 (**b**). Affected individuals are indicated by filled circles (females) or squares (males). Unaffected individuals are indicated by open symbols. Deceased individuals are identified by a slash. Aberrant SSCP conformers that co-segregate with the disease are shown below each pedigree. A common polymorphism (G38S) that is not related to LQT is also detected by these primers. The effect of mutations on hminK protein sequence is indicated. **c**, Schematic representation of hminK protein showing the location of LQT-associated mutations.

<sup>1</sup>Department of Human Genetics, <sup>2</sup>Department of Pediatrics, <sup>3</sup>Eccles Program in Human Molecular Biology and Genetics, <sup>4</sup>Department of Medicine and Division of Cardiology, <sup>5</sup>Howard Hughes Medical Institute, University of Utah, Salt Lake City, Utah 84112, USA. <sup>6</sup>Arrhythmia Center, Sinai Hospital, Detroit, Michigan 48235, USA. I.S. and M.T.-F. contributed equally to this work. Correspondence should be addressed to M.T.K.

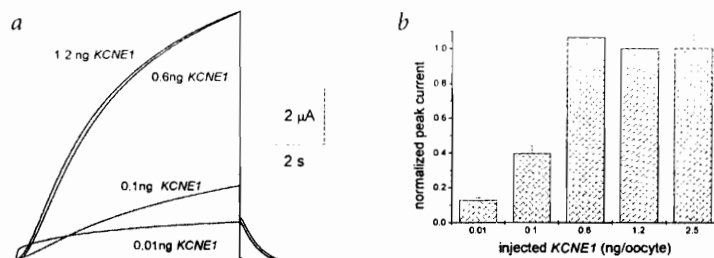


**Fig. 2** Magnitude of  $I_{Ks}$  varies as a function of injected *KCNE1* cRNA. **a**, Representative current tracings elicited by 7.5-s pulses to +40 mV following injection of oocytes with 6 ng/oocyte *KVLQT1* and a variable amount of *KCNE1* cRNA, as indicated. Note the presence of *KVLQT1* current and the absence of  $I_{Ks}$  with 0.01 ng *KCNE1*/oocyte. **b**, Current amplitude following a 7.5-s pulse to +40 mV was normalized to peak current obtained by injection of 1.2 ng *KCNE1*. Values represent mean  $\pm$  S.E.M.  $N=8$  oocytes/group.

channels, we characterized the voltage dependence of activation and the kinetics of deactivation for  $I_{Ks-D76N}$  and  $I_{Ks-WT}$ . The magnitude of  $I_{Ks}$  does not reach steady state even when elicited with pulses of 100 seconds' duration<sup>10</sup>. Therefore, tail current amplitude following 7.5-second test pulses was used as an empirical measure of the voltage dependence of  $I_{Ks}$ .  $I_{Ks-D76N}$  tail currents were half maximal at +28 mV, a +16 mV shift relative to  $I_{Ks-WT}$  (Fig. 3c). A shift in channel gating was confirmed by the voltage dependence of current deactivation. The rate of  $I_{Ks-D76N}$  channel closure (deactivation) was faster than  $I_{Ks-WT}$  at voltages of at least -80 mV (Fig. 3d). The voltage dependence of the time constants of deactivation were shifted by approximately +30 mV. Thus, D76N hminK reduces  $I_{Ks}$  by three mechanisms: a dominant-negative suppression of channel function, an increased rate of channel deactivation and a positive shift in the voltage dependence of channel activation. These effects would reduce outward current during the repolarization phase and lengthen the duration of a cardiac action potential.

Unlike D76N hminK, S74L hminK formed  $I_{Ks}$  channels when co-expressed with *KvLQT1*, albeit with altered function. Current induced by injection with S74L *KCNE1* (1.2 ng/oocyte) and *KVLQT1* (6.0 ng/oocyte) cRNA had a threshold for activation that was approximately 40 mV higher than  $I_{Ks-WT}$ . The resultant current was 66% smaller than  $I_{Ks-WT}$  after 7.5-second pulses to +60 mV ( $n=15$ , data not shown). When S74L *KCNE1* (0.6 ng/oocyte) and wild-type *KCNE1* (0.6 ng/oocyte) were co-injected with *KVLQT1* (6.0 ng/oocyte) cRNA, the resultant current ( $I_{Ks-S74L}$ ) was reduced by approximately 33% at +60 mV compared

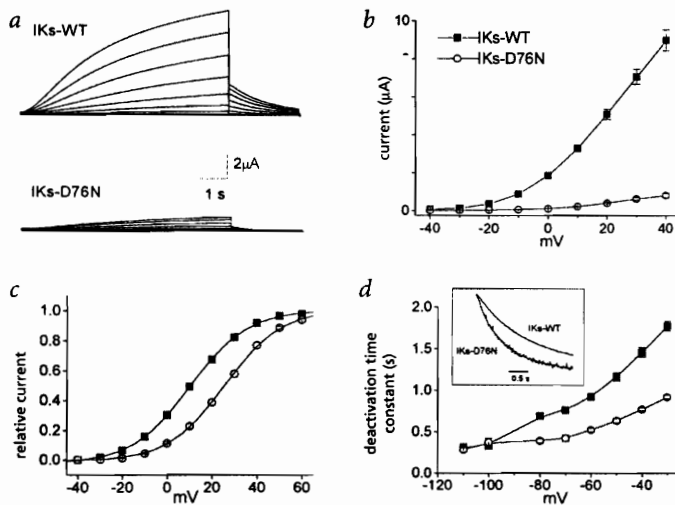
to  $I_{Ks-WT}$  (Fig. 4a,b). This reduction was due primarily to a positive shift in the voltage dependence of current activation (Fig. 4c). The voltage dependence of deactivation was shifted approximately +40 mV (Fig. 4d). This shift caused a marked increase in the rate of  $I_{Ks-S74L}$  deactivation. Thus, S74L hminK subunits form heteromultimeric channels with wild-type hminK and *KvLQT1*, and reduce  $I_{Ks}$  by a shift in the voltage dependence of channel activation and increased rate of channel deactivation. Because  $I_{Ks-S74L}$  did not equal  $I_{Ks-WT}$  at +60 mV (as expected for a simple shift in gating), it is possible that S74L mutant subunits also reduce the number of functional  $I_{Ks}$  channels and/or single-channel conductance.

The observation that LQT-associated mutations of *KCNE1* alter gating kinetics provides compelling evidence that hminK forms an integral part of the  $I_{Ks}$  channel rather than simply serving as a chaperone. Earlier studies of minK, performed before the discovery of *KvLQT1*, also support this conclusion<sup>11-14</sup>. In one of these studies, a mutant rat minK subunit (D77N), analogous to D76N hminK, co-assembled with wild-type minK and abolished  $I_{Ks}$  function, a dominant-lethal effect<sup>13</sup>.

We conclude that mutations in *KCNE1*, the gene that encodes  $\beta$ -subunits of  $I_{Ks}$  channels, cause arrhythmia susceptibility by reducing  $I_{Ks}$  and thereby delaying myocellular repolarization. Because regional heterogeneity in  $I_{Ks}$  exists within the myocardium<sup>15</sup>, mutations in *KCNE1* would cause abnormal regional disparity in action potential duration, creating a substrate for arrhythmia. The discovery of LQT-associated mutations in *KCNE1* will facilitate presymptomatic diagnosis of this disorder and may have implications for therapy.

**Fig. 3** Functional effects of D76N *KCNE1* mutation.

**a**,  $I_{Ks}$  was elicited by depolarizations of 7.5-s duration from a holding potential of -80 mV to test potentials of -40 to +40 mV. Deactivating tail currents were elicited by returning membrane potential to -50 mV. **b**, Isochronous current-voltage relation of  $I_{Ks-WT}$  ( $n=14$ ) and  $I_{Ks-D76N}$  ( $n=14$ ), demonstrating dominant negative suppression of  $I_{Ks}$  by D76N ( $P < 0.0001$ ). **c**, The voltage dependence of  $I_{Ks-D76N}$  activation, using a 7.5-s test pulse, is shifted by +16 mV compared to  $I_{Ks-WT}$ . Smooth curves are best fits of normalized tail currents to a Boltzmann function ( $V_{1/2}=10.8 \pm 0.8$  mV, slope factor =  $12.1 \pm 0.3$  mV for  $I_{Ks-WT}$ ; for  $I_{Ks-D76N}$   $V_{1/2}=25.7 \pm 1.0$  mV [ $P < 0.0001$ , compared to  $I_{Ks-WT}$ ], slope factor =  $12.0 \pm 0.2$  mV;  $n=14$ ). **d**,  $I_{Ks-D76N}$  deactivates faster than  $I_{Ks-WT}$ .  $I_{Ks}$  was activated by a 5-s pulse to +20 mV, and tail currents were measured at the indicated potentials. Tail currents were fitted to a single exponential function. Inset shows normalized deactivating tail currents at -50 mV, after a voltage step to +20 mV.



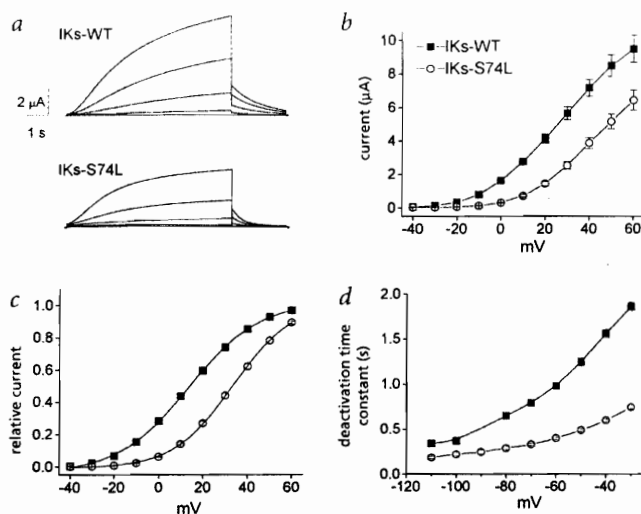


**Fig. 4** Functional effects of S74L *KCNE1* mutation. **a**,  $I_{Ks-WT}$  and  $I_{Ks-S74L}$  recorded during 7.5-s depolarizations to  $-40$ ,  $-20$ ,  $0$ ,  $+20$  and  $+40$  mV. Note the faster rate of deactivating  $I_{Ks-S74L}$  tail currents compared to  $I_{Ks-WT}$ . **b**, Isochronous current-voltage relation for  $I_{Ks-WT}$  and  $I_{Ks-S74L}$  ( $n=15$ ). **c**, Voltage dependence of  $I_{Ks-S74L}$  activation is shifted by  $+19$  mV relative to  $I_{Ks-WT}$ . Smooth curves are best fits of normalized tail currents to a Boltzmann function ( $V_{1/2} = 13.7 \pm 0.6$  mV, slope factor =  $16.0 \pm 0.3$  mV for  $I_{Ks-WT}$ ; for  $I_{Ks-S74L}$   $V_{1/2} = 33.6 \pm 0.8$  mV, slope factor =  $13.3 \pm 0.3$  mV [both  $P < 0.0001$  relative to  $I_{Ks-WT}$ ]). **d**,  $I_{Ks-S74L}$  deactivates faster than  $I_{Ks-WT}$ .

## Methods

**Phenotypic analyses.** Individuals were phenotypically characterized on the basis of the QT interval corrected for heart rate. Individuals were characterized as affected if  $QTc \leq 0.46$  s. Individuals were assigned as unaffected if  $QTc \leq 0.42$  s. Informed consent was obtained from all individuals or their guardians in accordance with local institutional review board guidelines. Phenotypic data were interpreted without knowledge of genotype.

**Mutation analyses.** Genomic samples were amplified by PCR with the following primer pairs: MINK1F 5'-CTGCAGCAGTGGAACTTAATG-3' and MINK1R 5'-GTTCCGAGTGTCTCCAGCTTCTTG-3'; MINK2F 5'-AGGGCATCATGCTGAGTACAT-3' and MINK2R 5'-TTTAGCCAGTGGTGGGGTTC-3'; MINK3F 5'-GTTTCAGCAGGTGGCAACAT and MINK3R 5'-GCCAGATGGTTTCAACGACA-3'. PCR products were used in SSCP analysis as described<sup>5</sup>. PCR was completed with 75 ng DNA in a volume of 10  $\mu$ l using a Perkin Elmer/Cetus 9600 thermocycler. Amplification conditions were 94 °C for 3 min, followed by 30 cycles of 94 °C for 10 s, 58 °C for 20 s, 72 °C for 20 s and a 5-min extension at 72 °C. Reactions were diluted with 40  $\mu$ l of 0.1% SDS/10 mM EDTA and with 30  $\mu$ l of 95% formamide load dye. The mixture was denatured at 94 °C for 5 min and placed on ice. Three microlitres of each sample was separated on 5% and 10% non-denaturing polyacrylamide gels (acrylamide:bisacrylamide 49:1) at 4 °C and on 0.5x and 1x mutation detection enhancement (MDE) gels (FMC) at room temperature. Electrophoreses on the 5% and 10% gels were completed at 40 W for 3–5 h; electrophoreses on 0.5x and 1x MDE gels were completed overnight, respectively, at 350 V and 600 V. Gels were dried on 3MM filter paper and exposed for 18 h at  $-70$  °C.

SSCP bands were cut out of the gel and eluted in 100  $\mu$ l ddH<sub>2</sub>O at 65 °C for 30 min. Eluted DNA (10  $\mu$ l) was re-amplified with the original primer

pair. Products were separated on 1% low-melting-point agarose gels (FMC), phenol-chloroform extracted and ethanol precipitated. DNA was sequenced in both directions by the dideoxy chain termination method on a model 373A DNA sequencer (Applied Biosystems).

**Functional expression.** *KCNE1* cDNA expression constructs were amplified by PCR from total human DNA and cloned in pSP64 transcription vector (Promega) with the following primers: MINKF 5'-CAGTGG-AAGCTTAATGCCAGGATGATC-3' and MINKR 5'-CAGGAGGATCCAGTTAGCCAGTGGTGGG-GGTTCA-3'. Nucleotides in bold denote the changes made to create *HindIII* and *BamHI* restriction sites (underlined). A full-length *KVLQT1* cDNA clone (identical to that reported by Yang *et al.*<sup>16</sup>) was isolated from a human cardiac cDNA library and subcloned into the pSP64 plasmid expression vector. All constructs were confirmed by DNA sequence analyses. Complementary RNAs were synthesized with the mCAP RNA capping kit (Stratagene).

Isolation of *Xenopus laevis* oocytes and cRNA injection were performed as described<sup>17</sup>. Voltage clamp data were acquired and analysed with PCLAMP v6.0 software (Axon Instruments). Isochronous (7.5 s) rather than steady-state measurements were used to estimate the voltage dependence of  $I_{Ks}$  activation. The voltage dependence of  $I_{Ks}$  activation was determined by fitting peak tail currents to a Boltzmann function.  $V_{1/2}$ , the voltage at which the current was half activated with this pulse protocol, and the slope factor were calculated from these data. Activating current was fitted to a bi-exponential function to obtain slow and fast time constants of activation. Deactivation time constants were obtained by fitting decaying tail currents at various test potentials to a single exponential function.

All data are mean  $\pm$  S.E.M. Statistical analyses were performed with repeated measures analysis of variance, with the Fisher's Least Significance *post hoc* test and the unpaired Student's *t*-test. A *P* value  $< 0.05$  was required for significance.

## Acknowledgements

We thank K. Timothy, Q. Xu, D. Atkinson, D. Frankovich, J. Shen and H. Orme for technical assistance. This work was supported by NHLBI RO1 HL48074, P50-HLS2338-02, PHS Grant M01 RR00064, the Technology Access Section of the Utah Genome Center, the American Heart Association and an award from Bristol-Myers/Squibb.

Received January 31; accepted 25 August 1997.

1. Rettig, J. *et al.* Inactivation properties of voltage-gated K<sup>+</sup> channels altered by presence of  $\beta$ -subunit. *Nature* **369**, 289–294 (1994).
2. Shi, G. *et al.*  $\beta$ -subunits promote K<sup>+</sup> channel surface expression through effects early in biosynthesis. *Neuron* **16**, 843–852 (1996).
3. Sanguinetti, M.C. *et al.* Coassembly of  $K_vLQT1$  and minK ( $I_{Ks}$ ) proteins to form cardiac  $I_{Ks}$  potassium channel. *Nature* **384**, 80–83 (1996).
4. Barhanin, J. *et al.*  $K_vLQT1$  and  $I_{Ks}$  (minK) proteins associate to form the  $I_{Ks}$  cardiac potassium current. *Nature* **384**, 78–80 (1996).
5. Wang, Q. *et al.* Positional cloning of a novel potassium channel gene: *KVLQT1* mutations cause cardiac arrhythmias. *Nature Genet.* **12**, 17–23 (1996).
6. Neyroud, N. *et al.* A novel mutation in the potassium channel gene *KVLQT1* causes the Jervell and Lange-Nielsen cardioauditory syndrome. *Nature Genet.* **15**, 186–189 (1997).
7. Splawski, I., Timothy, K.W., Vincent, G.M., Atkinson, D.L. & Keating, M.T. Molecular basis of the long-QT syndrome associated with deafness. *N. Engl. J. Med.* **336**, 1562–1567 (1997).
8. Keating, M. *et al.* Linkage of a cardiac arrhythmia, the long QT syndrome, and the Harvey ras-1 gene. *Science* **252**, 704–706 (1991).
9. Jiang, C. *et al.* Two long QT syndrome loci map to chromosomes 3 and 7 with evidence for further heterogeneity. *Nature Genet.* **8**, 141–147 (1994).
10. Swanson, R., Hice, R.E., Folander, K. & Sanguinetti, M.C. The  $I_{Ks}$  protein, a slowly activating voltage-dependent K<sup>+</sup> channel. *Semin. Neurosci.* **5**, 117–124 (1993).
11. Takumi, T. *et al.* Alteration of channel activities and gating by mutations of slow  $I_{Ks}$  potassium channel. *J. Biol. Chem.* **266**, 22192–22198 (1991).
12. Goldstein, S.A.N. & Miller, C. Site-specific mutations in a minimal voltage-dependent K<sup>+</sup> channel alter ion selectivity and open-channel block. *Neuron* **7**, 403–408 (1991).
13. Wang, K.-W. & Goldstein, S.A.N. Subunit composition of minK potassium channels. *Neuron* **14**, 1303–1309 (1995).
14. Wang, K., Tai, K. & Goldstein, S.A.N. MinK residues line a potassium channel pore. *Neuron* **16**, 571–577 (1996).
15. Liu, D.-W. & Antzelevitch, C. Characteristics of the delayed rectifier current ( $I_{Kr}$  and  $I_{Ks}$ ) in canine ventricular epicardial, midmyocardial, and endocardial myocytes: a weaker  $I_{Ks}$  contributes to the longer action potential of the M cell. *Circ. Res.* **76**, 351–365 (1995).
16. Yang, W.P. *et al.* *KvLQT1*, a voltage-gated potassium channel responsible for human cardiac arrhythmias. *Proc. Natl. Acad. Sci. USA* **94**, 4017–4021 (1997).
17. Sanguinetti, M.C., Jiang, C., Curran, M.E. & Keating, M.T. A mechanistic link between an inherited and an acquired cardiac arrhythmia: *HERG* encodes the  $I_{Kr}$  potassium channel. *Cell* **81**, 299–307 (1995).

## CHAPTER 7

### MOLECULAR BASIS OF THE LONG-QT SYNDROME ASSOCIATED WITH DEAFNESS

The following chapter is a reprint from an article coauthored by Timothy, K. W., Vincent, G. M., Atkinson, D., Keating, M. T. and me. It was originally published in New England Journal of Medicine, volume 336, pages 1562-1567, May 29, 1997 (Copyright Massachusetts Medical Society). It is reprinted here with the permission of the coauthors and the Massachusetts Medical Society.

## Brief Report

MOLECULAR BASIS OF THE  
LONG-QT SYNDROME  
ASSOCIATED WITH DEAFNESSIGOR SPLAWSKI, M.S., KATHERINE W. TIMOTHY, B.S.,  
G. MICHAEL VINCENT, M.D., DONALD L. ATKINSON, B.S.,  
AND MARK T. KEATING, M.D.

IN 1957, Jervell and Lange-Nielsen reported a syndrome of congenital sensory deafness associated with a prolonged QT interval in four children of a Norwegian family.<sup>1</sup> The affected children had multiple syncopal episodes, and three died suddenly at the ages of four, five, and nine years. Since 1957, other examples of the long-QT syndrome associated with deafness (the Jervell and Lange-Nielsen syndrome) have been described.<sup>2-4</sup> In all cases, the apparent mode of inheritance was autosomal recessive. This syndrome is rare (estimated incidence, 1.6 to 6 cases per million).<sup>2</sup> Affected persons are susceptible to recurrent syncope, and they have a high incidence of sudden death and short life expectancy. Syncope results from torsade de pointes ventricular tachycardia and ventricular fibrillation.<sup>5,6</sup>

The Romano-Ward syndrome is an autosomal dominant form of the long-QT syndrome and is not associated with deafness or other phenotypic abnormalities.<sup>7,8</sup> The incidence of the Romano-Ward syndrome is higher than that of the Jervell and Lange-Nielsen syndrome, but affected persons generally have milder symptoms.<sup>9,10</sup>

In previous studies, we mapped the genes for the autosomal dominant long-QT syndrome to chromosomes 11p15.5 (*LQT1*), 7q35-36 (*LQT2*), and 3p21-24 (*LQT3*).<sup>11-13</sup> A fourth gene (*LQT4*) was mapped to chromosome 4q25-27.<sup>14</sup> We subsequently identified genes for *LQT1* (*KVLQT1*), *LQT2* (*HERG*), and *LQT3* (*SCN5A*).<sup>15-18</sup> These genes encode cardiac ion channels and support the hypothesis that the long-QT syndrome results from delayed myocellular repolarization. Functional expression of *KVLQT1* in xenopus oocytes and mammalian cells induces a potassium current unlike any known cardiac current. In

recent experiments, we and others demonstrated that the *KVLQT1* protein joins with another protein known as minimal potassium-channel subunit (minK) to form a cardiac potassium channel expressing the cardiac slow delayed rectifier potassium current ( $I_{Kr}$ ), a channel that contributes to myocellular repolarization.<sup>19,20</sup>

In this study, we hypothesized that the Jervell and Lange-Nielsen syndrome results from mutations that affect both alleles of an autosomal dominant gene for the long-QT syndrome. We discovered that a patient with the Jervell and Lange-Nielsen syndrome had a homozygous mutation of *KVLQT1*. Other family members also had prolongation of the QT interval corrected for heart rate (QTc) with an autosomal dominant pattern of inheritance, but they had normal hearing and were heterozygotes. These data indicate that homozygous mutation of *KVLQT1* causes the Jervell and Lange-Nielsen syndrome.

## METHODS

## Ascertainment and Phenotyping of the Kindred

A patient with the Jervell and Lange-Nielsen syndrome was referred to us. A team of researchers attended a large family gathering organized by the patient's paternal aunt and grandmother. Information on the pedigree and the patient's history was collected at the gathering, and electrocardiograms and blood samples were obtained.

The members of the family ranged in age from 13 months to 82 years. Each subject was characterized phenotypically on the basis of the QTc and the presence of symptoms as described.<sup>11,13,21</sup> Subjects were classified as phenotypically affected by the long-QT syndrome if they had symptoms (syncope, seizures, or aborted sudden death) and QTc intervals of 0.45 sec<sup>1/2</sup> or more or were asymptomatic with QTc intervals of 0.47 sec<sup>1/2</sup> or more. Subjects were classified as unaffected if they were asymptomatic and had QTc intervals of 0.41 sec<sup>1/2</sup> or less. The status of asymptomatic persons with QTc intervals of between 0.42 and 0.46 sec<sup>1/2</sup> and symptomatic persons with QTc intervals of less than 0.45 sec<sup>1/2</sup> was classified as uncertain. The criteria for the assignment of phenotypes were not age-dependent. Informed consent was obtained from all the subjects or their guardians. The research protocol was reviewed and approved by the appropriate institutional review boards. Phenotypic data were interpreted by investigators who did not know the patients' genotypes.

## Linkage Analysis

Linkage analysis is a technique that can be used to determine whether a gene responsible for a phenotype is located on the same chromosomal segment as a genetic marker. With this technique, an investigator examines a family to determine whether a phenotype is inherited with a specific DNA-sequence variant (allele) of known chromosomal location. Genes or segments of DNA that have two or more forms are known as polymorphic markers and can be detected with the polymerase chain reaction (PCR).<sup>22</sup>

In this study, we used linkage analysis to determine whether the phenotype of the long-QT syndrome was inherited with the polymorphic markers *TH* and *D11S1318*, which are located near *KVLQT1*.<sup>17</sup> Small, synthetic DNA primers (oligonucleotides) were used to amplify DNA from each subject by PCR. The reactions were completed with 75 ng of DNA in a final volume of 10  $\mu$ l with a thermocycler (model 9600, Perkin-Elmer Cetus). The amplification conditions were as follows: 94°C for 3 minutes, followed by 30 cycles of 94°C for 10 seconds, 58°C for 20 seconds, and 72°C for 20 seconds. Ten microliters of 95 percent forma-

From the Eccles Institute of Human Genetics (I.S., D.L.A., M.T.K.), the Cardiology Division (K.W.T., G.M.V., M.T.K.), and the Howard Hughes Medical Institute (D.L.A., M.T.K.), University of Utah; and the Department of Medicine (K.W.T., G.M.V.), Latter-Day Saints Hospital — all in Salt Lake City. Address reprint requests to Dr. Keating at the Howard Hughes Medical Institute, Suite 5100 EIHG, University of Utah, Salt Lake City, UT 84112.  
©1997, Massachusetts Medical Society.



## BRIEF REPORT

ide loading dye was added to each reaction, and the samples were denatured at 94°C for 5 minutes and placed on ice. Three microliters of each sample was separated on 6 percent denaturing polyacrylamide gels. The gels were dried on 3MM filter paper (Whatman, Clifton, N.J.) and exposed to film for 12 hours at -70°C. The pattern of the alleles in each subject (the genotype), which appears as bands of variable size on the film, was determined by inspection.

The genotypes were scored without knowledge of the phenotypic data and were entered into a computerized relational database. The likelihood of odds (lod score) for linkage was determined with the Linkage version 5.1 software package.<sup>23</sup> Penetrance was assumed to be 95 percent, and the frequency of the gene for the long-QT syndrome (0.001) was assumed to be the same in male and female subjects. The allelic frequencies were set to 1/n, where n equals the number of alleles for each marker in this family (TH, alleles; *KVLQT1*, 2 alleles; *D11S1318*, 10 alleles).

#### Mutation Analysis

Single-strand conformation polymorphism (SSCP) analysis was used to screen for mutations in *KVLQT1*.<sup>15</sup> With this technique a small (approximately 200-bp) section of a patient's genomic DNA is amplified by PCR. If the patient has a mutation, both the normal and the mutant alleles are amplified. The two products can then be separated on nondenaturing gels and distinguished. The principle underlying SSCP analysis is that a single strand of DNA migrates through a nondenaturing gel at a rate dependent on the size and the specific sequence of the strand.<sup>24</sup> Another strand identical in size that contains a substitution of a single nucleotide will travel through the same gel at a slightly different rate. The difference in mobility results from an altered conformation in the DNA molecule that has the nucleotide substitution, and an abnormal SSCP band is produced.

PCR was completed with 75 ng of DNA in a volume of 10  $\mu$ l with a thermocycler (model 9600, Perkin-Elmer Cetus). The amplification conditions were as follows: 94°C for 3 minutes, followed by 5 cycles of 94°C for 10 seconds, 64°C for 20 seconds, and 72°C for 20 seconds and 30 cycles of 94°C for 10 seconds, 60°C for 20 seconds, and 72°C for 20 seconds. The reaction mixtures were diluted with 40  $\mu$ l of 0.1 percent sodium dodecyl sulfate and 10 mM EDTA and with 30  $\mu$ l of 95 percent formamide loading dye. The mixture was denatured at 94°C for 5 minutes and placed on ice. Three microliters of each sample was separated on 5 percent and 10 percent nondenaturing polyacrylamide gels (acrylamide:bisacrylamide, 49:1) at 4°C and on 0.5 $\times$  and 1 $\times$  Mutation Detection Enhancement gels (MDE, FMC BioProducts, Rockland, Me.) at room temperature. Electrophoresis of the 5 percent and 10 percent gels was completed at 40 W for three to five hours; electrophoresis of the 0.5 $\times$  and 1 $\times$  MDE gels was completed overnight at 350 V and 600 V, respectively. The gels were dried on 3MM filter paper and exposed to film for 18 hours at -70°C.

#### DNA-Sequence Analysis

SSCP bands were cut out of the gel and eluted in 100  $\mu$ l of double-distilled water at 65°C for 30 minutes. Ten microliters of eluted DNA was used as a template in a second PCR reaction with the original primer pair. The products were separated on 1 percent low-melting-temperature agarose gels (FMC BioProducts), extracted with phenol-chloroform, and precipitated in ethanol. DNA was sequenced in both directions by the dideoxy chain-termination method with a DNA sequencer (model 373A, Applied Biosystems).

### RESULTS

#### Phenotypic Characteristics

We studied a family of Scottish descent in which one child had the Jervell and Lange-Nielsen syndrome. This female infant (Patient V-5, Fig. 1) was

born to a consanguineous marriage of second cousins. At 35 weeks' gestation, the obstetrician informed the 25-year-old mother that the fetal heart rate had dropped to 70 to 80 beats per minute. An ultrasound study showed normal growth and development, with a heart rate of 80 and a regular rhythm. At 38 weeks the heart rate continued to be slow. A second ultrasound study confirmed normal development, bradycardia, and regular rhythm. The infant was born without complications by normal vaginal delivery.

The slow heart rate persisted after birth. One hour after delivery, at the time of the first bottle feeding, the infant had cyanosis and hypotonia. She was rushed to the pediatric intensive care unit. Her serum electrolytes and a hematologic evaluation were normal. Blood cultures, urinalysis, urine cultures, and a chest film were negative. An electrocardiogram showed sinus bradycardia with a rate of 82 beats per minute and prolongation of the QT interval, with a QTc of 0.61 sec<sup>1/2</sup>. On the third hospital day, a pediatric cardiologist made the diagnosis of the long-QT syndrome and treatment with propranolol was started. On the eighth day, audiograms indicated bilateral sensory deafness. A neurologic evaluation was otherwise unremarkable, and no evidence of brain-stem dysfunction was found. There was no evidence of dysmorphism.

On day 10, the infant was sent home with an apnea monitor. At the age of four weeks, serial audiograms revealed no responses to auditory stimuli in a soundproof room or through earphones. Trials with battery-powered behind-the-ear hearing aids also indicated no responses. There was no evidence of infection, meningitis, or temporal bone fractures and no history of treatment with ototoxic drugs. At 26 months the proband continued to be treated with propranolol and had no documented syncope, seizures, or tachyarrhythmia.

The family members were not evaluated further. Seven months after the delivery of the proband, her mother had a cardiac arrest and died when her alarm clock sounded. She was exhausted and extremely anxious at the time.

After the mother's death, the family was referred to our laboratory for genetic evaluation. Phenotypic analysis revealed that 14 family members had prolonged QTc intervals ranging from 0.47 to 0.53 sec<sup>1/2</sup> (Fig. 1). Thirty-two family members had borderline QTc intervals, ranging from 0.42 to 0.46 sec<sup>1/2</sup>. Six family members reported a history of syncope. Three had had one syncopal episode each: Subject II-13 (QTc, 0.46 sec<sup>1/2</sup>; precipitating cause of syncope unknown), Subject III-29 (QTc, 0.49 sec<sup>1/2</sup>; syncope while smoking marijuana), and Subject IV-4 (QTc, 0.51 sec<sup>1/2</sup>; syncope while exercising). Three other family members had multiple episodes of syncope: Subject III-27 (QTc, 0.53 sec<sup>1/2</sup>; syncope while exer-

cising), Subject III-33 (QTc, 0.46 sec<sup>1/2</sup>; precipitating cause of syncope unknown), and Subject IV-14 (QTc, 0.41 sec<sup>1/2</sup>; syncope while exercising or at rest). None of the family members reported hearing deficits. Formal audiometric analyses of Subjects IV-4, V-1, and V-3 showed normal hearing.

On the basis of this inspection, it is apparent that

**TABLE 1. PAIRWISE LOD SCORES FOR THE KINDRED STUDIED, RELATING THE PHENOTYPE OF THE LONG-QT SYNDROME TO MARKERS AT CHROMOSOME 11p15.5, INCLUDING THE *KVLQT1* MUTATION.\***

MARKER	RECOMBINATION FRACTION						MAXIMAL LOD SCORE†
	0.00	0.001	0.01	0.05	0.1	0.2	
<i>TH</i>	4.70	4.70	4.63	4.31	3.89	2.98	4.70
<i>KVLQT1</i>	5.08	5.07	4.98	4.60	4.09	3.03	5.08
<i>D11S1318</i>	5.46	5.45	5.37	4.99	4.50	3.44	5.46

\*Markers at chromosome 11p15.5 were completely linked to the disease phenotype. Lod scores were computed with the assumption of 95 percent penetrance, a frequency of 0.001 for the disease allele, and equal recombination frequencies in both sexes. When penetrance was varied from 60 percent to 100 percent, the maximal lod scores ranged from 4.09 to 4.81 for *TH*, from 4.38 to 5.19 for the *KVLQT1* mutation, and from 4.77 to 5.57 for *D11S1318*.

†The estimated recombination fraction at the maximal lod score for each marker was 0.00.

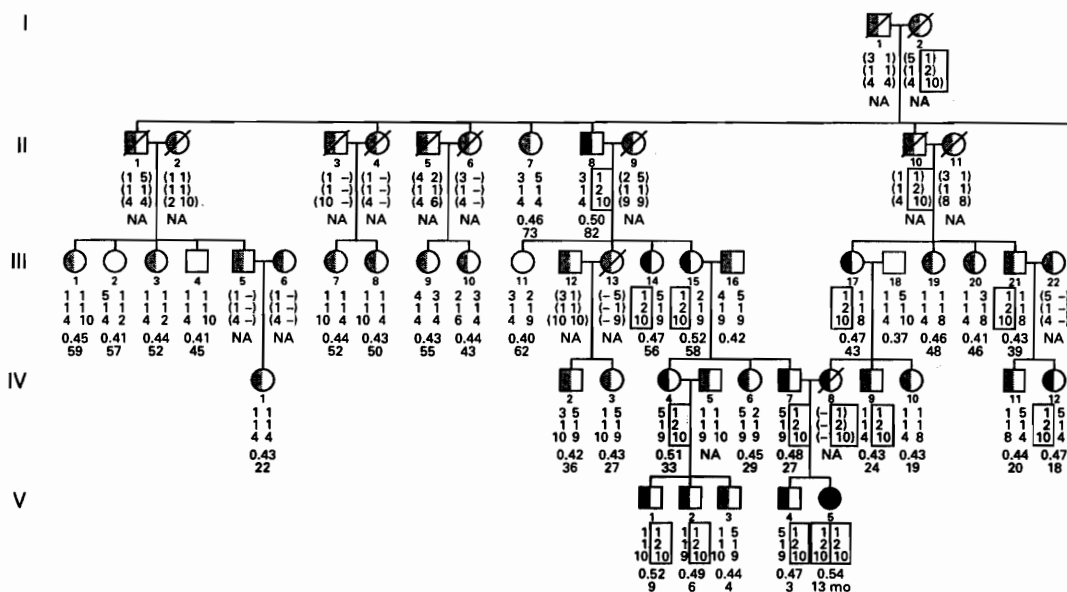
the phenotype of the long-QT syndrome is inherited as an autosomal dominant trait in this kindred (Fig. 1). This pattern of inheritance is characterized by transmission of the disease phenotype from parent to child, the presence of the phenotype in each generation, and the involvement of both sexes. Father-to-son transmission is observed in this family, a fact that rules out X-linked inheritance.

#### Linkage Analysis

We used linkage analysis to determine whether the gene responsible for the long-QT syndrome in this kindred was located on the same chromosome as one of the known autosomal dominant genes for the long-QT syndrome. The polymorphic markers *TH* and *D11S1318*, which map to the *KVLQT1* region of chromosome 11, were completely linked to the long-QT syndrome phenotype.<sup>17</sup> The lod scores for linkage were 4.70 and 5.46 at a recombination fraction of 0.00 for *TH* and *D11S1318*, respectively ( $P < 0.001$  for both markers) (Table 1). These data indicate that *KVLQT1* is an excellent candidate for the gene that causes the long-QT syndrome in this family.

#### Mutation Analysis

We screened DNA samples from affected subjects for functional mutations in *KVLQT1*, using SSCP to detect mutations. An abnormal band was observed



## BRIEF REPORT

in affected members of the family, but not unaffected ones (Fig. 1 and 2). The proband with the Jervell and Lange-Nielsen syndrome (Patient V-5) had two copies of the abnormal SSCP band. Linkage analysis indicated that the abnormal band was completely linked to the long-QT syndrome phenotype in this family, with a lod score of 5.08 at a recombination fraction of 0.00 (Table 1). This indicates odds of more than 100,000 to 1 in favor of linkage and corresponds to  $P < 0.001$ . The abnormal SSCP band was not observed in DNA samples from 200 unrelated control subjects (a total of 400 chromosomes).

DNA-sequence analysis revealed that the abnormal SSCP band contained the insertion of a single nucleotide (G) after nucleotide 282 of the *KVLQT1* sequence (numbering started at the A nucleotide in the ATG initiation codon; GenBank accession number U89364). This insertion causes a frame shift, disrupting the coding sequence after the second putative membrane-spanning domain of the *KVLQT1* protein and leading to a premature stop codon at nucleotide 564.

We next assessed the range of QTc intervals in this genotypically defined population. For the proband, who had a homozygous mutation of *KVLQT1*, the mean ( $\pm$ SD) QTc as calculated on the basis of eight electrocardiograms was  $0.54 \pm 0.05$  sec<sup>1/2</sup>. By contrast, the mean QTc in 24 persons with one mutant *KVLQT1* allele (who were tested with one electro-

cardiogram each) was  $0.47 \pm 0.04$  sec<sup>1/2</sup>. In the 28 family members with no *KVLQT1* mutations, the mean QTc was  $0.43 \pm 0.02$  sec<sup>1/2</sup>. Although no formal statistical analysis could be performed because there was only one homozygote in the family, the QTc interval of the proband ( $0.54$  sec<sup>1/2</sup>) was markedly higher than the mean value in the heterozygotes ( $0.47$  sec<sup>1/2</sup>). This suggests that patients with two copies of a mutant *KVLQT1* gene may have longer QTc intervals than those with a single mutant copy.

## DISCUSSION

We have described a family with an autosomal dominant long-QT syndrome resulting from a mutation of *KVLQT1*. Family members with one mutant *KVLQT1* allele had the long-QT syndrome but had normal hearing. One family member had the typical features of the Jervell and Lange-Nielsen syndrome: marked QTc prolongation and congenital sensory deafness.<sup>1,2,4</sup> This person presented with bradycardia in utero. She was the offspring of a consanguineous marriage and had two copies of the mutant *KVLQT1* allele. We conclude that homozygous mutation of *KVLQT1* causes the Jervell and Lange-Nielsen syndrome.

Recent genetic and physiologic data support the conclusion that homozygous *KVLQT1* mutations cause deafness. We and others recently discovered that *KVLQT1* protein joins with minK protein to

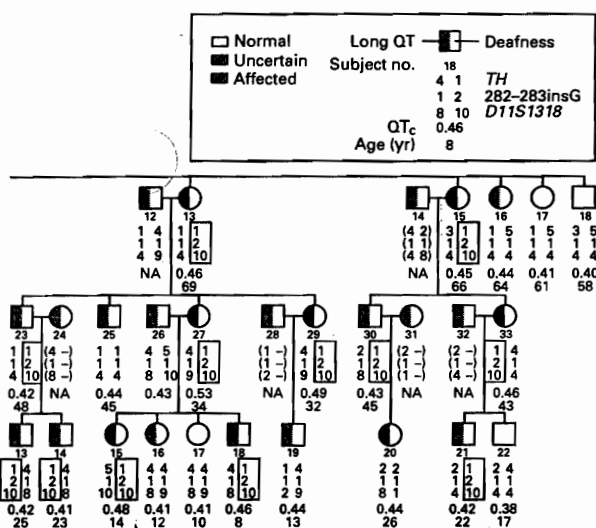
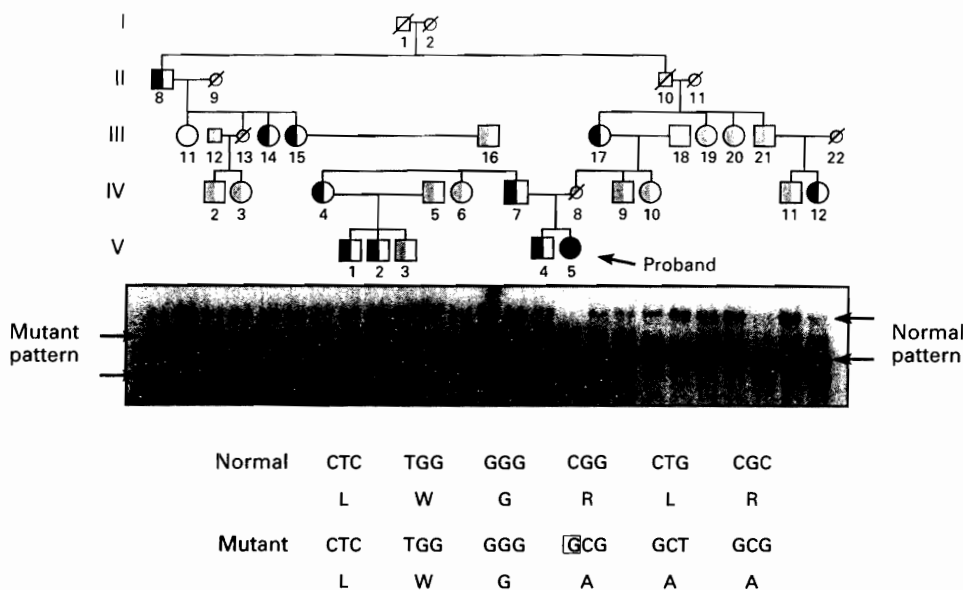


Figure 1. Genotypic Analysis of the Kindred of the Proband with the Jervell and Lange-Nielsen Syndrome, Showing the Linkage between *KVLQT1* and the Phenotype of the Long-QT Syndrome.

Circles indicate female family members, squares male family members, and slashes deceased family members. The left side of each symbol indicates whether the subject had the phenotype of the long-QT syndrome; the right side denotes the subject's hearing status. Black denotes affected status, gray uncertain status, and white unaffected status. The proband (Patient V-5) is indicated by the solid circle representing both the long-QT syndrome and deafness. The genotypes of the polymorphic markers *TH* and *D11S1318* and the *KVLQT1* mutation (282-283insG) are shown beneath each symbol, with inferred genotypes given in parentheses and hyphens indicating unknown alleles. For *KVLQT1*, the normal allele is designated by 1 and the mutant allele by 2. Genotypes associated with the long-QT syndrome are shown in boxes. The subjects' QTc intervals are given immediately below the genotypes, with their ages (in years) below the QTc intervals. NA denotes not available. The *KVLQT1* mutant allele cosegregates with the phenotype of the long-QT syndrome in this family, and the proband with the Jervell and Lange-Nielsen syndrome is homozygous for the mutation.



**Figure 2.** Cosegregation of the Abnormal SSCP Band with the Phenotype of the Long-QT Syndrome in the Kindred of the Proband with the Jervell and Lange-Nielsen Syndrome, with the DNA Sequence of the *KVLQT1* Mutation.

The top panel shows a subgroup of the kindred. The symbols are as described in the legend and key to Figure 1. Small symbols denote family members for whom no bands are shown but who are included to clarify the family relationships. The abnormal SSCP band cosegregates with the phenotype of the long-QT syndrome. The bottom panel shows the DNA and protein sequences of the normal and mutant *KVLQT1* alleles. The mutant allele contains an insertion of a single nucleotide (G) after nucleotide 282. This insertion causes a frame shift that leads to a premature stop codon.

**TABLE 2.** MOLECULAR GENETICS OF THE LONG-QT SYNDROME.

SYNDROME, TYPE OF INHERITANCE, AND LOCUS	CHROMOSOME	GENE
<b>Romano-Ward syndrome (long QT)</b>		
Autosomal dominant		
LQT1	11p15.5	<i>KVLQT1</i>
LQT2	7q35-36	<i>HERG</i>
LQT3	3p21-24	<i>SCN5A</i>
LQT4	4q25-27	?
LQT5	?	?
<b>Jervell and Lange-Nielsen syndrome (long QT and deafness)</b>		
Autosomal recessive		
LQT1	11p15.5	<i>KVLQT1</i>

form cardiac  $I_{Ks}$  potassium channels.<sup>19,20</sup> Although most studies have focused on the function of minK in the heart, the gene that encodes it is also expressed in the inner ear. *MinK* knockout mice are deaf and have inner-ear disease similar to that of patients with the Jervell and Lange-Nielsen syndrome.<sup>25,26</sup> The loss of functional minK protein apparently disrupts the production of endolymph, leading to deafness. Recently, Neyroud and colleagues showed that *KVLQT1* is expressed in the stria vascularis of the inner ear in mice.<sup>27</sup> Other known genes located near *KVLQT1* (*p57<sup>KIP2</sup>*, *H19*, and the genes for insulin-like growth factor II, insulin, and tyrosine hydroxylase) are not likely to contribute to the disease observed in the Jervell and Lange-Nielsen syndrome. These data are consistent with the finding that homozygous mutations of *KVLQT1* cause deafness in humans.

The *KVLQT1* mutation described here causes a frame shift, disrupting the coding sequence and leading to a premature stop codon. The resulting truncated protein would lack a pore region and could not function as an ion channel. Thus, the proband represents a case of functional knockout of *KVLQT1*. The result is prolonged myocellular repolarization, lack of

## BRIEF REPORT

homogeneity of cardiac repolarization, increased risk of torsade de pointes arrhythmias, and deafness.

It is not yet clear whether *KVLQT1* is the only gene responsible for the Jervell and Lange-Nielsen syndrome. Genetic heterogeneity has been identified in the autosomal dominant long-QT syndrome (Table 2),<sup>15-17</sup> and Jeffrey and colleagues described a family with the Jervell and Lange-Nielsen syndrome in which the phenotype was not linked to a chromosome 11p15.5 marker.<sup>28</sup> In findings consistent with ours, Neyroud and colleagues recently reported homozygous *KVLQT1* mutations associated with the Jervell and Lange-Nielsen syndrome in two kindreds.<sup>27</sup> Because minK joins with *KVLQT1* protein to form  $I_{Ks}$  channels, *minK* is another excellent candidate gene for this disorder.<sup>19,20</sup>

Previous reports describing the clinical characteristics of patients with the Jervell and Lange-Nielsen syndrome have focused on the dramatic features observed, which generally include marked prolongation of the QTc interval, frequent tachyarrhythmias, and deafness. Some studies have documented moderate prolongation of QTc in family members with normal hearing, but the Romano-Ward long-QT syndrome was not diagnosed.<sup>2,3</sup> The family described in our study came to our attention because the proband's mother died suddenly, presumably of a cardiac arrhythmia. Phenotypic evaluation of the extended family revealed autosomal dominant inheritance of the long-QT syndrome in other family members. Deafness, however, was found only in the proband, who was homozygous for the *KVLQT1* mutation. Thus, one feature of the phenotype of the Jervell and Lange-Nielsen syndrome, deafness, is inherited as an autosomal recessive trait. QTc prolongation, by contrast, is inherited as a dominant trait, but that phenotype may be more severe if both alleles are mutant. It is important to note that the parents (and possibly other family members) of patients with the Jervell and Lange-Nielsen syndrome are obligate heterozygotes for long-QT-associated mutations and are at increased risk for arrhythmia. The untimely death of the proband's mother points to the importance of electrocardiographic and genetic screening of families with the Jervell and Lange-Nielsen syndrome.

Supported by a grant (RO1 HL48074) from the National Heart, Lung, and Blood Institute, by a Specialized Center of Research Grant (HL53773), by a grant (M01 RR00064) from the Public Health Service, by the Technology Access Section of the Utah Genome Center, by the American Heart Association, and by an award from Bristol-Myers Squibb.

We are indebted to the family members for their participation; to Dr. S. Appleton for referring the family; to M. Sanguinetti, L. Urness, and S. Odelberg for critical review of the manuscript; to S. Wilson for blood collection; and to the Sudden Arrhythmia Death Syndrome Foundation.

## REFERENCES

- Jervell A, Lange-Nielsen F. Congenital deaf-mutism, functional heart disease with prolongation of the Q-T interval, and sudden death. *Am Heart J* 1957;54:59-68.
- Fraser GR, Froggatt P, James TN. Congenital deafness associated with electrocardiographic abnormalities, fainting attacks and sudden death: a recessive syndrome. *Q J Med* 1964;33:361-85.
- Jervell A, Thingstad R, Endsjø TO. The surdo-cardiac syndrome: three new cases of congenital deafness with syncopal attacks and Q-T prolongation in the electrocardiogram. *Am Heart J* 1966;72:582-93.
- Tesson F, Donger C, Denjoy I, et al. Exclusion of KCNE1 (IsK) as a candidate gene for Jervell and Lange-Nielsen Syndrome. *J Mol Cell Cardiol* 1996;28:2051-5.
- Till JA, Shinebourne EA, Pepper J, Camm AJ, Ward DE. Complete denervation of the heart in a child with congenital long QT and deafness. *Am J Cardiol* 1988;62:1319-21.
- Holland JJ. Cardiac arrest under anesthesia in a child with previously undiagnosed Jervell and Lange-Nielsen syndrome. *Anaesthesia* 1993;48:149-51.
- Romano C, Gemme G, Pongiglione R. Aritmie cardiache rare dell'età pediatrica. II. Accessi sincopali per fibrillazione ventricolare parossistica. *Clin Pediatr* 1963;45:656-83.
- Ward OC. A new familial cardiac syndrome in children. *J Ir Med Assoc* 1964;54:103-6.
- Moss AJ, Schwartz PJ, Crampton RS, Locati E, Carleen E. The long QT syndrome: a prospective international study. *Circulation* 1985;71:17-21.
- Moss AJ, Schwartz PJ, Crampton RS, et al. The long QT syndrome: prospective longitudinal study of 328 families. *Circulation* 1991;84:1136-44.
- Keating M, Atkinson D, Dunn C, Timothy K, Vincent GM, Leppert M. Linkage of a cardiac arrhythmia, the long QT syndrome, and the Harvey *ras-1* gene. *Science* 1991;252:704-6.
- Keating M, Dunn C, Atkinson D, Timothy K, Vincent GM, Leppert M. Consistent linkage of the long-QT syndrome to the Harvey *ras-1* locus on chromosome 11. *Am J Hum Genet* 1991;49:1335-9.
- Jiang C, Atkinson D, Towbin JA, et al. Two long QT syndrome loci map to chromosomes 3 and 7 with evidence for further heterogeneity. *Nat Genet* 1994;8:141-7.
- Schott JJ, Charpentier F, Peltier S, et al. Mapping of a gene for long QT syndrome to chromosome 4q25-27. *Am J Hum Genet* 1995;57:1114-22.
- Curran ME, Splawski I, Timothy KW, Vincent GM, Green ED, Keating MT. A molecular basis for cardiac arrhythmia: *HERG* mutations cause long QT syndrome. *Cell* 1995;80:795-803.
- Wang Q, Shen J, Splawski I, et al. *SCN5A* mutations associated with an inherited cardiac arrhythmia, long QT syndrome. *Cell* 1995;80:805-11.
- Wang Q, Curran ME, Splawski I, et al. Positional cloning of a novel potassium channel gene: *KVLQT1* mutations cause cardiac arrhythmias. *Nat Genet* 1996;12:17-23.
- Wang Q, Shen J, Li Z, et al. Cardiac sodium channel mutations in patients with long QT syndrome, an inherited cardiac arrhythmia. *Hum Mol Genet* 1995;4:1603-7.
- Sanguinetti MC, Curran ME, Zou A, et al. Coassembly of K(V)LQT1 and minK (IsK) proteins to form cardiac I(Ks) potassium channel. *Nature* 1996;384:80-3.
- Barhanin J, Lesage F, Guillemare E, Fink M, Lazdunski M, Romey G. K(V)LQT1 and IsK (minK) proteins associate to form the I(Ks) cardiac potassium current. *Nature* 1996;384:78-80.
- Vincent GM, Timothy KW, Leppert M, Keating M. The spectrum of symptoms and QT intervals in carriers of the gene for the long-QT syndrome. *N Engl J Med* 1992;327:846-52.
- Keating M. Linkage analysis and long Q1 syndrome: using genetics to study cardiovascular disease. *Circulation* 1992;85:1973-86.
- Lathrop GM, Lalouel J-M, Julier C, Ott J. Multilocus linkage analysis in humans: detection of linkage and estimation of recombination. *Am J Hum Genet* 1985;37:482-98.
- Orita M, Iwahana H, Kanazawa H, Hayashi K, Sekiya T. Detection of polymorphisms of human DNA by gel electrophoresis as single strand conformation polymorphisms. *Proc Natl Acad Sci U S A* 1989;86:2766-70.
- Vetter DE, Mann JR, Wangemann P, et al. Inner ear defects induced by null mutation of the *isk* gene. *Neuron* 1996;17:1251-64.
- Friedmann I, Fraser GR, Froggatt P. Pathology of the ear in the cardioauditory syndrome of Jervell and Lange-Nielsen (recessive deafness with electrocardiographic abnormalities). *J Laryngol Otol* 1964;80:451-70.
- Neyroud N, Tesson F, Denjoy I, et al. A novel mutation in the potassium channel gene *KVLQT1* causes the Jervell and Lange-Nielsen cardioauditory syndrome. *Nat Genet* 1997;15:186-9.
- Jeffrey S, Jamieson R, Patton MA, Till J. Long QT and Harvey-ras. *Lancet* 1992;339:255.

## CHAPTER 8

### GENOMIC STRUCTURE OF THREE LONG QT SYNDROME GENES: *KVLQT1*, *HERG* AND *KCNE*

The following chapter is a reprint from an article coauthored by Shen, J., Timothy, K. W., Vincent, G. M., Lehmann, M. H., Keating, M. T., and me. It was originally published in *Genomics*, volume 51, pages 86-97, July 1, 1998 (Copyright Academic Press). It is reprinted here with the permission of the coauthors. It is a policy of Academic Press that authors do not need permission to include their papers as part of their dissertation.

## Genomic Structure of Three Long QT Syndrome Genes: *KVLQT1*, *HERG*, and *KCNE1*

Igor Splawski,<sup>\*</sup>† Jiaxiang Shen,<sup>†</sup>‡ Katherine W. Timothy,<sup>§</sup>¶ G. Michael Vincent,<sup>§</sup>¶  
Michael H. Lehmann,<sup>||</sup> and Mark T. Keating<sup>\*</sup>†,§,¶,||

<sup>\*</sup>Department of Human Genetics, <sup>†</sup>Eccles Institute of Human Genetics, <sup>‡</sup>Howard Hughes Medical Institute,  
and <sup>§</sup>Department of Medicine, Cardiology Division, University of Utah, Salt Lake City, Utah 84112;

<sup>¶</sup>Department of Medicine, Latter-Day Saints Hospital, Salt Lake City, Utah 84037;  
and <sup>||</sup>Arrhythmia Center, Sinai Hospital, Detroit, Michigan 48235

Received February 27, 1998; accepted May 1, 1998

Long QT syndrome (LQT) is a cardiac disorder causing syncope and sudden death from arrhythmias. LQT is characterized by prolongation of the QT interval on electrocardiogram, an indication of abnormal cardiac repolarization. Mutations in *KVLQT1*, *HERG*, *SCN5A*, and *KCNE1*, genes encoding cardiac ion channels, cause LQT. Here, we define the complete genomic structure of three LQT genes and use this information to identify disease-associated mutations. *KVLQT1* is composed of 16 exons and encompasses approximately 400 kb. *HERG* consists of 16 exons and spans 55 kb. Three exons make up *KCNE1*. Each intron of these genes contains the invariant GT and AG at the donor and acceptor splice sites, respectively. Intron sequences were used to design primer pairs for the amplification of all exons. Familial and sporadic cases affected by mutations in *KVLQT1*, *HERG*, and *KCNE1* can now be genetically screened to identify individuals at risk of developing this disorder. This work has clinical implications for presymptomatic diagnosis and therapy. © 1998 Academic Press

### INTRODUCTION

Long QT (LQT) syndrome is a cardiac disorder that causes syncope, seizures, and sudden death, usually in young, otherwise healthy individuals. Affected individuals manifest prolongation of the QT interval on electrocardiograms, a sign of abnormal cardiac repolarization (Vincent *et al.*, 1992). The clinical features of LQT result from episodic cardiac arrhythmias, such as *torsade de pointes* and ventricular fibrillation. Two inherited forms of LQT exist. The

more common form, Romano-Ward syndrome, is not associated with other phenotypic abnormalities and is inherited as an autosomal dominant trait (Romano *et al.*, 1963; Ward, 1964). Jervell and Lange-Nielsen syndrome (JLN) is characterized by the presence of deafness (Jervell and Lange-Nielsen, 1957), a phenotypic abnormality inherited as an autosomal recessive trait.

In previous studies, we mapped genes for Romano-Ward syndrome to chromosomes 11p15.5 (LQT1), 7q35–q36 (LQT2), and 3p21–p24 (LQT3) (Keating *et al.*, 1991a,b; Jiang *et al.*, 1994). A fourth locus (LQT4) was mapped to chromosome 4q25–q27 (Schott *et al.*, 1995). We subsequently identified the genes for LQT1 (*KVLQT1*), LQT2 (*HERG*), and LQT3 (*SCN5A*) and the gene for another LQT locus, LQT5 (*KCNE1*), on chromosome 21q22.1–q22.2 (Wang *et al.*, 1995, 1996; Curran *et al.*, 1995; Warmke and Ganetzky, 1994; Gellens *et al.*, 1992; Splawski *et al.*, 1997b; Murai *et al.*, 1989). These genes encode ion channels involved in generation of the cardiac action potential (Sanguinetti *et al.*, 1995, 1996b; Barhanin *et al.*, 1996; Trudeau *et al.*, 1995; Gellens *et al.*, 1992). Mutations can lead to channel dysfunction and delayed myocellular repolarization. Because of regional heterogeneity of channel expression within the myocardium, the aberrant cardiac repolarization creates a substrate for arrhythmia. *KVLQT1* and *KCNE1* are also expressed in the inner ear (Neyroud *et al.*, 1997; Vetter *et al.*, 1996). We and others demonstrated that homozygous or compound heterozygous mutations in each of these genes can cause deafness and the severe cardiac phenotype of the Jervell and Lange-Nielsen syndrome (Neyroud *et al.*, 1997; Splawski, *et al.*, 1997b; Schulze-Bahr *et al.*, 1997; Tyson *et al.*, 1997; Duggal *et al.*, 1998). Loss of functional channels in the ear apparently disrupts the production of endolymph, leading to deafness. Additional mutation and expression studies have contributed to and expanded our understanding of

<sup>†</sup> To whom correspondence should be addressed at Eccles Institute of Human Genetics, 15 N 2030 E Room 6110B, University of Utah, Salt Lake City, UT 84112. Telephone: (801) 581-8904. Fax: (801) 585-7423. E-mail: mark@howard.genetics.utah.edu.

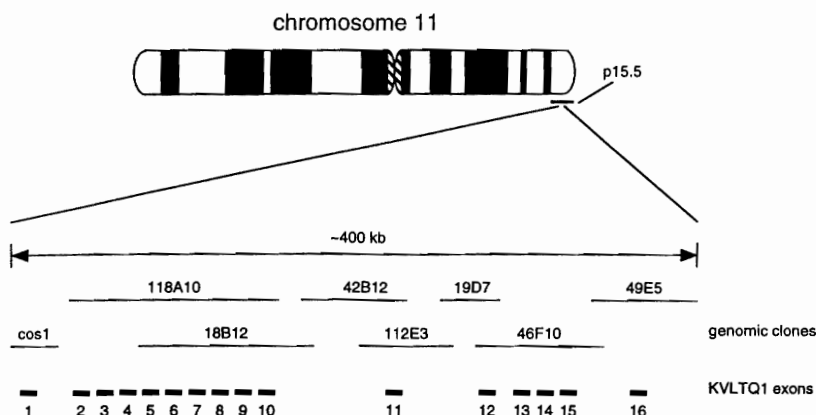


FIG. 1. Physical map and exon organization of *KVLQT1*. The genomic region of *KVLQT1* encompasses approximately 400 kb. Physical map of the minimal contig of overlapping P1 clones and of the cosmid containing exon 1 is shown. The location of *KVLQT1* exons relative to genomic clones is indicated. Sizes of exons and distances are not drawn to scale.

the molecular mechanisms of LQT (Donger *et al.*, 1997; Saarinen *et al.*, 1998; Tanaka *et al.*, 1997; Russell *et al.*, 1996; Schulze-Bahr *et al.*, 1995; Shalaby *et al.*, 1997; Wollnik *et al.*, 1997; Chouabe *et al.*, 1997; Sanguinetti *et al.*, 1996a; Bennett *et al.*, 1995; Dumaine *et al.*, 1996; Makita *et al.*, 1998; Kambouris *et al.*, 1998). Presymptomatic diagnosis of LQT is currently based on prolongation of the QT interval on electrocardiograms. QTc (QT interval corrected for heart rate) greater than 0.44 s has traditionally classified an individual as affected. Most LQT patients, however, are young, otherwise healthy individuals, who do not have electrocardiograms. Moreover, genetic studies have shown that QTc is neither sensitive nor specific (Vincent *et al.*, 1992). The spectrum of QTc intervals for gene carriers and noncarriers overlaps, leading to misclassifications. Noncarriers can have prolonged QTc intervals and be diagnosed as affected. Conversely, some LQT gene carriers have QTc intervals of  $\leq 0.44$  s but are still at increased risk for arrhythmia.

Genetic screening using mutational analysis can improve presymptomatic diagnosis. The presence of a mutation would unequivocally distinguish affected individuals and identify the gene underlying LQT even in small families and sporadic cases. To facilitate the identification of LQT-associated mutations, we defined the genomic structure of three LQT genes (*KVLQT1*, *HERG*, and *KCNE1*) and designed primer pairs for the amplification of each exon. Single-strand conformational polymorphism (SSCP) analyses identified additional mutations in *KVLQT1* and *HERG*.

## MATERIALS AND METHODS

**Isolation of cDNA clones.** (1) A cDNA probe containing exons 3 through 6 was used to isolate three full-length *KVLQT1* cDNA clones from an adult heart cDNA library prepared in the laboratory using SuperScript Choice system (Gibco BRL). (2) PCR products amplified from total human DNA containing *HERG* coding sequence were used as probes to screen the adult heart cDNA library and a hippocampal cDNA library (Stratagene). Isolated cDNA clones were used in subsequent rounds of screening. (3) *KCNE1* cDNA clones were isolated by screening the adult heart cDNA library with a PCR product amplified from total human DNA and containing the entire coding sequence.

**Isolation of genomic clones.** (1) *KVLQT1* P1 clones were isolated as described (Wang *et al.*, 1996). The cosmid containing exon 1 was isolated by screening a human genomic cosmid library (Stratagene) with a cDNA probe from exon 1. (2) PCR products containing *HERG* intronic sequences and amplified from total human DNA were used as probes to isolate *HERG* cosmid clones. (3) Full-length *KCNE1* cDNA was used as a probe to isolate two *KCNE1* cosmid clones.

**Exon-intron boundary determination.** All genomic clones were sequenced using primers designed to the cDNA sequences. The *KVLQT1* P1 clones were cycle sequenced using ThermoSequenase (Amersham Life Science). The *KVLQT1*, *HERG*, and *KCNE1* cosmids were sequenced by the dideoxy chain termination method on an Applied Biosystems Model 373A DNA sequencer. The exact exon-intron boundaries were determined by comparison of cDNA, genomic sequences, and known splice site consensus sequences.

**Design of PCR primers and PCR conditions.** Primers to amplify exons of the three genes were designed empirically or using OLIGO 4.0 (NBI). Amplification conditions were as follows:

(1) 94°C for 3 min followed by 30 cycles of 94°C for 10 s, 58°C for 20 s, and 72°C for 20 s, and a 5-min extension at 72°C.

(2) The same conditions as above were used but reactions had a final concentration of 10% glycerol and 4% formamide and were overlaid with mineral oil.

FIG. 2. Genomic organization of *KVLQT1* coding and 5'- and 3'- untranslated regions. Positions of the introns are indicated with arrowheads, and exons are numbered. The six putative transmembrane segments (S1 to S6) and the putative pore region (Pore) are underlined. The stop codon is denoted by an asterisk.





TABLE 1  
Intron-Exon Boundaries in *KVLQT1*

Exon	Intron	Exon	Intron
1	.. 5'-UTR...ATGGCCGCGG	(386+)	ACTTCGCCGTgtgagtatcg
2	tgtcttgcagCTTCCTCATC	(91)	CTTCTGGATGgtacgtagca
3	gtccctgcagGAGATCGTGC	(127)	TCCATCATCGgtgagtcacg
4	cactccacagACCTCATCGT	(79)	GGGCCATCAGgtgctgtgt
5	tccttcgcagGGGCATCCGC	(97)	CCACGCCAGgtgggtggcc
6	tctggcctagGAGCTGATAA	(141)	GTGGGGGTGgttaagtcgga
7	ctccctgcagGTACAGTCA	(111)	GCTCCAGCGgttaggtgccc
8	tccttcccagGGGATTCTTG	(96)	ACTCATTCAGgtgcggtgcc
9	ccacctcagACCGCATGGA	(123)	GTCTGTGGTGTgagtagcc
10	tttttttagTAAAGAAAA	(142)	GACAGTCTGTgtagaaccc
11	ttctcctcagTAAGGAAGAG	(121)	ACATCTCACagtgagtgcc
12	tcactgcagGCTGCGGGA	(76)	GAAATTCAGgttaagccctg
13	tgccccgcagCAAGCGCGGA	(95)	TGCAGAGGAGgtgggacgg
14	ttctctccagGCTGGACAG	(47)	TCCGTCTCAGgtgggtttct
15	tcctccatagAAAAGAGCAA	(62)	AGAAGACAAGgttaggtcac
16	gtccccgcagGTGACGCAGC	(237+)	GGGTCTCTGAT... 3'-UTR

TABLE 2  
Primers Used to Amplify *KVLQT1* Exons

Exon	Forward primer	Reverse primer	Size	(c) <sup>a</sup>
1	CTCGCCTTCGCTGCAGTCTC	GCGCGGGTCTAGGCTCACC	334	(2)
1	CGCCGCGCCCCAGTTGC	CAGAGCTCCCCACACCAG	224	(2)
2	ATGGGAGAGGCCGTGATGCTGAC	ATCCAGCCATGCCCTCAGATGC	165	(3)
3	GTTCAAACAGGTTGCAGGGTCTGA	CTTCTGTGCTGGAAACCTGG	256	(3)
4	CTCTTCCCTGGGGCCCTGGC	TGCGGGGAGCTTGTGGCACAG	170	(3)
5	TCAGCCCCACACCATCTCCTTC	CTGGGCCCCCTACCTTAACCC	154	(3)
6	TCCTGGAGCCCGACACTGTGTGT	TGTCTTGCCCACTCCTCAGCCT	238	(2)
7	TGGCTGACCACTGTCCCTCT	CCCCAGGACCCAGCTGTCCAA	195	(3)
8	GCTGGCAGTGGCCTGTGTGGA	AACAGTGACCAAAATGACAGTGAC	191	(3)
9	TGGCTCAGCAGGTGACAGC	TGGTGGCAGGTGGGCTACT	185	(1)
10	GCCTGGCAGACGATGTCCA	CAACTGCCCTGAGGGTTCCT	216	(1)
11	CTGTCCCCACACTTCTCCT	TGAGCTCCAGTCCCTCCAG	195	(1)
12	TGGCACTCACAATCTCCT	GCCTTGACACCCCTCCACTA	222	(1)
13	GGCACAGGAGGAGAAGTG	CGGCACCGCTGATCATGCA	216	(1)
14	CCAGGGCCAGGTGTGACTG	TGGGCCAGAGTAAGTGACA	119	(2)
15	GGCCCTGATTGGGTGTTTA	GGACGCTAACCAGAACCCAC	135	(2)
16	CACCACTGACTCTCTCGTCT	CCATCCCCAGCCCCATC	297	(2)

<sup>a</sup> Conditions of PCR (details under Materials and Methods).

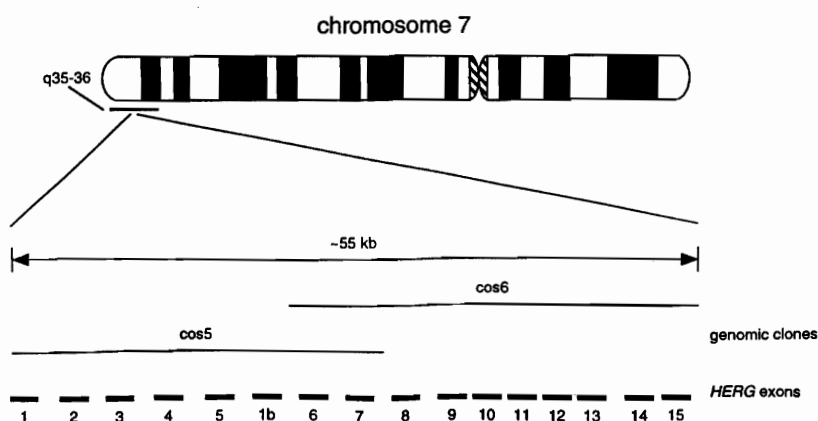
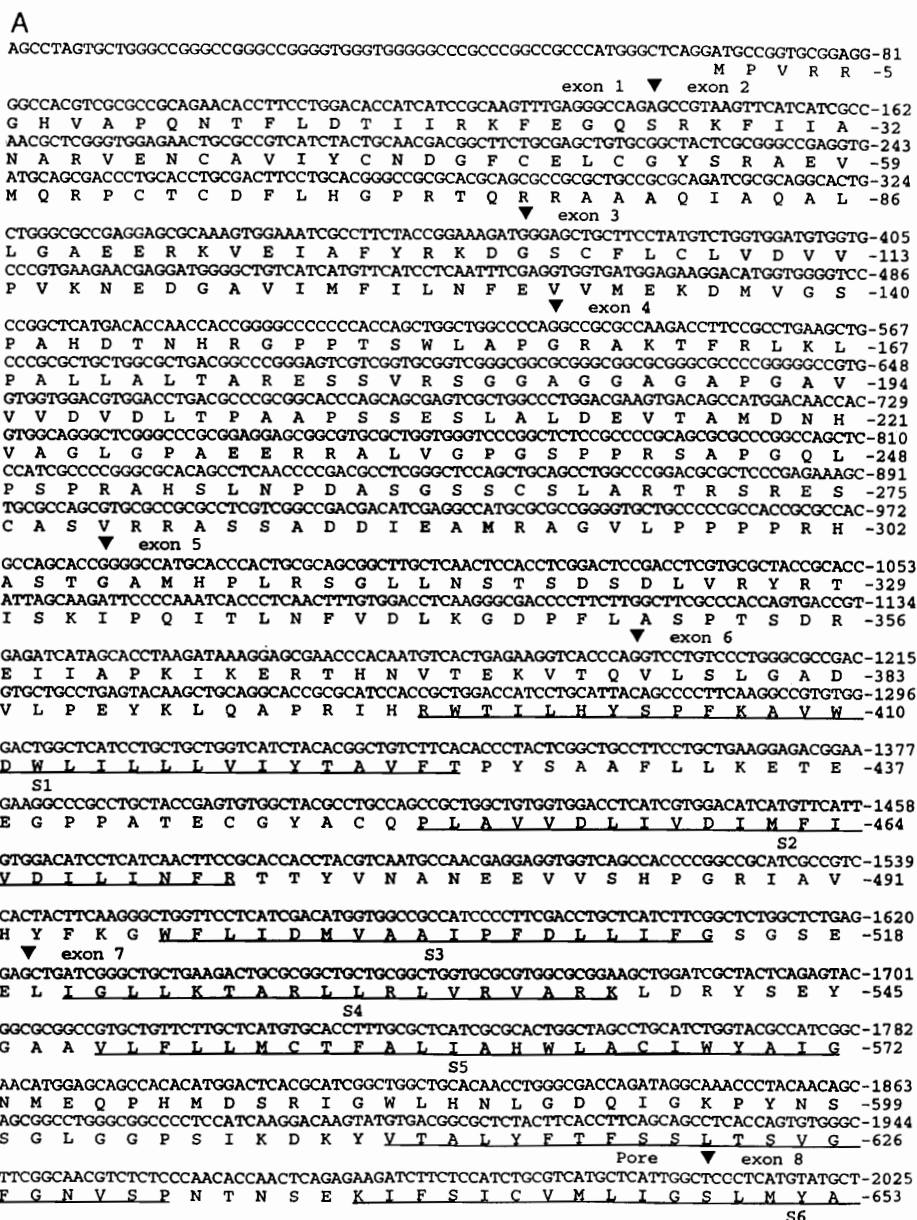


FIG. 3. Physical map and exon organization of *HERG*. The genomic region of *HERG* encompasses approximately 55 kb. The overlapping cosmid clones containing the entire *HERG* transcript sequence are shown. The location of *HERG* exons relative to genomic clones is indicated. Sizes of exons and distances are not drawn to scale.



**FIG. 4.** Genomic organization of *HERG* coding and 5'- and 3'- untranslated sequences. Positions of introns are indicated with arrowheads, and exons are numbered. The six putative membrane-spanning segments (S1 to S6) and the putative pore (Pore) and cyclic nucleotide-binding (cNBD) regions are underlined. The asterisks mark stop codons. (A) *HERG* splice form A. (B) Partial sequence of putative *HERG* splice form B. Exon 1b is spliced to exon 6 of *HERG* splice form A. The sequence of exon 1b is derived from genomic sequence.

(3) 94°C for 3 min followed by 5 cycles of 94°C for 10 s, 64°C for 20 s, and 72°C for 20 s, and 30 cycles of 94°C for 10 s, 62°C for 20 s, and 72°C for 20 s, and a 5-min extension at 72°C.

In the nested PCR for exons 1 and 11 of *HERG*, a 2- $\mu$ l aliquot from the initial reaction was used in the second reaction.

**Mutation analyses.** PCR samples were used in mutation detection and sequencing experiments as previously described (Splawski et al., 1997b).

**Phenotypic characterization.** Phenotypic criteria were identical to those used in our previous studies (Splawski et al., 1997a).

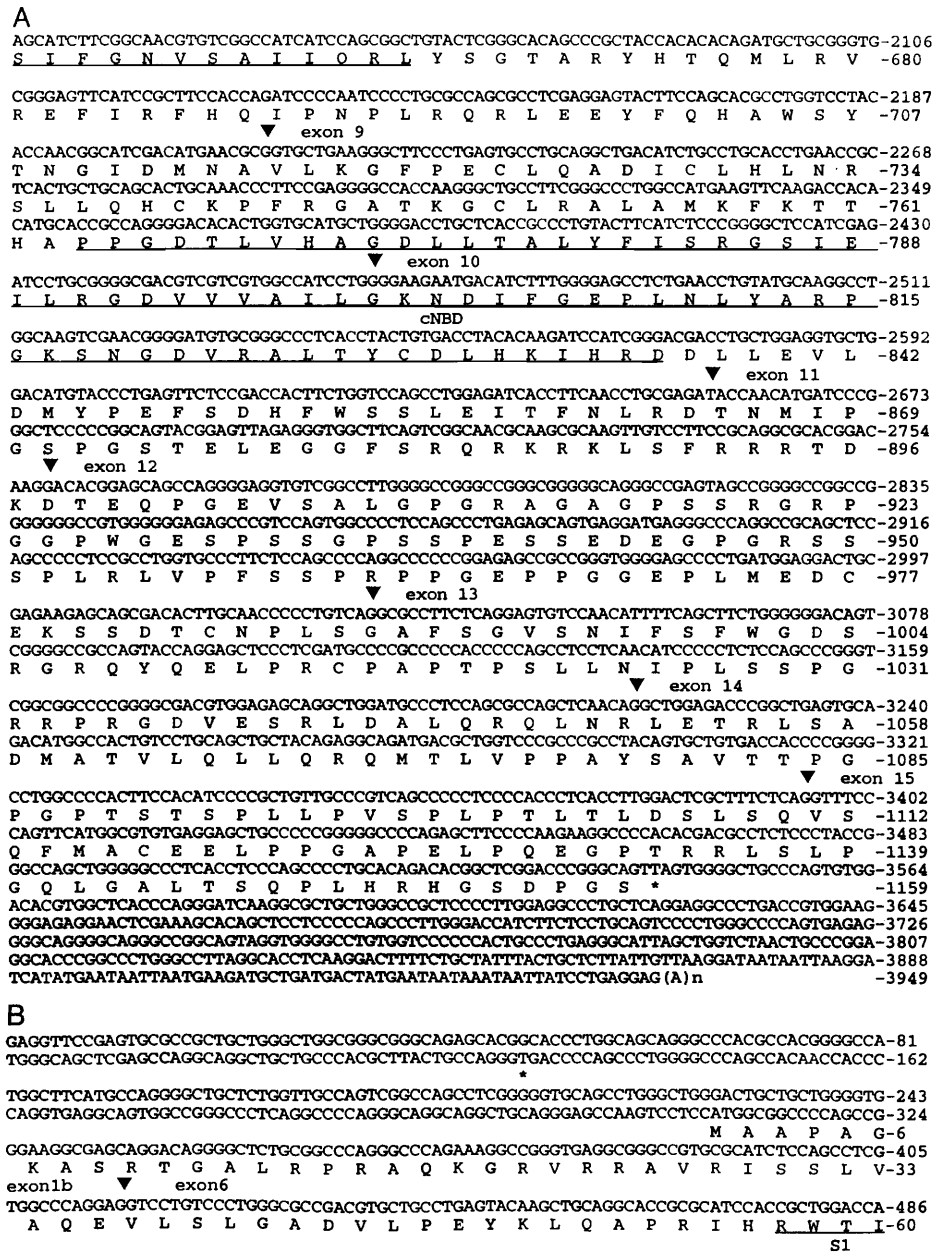


FIG. 4—Continued

## RESULTS

*KVLQT1* Genomic Structure and Primer Sets

Three full-length cDNA clones were isolated from an adult heart cDNA library. A 5'-cDNA probe gen-

erated from one of these clones was used to isolate cos1, a genomic cosmid clone containing exon 1. P1 genomic clones encompassing the rest of the *KVLQT1* cDNA were previously isolated (Wang *et al.*, 1996). These genomic clones span approxi-

TABLE 3  
Intron-Exon Boundaries in *HERG*

Exon	Intron	Exon	Intron
1	..5'UTR...ATGCCGGTGC	(76+)	GAGGGCCAGAgtagtgagg
2	gccccctagGCCGTAAGTT	(231)	CGGAAAGATGtaggagcgg
3	cactctgcaggGAGCTGCTT	(165)	CTGGCCCCAGtagtgtag
4	tetccccagGCCGCGCCAA	(444)	GCCAGCACCgtagggcgcc
5	ctccacctagGGCCATGCA	(212)	GGTCACCCAGtagggcgcc
1b	..5'UTR...ATGGCGCCCC	(108+)	GGCCAGGAGtaggtgaca
6	ccgggtgcagGTCTGTCTCC	(429)	CTCTGAGAGtaggggtcag
7	tgtccccagCTGATCGGGC	(388)	CTCATTGGCTgtgagtgtgc
8	acgccccagCCCTCATGTA	(200)	CATGAACGCGtagggccac
9	ctgccccagGTCTGAAGG	(253)	GCCATCTGGtagtggtg
10	tggcctccagGGAAGATGA	(194)	CCTCGAGATgtgagttggc
11	ttggttccagACCAACATGA	(100)	ACGGACAAGgtgaggcgcc
12	tttccacagACAGGAGCA	(273)	CCCCGTGACgtagtccggg
13	ctggctgcagCGCCTTCTC	(187)	AGCTCAACAGtagggaggt
14	cctgccccagGCTGGAGACC	(178)	GCTTCTCAGtagtcca
15	tgtattgcagGTTCCAGT	(150+)	GGGCAGTTAG...3'UTR

mately 400 kb on chromosome 11p15.5 (Fig. 1). To determine the exon structure and exon-intron boundaries, cos1 and P1 clones 118A10, 112E3, 46F10, and 49E5 were sequenced using primers designed to the cDNA. Comparison of the genomic and cDNA sequences of *KVLQT1* revealed the presence of 16 exons (Figs. 1 and 2 and Table 1). Exon size ranged from 47 bp (exon 14) to 1122 bp (exon 16). All intronic sequences contained the invariant GT and AG at the donor and acceptor splice sites, respectively (Table 1). One pair of PCR primers was designed to intron sequences flanking exons 2 through 16, and two pairs of primers with overlapping prod-

ucts were designed to exon 1 due to its large size (Table 2). These primers can be used to screen all *KVLQT1* exons.

#### *HERG Genomic Structure and Primer Sets*

Two full-length cDNA clones for splice form A were isolated by screening adult heart and hippocampal cDNA libraries. Neither splice form B nor other splice forms were found in 14 clones of different lengths isolated from the two libraries. Screening of a human cosmid library yielded two cosmids spanning approximately 55 kb and encompassing

TABLE 4  
Primers Used to Amplify *HERG* Exons

Exon	Forward primer	Reverse primer	Size	(c)
1o <sup>a</sup>	GGGCCACCCGAAGCCTAGT	CCGTCCCCTCGCCAAAGC	298	(2)
1i <sup>a</sup>	CCGCCCATGGGCTCAGG	CATCCACACTCGGAAGAGCT	162	(2)
2	GGTCCCGTCACGCGACTCT	TTGACCCCGCCCTGGTCGT	312	(2)
3	GGGCTATGTCTCCACTCT	AGCCTGCCCTAAAGCAAGTACA	213	(2)
4	CTCCGGGGTGTCTGGGAT	CACCAGCGCACGCCGCTCCT	284	(2)
4	GCCATGGACAACCACGTGGCA	CCCAGAATGCAGCAAGCCTG	339	(2)
5	GGCCTGACCACGCTGCCTCT	CCCTCTCCAAGCTCCTCAA	293	(2)
1b	GGTGCAGGTGAGGCAGTGG	CGGCCCCAGAAAGAAGAGGAA	216	(2)
6	CAGAGATGTCATCGCTCCTG	CAGGCGTAGCCACACTCGGTAG	295	(1)
6	TTCTGTCTGAAGGAGACGGAAG	TACACCACCTGCCCTCTGTCTGA	296	(1)
7	TGCCCCATCAACGGAATGTGC	GAAGTAGAGCGCGTCACATAC	333	(1)
7	GCCTGGGCGGCCCTCCATCAA	AGTTTCTTCCAACTTGGGTTT	210	(1)
8	GCAGAGGCTGACGGCCCCA	ACTTGTCTGTGTGCCAAGAG	321	(2)
9	ATGGTGGAGTGGAGTGTGGGTT	AGAAGGCTCGCACCTCTTGAG	390	(2)
10	GAGAGGTGCTGTGCTCTGG	ACAGCTGGAAGCAGGAGGATG	307	(2)
11o <sup>a</sup>	GGGCCCTGATACTGATTTTG	GCCCTGTGAAGTCCAAAAAGC	372	(2)
11i <sup>a</sup>	CCCTGATACTGATTTTGGTT	CACCCCGCCTTCCAGCTCC	193	(2)
12	TGAGGCCATCTCTGTCTTCC	GTAAGCGCACCAACCGCTGCCA	358	(2)
13	CTCACCAGCTCTGTCTCTG	CACCAGGACCTGGACCAAGCT	273	(2)
14	GTGGAGGCTGTCACTGGTGT	GAGGAAGCAGGGCTGGAGCTT	258	(2)
15	TGCCCATGCTCTGTGTATTG	CGGCCAGCAGCGCTTGATC	232	(2)

<sup>a</sup> Nested PCR was used to amplify exons 1 and 11 due to repetitive DNA sequences (o denotes outer and i denotes inner pair of primers).

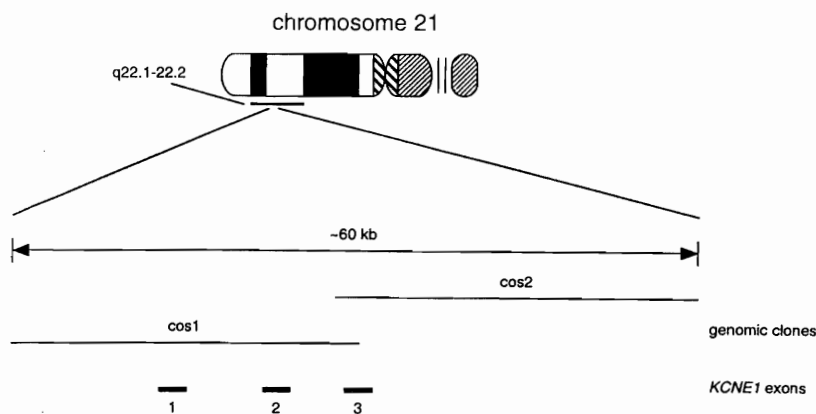


FIG. 5. Physical map and exon organization of *KCNE1*. The two cosmid clones spanning the entire *KCNE1* transcript are shown. Cosmid 1 does not extend to the end of exon 3, and cosmid 2 does not include exons 1 and 2. Sizes of the exons and distances are not drawn to scale.

all exons (Fig. 3). Exon-intron boundaries were determined by sequencing these cosmids with primers designed to the cDNA. Sequencing revealed the presence of 16 exons (Figs. 3 and 4 and Table 3) with sizes ranging from 100 bp (exon 11) to 553 bp (exon 15). Exon 1b sequence of putative *HERG* splice form B was derived from cos5 using primers designed to the published partial human sequence (Lees-Miller *et al.*, 1997). The 5'-end of exon 1b (Fig. 4B) was determined based on the mouse cDNA for

this splice form (Lees-Miller *et al.*, 1997). Intron donor and acceptor splice sites did not diverge from the invariant GT and AG. A single pair of primers was designed for most exons, and two pairs with overlapping products were designed for exons 4 through 7 (Table 4). Due to repetitive DNA sequences in flanking introns, nested PCR was used to amplify exons 1 and 11. This set of primers can be used to screen the entire coding sequence of *HERG* for mutations.

exon 1 ▼ exon 2  
ACACCCGGCTCTCTCGGCATCTCAGACCCGGGAAAAATCCCTCTGCTTTCTCTGGCCAGTTTTCACACAATCATCAGGTGAG-81  
▼ exon 3  
CCGAGGATCCATTTGGAGGAAGGCATTTATCTGTATCCAGAGGAATAGCCAAGGATATTCAGAGGTGTGCTGGGAAGTTTG-162  
AGCTGCAGCAGTGGAAACCTTAATGCCCCAGGATGATCTGTCTAACACCCACAGCGGTGACGCCCTTTCTGACCAAGCTGTGG-243  
M I L S N T T A V T P F L T K L W -17  
CAGGAGACAGTTTCAGCAGGGTGGCAACATGTCTGGCCCTGGCCCGCAGGTCCCCCGCAGCGGTGACGGCAAGCTGGAGGCC-324  
Q E T V Q Q G G N M S G L A R R S P R S G D G K L E A -44  
CTCTACGTCTCATGTTACTGGGATTTCTCGGCTTCTTACCTGGGCATCATGCTGAGCTACATCCGCTCCAGAAGCTG-405  
L Y V L M V L G F F G F F T L G I M L S Y I R S K K L -71  
GAGCACTCGAACGACCATTCACGCTACATCGAGTCCGATGCCCTGGCAAGAGAAGGACAAGGCCATATGTCCAGGCCCGG-486  
E H S N D P F N V Y I E S D A W Q E K D K A Y V Q A R -98  
GTCTGGAGAGCTACAGGTCGTGCTATGTCTGTTGAAAACCATCTGGCCATAGAACCAACCAACACACACCTTCTGAGAGC-567  
V L E S Y R S C Y V V E N H L A I E Q P N T H L P E T -125  
AAGCCTTCCCATGAACCCACCACTGGCTAACTGGACACCTCTGCTGGNNNNNAGATTTTCTAATCATCTCCTCTCA-648  
K P S P \*  
TACTCTTTATTGTGATGGATACCACTGGATTCTTTTGGCTGTTGTAANGGTGAGGGGTGGATTATGACACTGTTTCA-729  
CTGTTTCTCTAAAATCACGTTCTTTTGTGATAGACTGTCAAGTGTCCCCCATATCTGTCCCTGCCCTTGCTAAATTTAGCA-810  
GAATCCCTGAGGACATGGCCTCTGAGAATAGCAGTGCATTTCCACAGACTCCCTTGCACTAGCAAGGTGTGTGACTAAG-891  
CCCTGGCCAGTAGGCATGGAAAGTGAAGACTGTAATGTCCAAGTAATCTTGGAAAGAAAAGAACGTCGCCCTTAACCTTAACT-972  
TGTCCTGCTTCCAGTGGCTGGATGTGGAGGAGGTGGAGAGCAGTTATGAGACTGGGAAAGTTCGGGGCACTCAAAGAGCC-1053  
ACACACATCTGGGCCCTGGGCGACGTGGATCCTCTTACCACCCACAGGCCAGATTACAGGAGAGAGAAATCCACTCCAC-1134  
TCTTCTTAAGCCACTGTTATTCTGATCTCTGTTAAGGTGCGAGAAATCAATGCCCTTACTGATACACCTACCTTATAGGAC-1215  
TGAACCTAAAGGATGACATTTCCATACCTTGTACACAGCACACATGATCTGCCCCCTTGTCACCTTCTGTGCTCACTCTTGT-1296  
GGCTCTATCTCTCTGCCCCCTTCCGCTTCCACTCTCTCCCTTGACCCCATCTGCACACATCTCCCTGAAAACACACAGG-1377  
CACATACACTCATATACATAGACACACATACACACCTCAATCTAGAAAGAACTTGCTTTGTACAGGGCTGAGATGGAGGAG-1458  
AAAAAATGCCCTTCAGAAATGCATACCAAGGGGAAGGTGCTCGGTCACTGTGGGAGCAGGAAAGGTGCCCTCACTCCC-1539  
CGAGAGCCAGGGGAAGGAGTGGCTCTGGGCAGAGAGGACACATAGCACTGGGGTGGCAGGTCTTTTGGAGTGATGGGCC-1620  
GGTTTGTGAGATGAATTGTATCCCCAAAAAGACAGGTACCTTCAATGTGACCTAATTTGGGAAATAGAGTCTTTGCAGAT-1701  
G(A)<sub>n</sub> -1702

FIG. 6. Genomic organization of the *KCNE1* coding and 5'- and 3'- untranslated regions. Positions of the introns are indicated with arrowheads, and exons are numbered. The putative transmembrane segment is underlined. Note that both introns are within the 5'-untranslated region. The asterisk indicates the stop codon.



TABLE 7  
Summary of *KVLQT1* and *HERG* Mutations

Gene	Kindred number	Nucleotide change	Coding effect	Region of gene
<i>KVLQT1</i>	2625	G502A	Gly168Arg	S2
<i>KVLQT1</i>	2673	G502A	Gly168Arg	S2
<i>KVLQT1</i>	3698	G502A	Gly168Arg	S2
<i>KVLQT1</i>	19187	G940A	Gly314Ser	Pore
<i>KVLQT1</i>	22709	A944G	Tyr315Cys	Pore
<i>KVLQT1</i>	2762	G954C	Lys318Asn	Pore
<i>KVLQT1</i>	3401	T1058C	Leu353Pro	S6
<i>KVLQT1</i>	2824	C1096T	Arg366Trp	C-terminus
<i>HERG</i>	1663	G1714T	Gly572Cys	S5
<i>HERG</i>	2548	A1762G	Asn588Asp	S5/Pore
<i>HERG</i>	2554	C1841T	Ala614Val	Pore
<i>HERG</i> <sup>a</sup>	1697	C1841T	Ala614Val	Pore
<i>HERG</i> <sup>a</sup>	1789	T1889C	Val630Ala	Pore

<sup>a</sup> Mutations arose *de novo*.

familial cases and five were in sporadic cases. An abnormal band was observed in kindreds 2625, 2673, and 3698. The abnormal band was not observed in unaffected members of the three kindreds or in more than 200 control individuals. Sequencing revealed a nucleotide change causing an amino acid substitution (Table 7).

Further analysis identified abnormal conformers in five sporadic cases (Fig. 7). The abnormal conformers were not observed in more than 200 control individuals. Sequencing of the anomalous bands revealed point mutations leading to amino acid substitutions in all five individuals. The nucleotide changes, their coding effect, and their location in *KVLQT1* are summarized in Table 7.

SSCP analyses of *HERG* identified anomalous bands in affected individuals of five kindreds (Fig. 8 and Table 7). The anomalous conformers were absent in unaffected members of the families and in more than 200 controls. Sequencing revealed point mutations causing amino acid changes in all cases (Table 7). Two of the *HERG* mutations (K1697 and K1789) arose *de novo*. Highly polymorphic short tandem repeats were used to confirm maternity and paternity in both cases (data not shown).

No additional mutations were identified in *KCNE1*. This form of LQT is rare as we identified only two mutations in 280 unrelated individuals with LQT (Splawski *et al.*, 1997b).

## DISCUSSION

In this study we determined the genomic structure of three LQT genes, *KVLQT1*, *HERG* and *KCNE1*. Using intronic sequences, we designed PCR primers for the

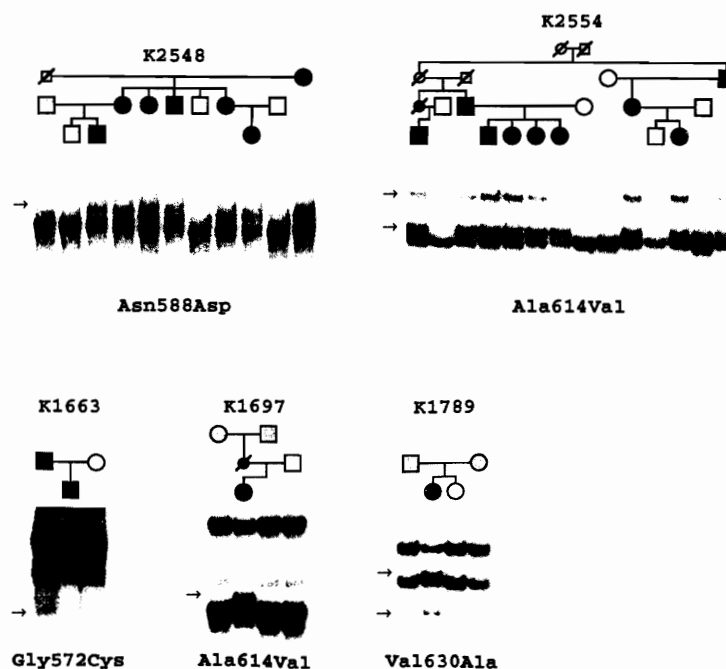


FIG. 8. *HERG* missense mutations associated with LQT. Results from SSCP analyses and the mutation effect on amino acid sequence are shown below each pedigree. Note that aberrant SSCP conformers (indicated by an arrow) cosegregate with the disease phenotype. Mutation information is summarized in Table 7.



amplification of newly defined exons. The entire coding sequence and the adjacent splice sites for *KVLQT1*, *HERG* and *KCNE1* can now be genetically screened for LQT-causing mutations. Mutation identification will improve presymptomatic diagnosis and therapy of this disorder.

Historically, diagnosis of LQT has been based on electrocardiographic findings of QTc greater than 0.44 s, presence of symptoms (syncope, seizures, and sudden death), and family history. Many LQT gene carriers have a prolonged QT interval on electrocardiograms, but diagnosis of LQT based solely on these criteria is difficult. The QT interval varies with gender, age, drug treatment, electrolytic abnormalities, and presence of other disease. Furthermore, the presence of symptoms and family history are not completely indicative of LQT. Genetic studies have shown overlap between QTc in LQT carriers and a control population. In one of our studies, using 0.44 s as a critical value resulted in misclassification rate of 11% (Vincent *et al.*, 1992). The rate was 20% in another study (Splawski *et al.*, 1997a). Misclassification leads to false-positive diagnosis with potential for unnecessary treatment. Misclassification can also result in false-negatives. The latter group (LQT carriers with QTc of 0.44 s or less) is more important as these patients may be at risk for tachyarrhythmias and sudden death. Another problem is that young people, the age group most often affected by arrhythmia in LQT, rarely undergo electrocardiographic screening.

The identification of mutations has implications for ion channel studies as well. The expression of mutant channels in *Xenopus* oocytes or mammalian cells can reveal how structural changes influence the behavior of the channel. These studies improve our understanding of channel function and provide insights into mechanisms of disease.

#### ACKNOWLEDGMENTS

We are indebted to the family members for their participation, to Dr. G. Vasudevan for referring patients, and to S. Odelberg and T. Olson for critically reading the manuscript. This work was supported by NHLBI RO1 HL48074, P50-HL52338-02, PHS Grant M01 RR00064, the Technology Access Section of the Utah Genome Center, and an award from Bristol-Myers Squibb.

#### REFERENCES

- Barhanin, J., Lesage, F., Guillemare, E., Fink, M., Lazdunski, M., and Romey, G. (1996). KvLQT1 and IsK (minK) proteins associate to form the IKs cardiac potassium current. *Nature* **384**: 78–80.
- Bennett, P. B., Yazawa, K., Makita, N., and George, A. L. (1995). Molecular mechanism for an inherited cardiac arrhythmia. *Nature* **376**: 683–685.
- Chouabe, C., Neyroud, N., Guicheney, P., Lazdunski, M., Romey, G., and Barhanin, J. (1997). Properties of KvLQT1 K<sup>+</sup> channel mutations in Romano-Ward and Jervell and Lange-Nielsen inherited cardiac arrhythmias. *EMBO J.* **16**: 5472–5479.
- Curran, M. E., Splawski, I., Timothy, K. W., Vincent, G. M., Green, E. D., and Keating, M. T. (1995). A molecular basis for cardiac arrhythmia: *HERG* mutations cause long QT syndrome. *Cell* **80**: 795–803.
- Donger, C., Denjoy, I., Berthet, M., Neyroud, N., Cruaud, C., Ben-naceur, M., Chivoret, G., Schwartz, K., Coumel, P., and Guicheney, P. (1997). KVLQT1 C-terminal missense mutation causes a forme fruste long-QT syndrome. *Circulation* **96**: 2778–2781.
- Duggal, P., Vesely, M. R., Wattanasirichaigoon, D., Villafane, J., Kaushik, V., and Beggs, A. H. (1998). Mutation of the gene for IsK associated with both Jervell and Lange-Nielsen and Romano-Ward forms of Long-QT syndrome. *Circulation* **97**: 142–146.
- Dumaine, R., Wang, Q., Keating, M. T., Hartmann, H. A., Schwartz, P. J., Brown, A. M., and Kirsch, G. E. (1996). Multiple mechanisms of sodium channel-linked long QT syndrome. *Circ. Res.* **78**: 916–924.
- Gellens, M., George, A., Chen, L., Chahine, M., Horn, R., Barchi, R., and Kallen, R. (1992). Primary structure and functional expression of the human cardiac tetrodotoxin-insensitive voltage-dependent sodium channel. *Proc. Natl. Acad. Sci. USA* **89**: 554–558.
- Jervell, A., and Lange-Nielsen, F. (1957). Congenital deaf-mutism, functional heart disease with prolongation of the QT interval, and sudden death. *Am. Heart J.* **54**: 59–68.
- Jiang, C., Atkinson, D., Towbin, J., Splawski, I., Lehmann, M., Li, H., Timothy, K., Taggart, R., Schwartz, P., Vincent, G., Moss, A., and Keating, M. (1994). Two long QT syndrome loci map to chromosome 3 and 7 with evidence for further heterogeneity. *Nat. Genet.* **8**: 141–147.
- Kambouris, N. G., Nuss, H. B., Johns, D. C., Tomaselli, G. F., Marban, E., and Balser, J. R. (1998). Phenotypic characterization of a novel long-QT syndrome mutation (R1623Q) in the cardiac sodium channel. *Circulation* **97**: 640–644.
- Keating, M., Atkinson, D., Dunn, C., Timothy, K., Vincent, G. M., and Leppert, M. (1991a). Linkage of a cardiac arrhythmia, the long QT syndrome, and the Harvey ras-1 gene. *Science* **252**: 704–706.
- Keating, M., Dunn, C., Atkinson, D., Timothy, K., Vincent, G. M., and Leppert, M. (1991b). Consistent linkage of the long QT syndrome to the Harvey ras-1 locus on chromosome 11. *Am. J. Hum. Genet.* **49**: 1335–1339.
- Lees-Miller, J. P., Kondo, C., Wang, L., and Duff, H. J. (1997). Electrophysiological characterization of an alternatively processed ERG K<sup>+</sup> channel in Mouse and Human Hearts. *Circ. Res.* **81**: 719–726.
- Makita, N., Shirai, N., Nagashima, N., Matsuo, R., Yamada, Y., Tohse, N., and Kitabatake, A. (1998). A de novo missense mutation of human cardiac Na<sup>+</sup> channel exhibiting novel molecular mechanisms of long QT syndrome. *FEBS Lett.* **423**: 5–9.
- Murai, T., Kakizuka, A., Takumi, T., Ohkubo, H., and Nakanishi, S. (1989). Molecular cloning and sequence analysis of human genomic DNA encoding a novel membrane protein which exhibits a slowly activating potassium channel activity. *Biochem. Biophys. Res. Commun.* **161**: 176–181.
- Neyroud, N., Tesson, F., Denjoy, I., Leibovici, M., Donger, C., Barhanin, J., Faure, S., Gary, F., Coumel, P., Petit, C., Schwartz, K., and Guicheney, P. (1997). A novel mutation in the potassium channel gene *KVLQT1* causes the Jervell and Lange-Nielsen cardioauditory syndrome. *Nat. Genet.* **15**: 186–189.
- Romano, C., Gemme, G., and Pongiglione, R. (1963). Artimie cardiach rare dell'eta pediatrica. II. Accessi sincopali per fibrillazione ventricolare parossistica. *Clin. Pediatr.* **45**: 656–683.
- Russell, M. W., Dick, M., Collins, F. S., and Brody, L. C. (1996). KVLQT1 mutations in three families with familial or sporadic long QT syndrome. *Hum. Mol. Genet.* **5**: 1319–1324.
- Saarela, K., Swan, H., Kainulainen, K., Toivonen, L., Viitasalo, M., and Kontula, K. (1998). Molecular genetics of the long QT syndrome: Two novel mutations of the KVLQT1 gene and phenotypic expression of the mutant gene in a large kindred. *Hum. Mutat.* **11**: 158–165.

- Sanguinetti, M. C., Curran, M. E., Spector, P. S., and Keating, M. T. (1996a). Spectrum of HERG K<sup>+</sup> channel dysfunction in an inherited cardiac arrhythmia. *Proc. Natl. Acad. Sci. USA* **93**: 2208–2212.
- Sanguinetti, M. C., Curran, M. E., Zou, A., Shen, J., Spector, P. S., Atkinson, D. L., and Keating, M. T. (1996b). Coassembly of KvLQT1 and minK (IsK) proteins to form cardiac IKs potassium channel. *Nature* **384**: 80–83.
- Sanguinetti, M. C., Jiang, C., Curran, M. E., and Keating, M. T. (1995). A mechanistic link between an inherited and an acquired cardiac arrhythmia: HERG encodes the IKr potassium channel. *Cell* **81**: 299–307.
- Schott, J., Charpentier, F., Peltier, S., Foley, P., Drouin, E., Bouhour, J., Donnelly, P., Vergnaud, G., Bachner, L., Moisan, J., Le Marec, H., and Pascal, O. (1995). Mapping of a gene for long QT syndrome to chromosome 4q25–27. *Am. J. Hum. Genet.* **57**: 1114–1122.
- Schulze-Bahr, E., Haverkamp, W., and Funke, W. (1995). The long-QT syndrome. *N. Engl. J. Med.* **333**: 1783–1784.
- Schulze-Bahr, E., Wang, Q., Wedekind, H., Haverkamp, W., Chen, Q., Sun, Y., Rubie, C., Hordt, M., Towbin, J., Borggrefe, M., Assmann, G., Qu, X., Somberg, J. C., Breithardt, G., Oberti, C., and Funke, H. (1997). *KCNE1* mutations cause Jervell and Lange-Nielsen syndrome. *Nat. Genet.* **17**: 267–268.
- Shalaby, F. Y., Levesque, P. C., Yang, W. P., Little, W. A., Conder, M. L., Jenkins-West, T., and Blarney, M. A. (1997). Dominant-negative KvLQT1 mutations underlie the LQT1 form of long QT syndrome. *Circulation* **96**: 1733–1736.
- Splawski, I., Timothy, K. W., Vincent, G. M., Atkinson, D. L., and Keating, M. T. (1997a). Molecular basis of the long-QT syndrome associated with deafness. *N. Engl. J. Med.* **336**: 1562–1567.
- Splawski, I., Tristani-Firouzi, M., Lehmann, M. H., Sanguinetti, M. C., and Keating, M. T. (1997b). Mutations in the hminK gene cause long QT syndrome and suppress I<sub>Kr</sub> function. *Nat. Genet.* **17**: 338–340.
- Tanaka, T., Nagai, R., Tomoike, H., Takata, S., Yano, K., Yabuta, K., Haneda, N., Nakano, O., Shibata, A., Sawayama, T., Kasai, H., Yazaki, Y., and Nakamura, Y. (1997). Four novel KVLQT1 and four novel HERG mutations in familial long-QT syndrome. *Circulation* **95**: 565–567.
- Trudeau, M. C., Warmke, J. W., Ganetzky, B., and Robertson, G. A. (1995). HERG, a human inward rectifier in the voltage-gated potassium channel family. *Science* **269**: 92–95.
- Tyson, J., Tranebjaerg, L., Bellman, S., Wren, C., Taylor, J. F. N., Bathen, J., Aslaksen, B., Sorland, S. J., Lund, O., Malcolm, S., Pembrey, M., Bhattacharya, S., and Bitner-Glindzicz, M. (1997). IsK and KvLQT1: Mutation in either of the two subunits of the slow component of the delayed rectifier potassium channel can cause Jervell and Lange-Nielsen syndrome. *Hum. Mol. Genet.* **6**: 2179–2185.
- Vetter, D. E., Mann, J. R., Wangemann, P., Liu, J., McLaughlin, K. J., Lesage, F., Marcus, D. C., Lazdunski, M., Heinemann, S. F., and Barhanin, J. (1996). Inner ear defects induced by null mutation of the isk gene. *Neuron* **17**: 1251–1264.
- Vincent, G. M., Timothy, K., Leppert, M., and Keating, M. (1992). The spectrum of symptoms and QT intervals in carriers of the gene for the long QT syndrome. *N. Engl. J. Med.* **327**: 846–852.
- Wang, Q., Curran, M. E., Splawski, I., Burn, T. C., Millholland, J. M., VanRaay, T. J., Shen, J., Timothy, K. W., Vincent, G. M., de Jager, T., Schwartz, P. J., Towbin, J. A., Moss, A. J., Atkinson, D. L., Landes, G. M., Connors, T. D., and Keating, M. T. (1996). Positional cloning of a novel potassium channel gene: KVLQT1 mutations cause cardiac arrhythmias. *Nat. Genet.* **12**: 17–23.
- Wang, Q., Shen, J., Splawski, I., Atkinson, D., Zhizhong, L., Robinson, J., Moss, A., Towbin, J., and Keating, M. (1995). *SCN5A* mutations associated with an inherited cardiac arrhythmia, long QT syndrome. *Cell* **80**: 805–811.
- Ward, O. (1964). A new familial cardiac syndrome in children. *J. Ir. Med. Assoc.* **54**: 103–106.
- Warmke, J., and Ganetzky, B. (1994). A family of potassium channel genes related to *eag* in *Drosophila* and mammals. *Proc. Natl. Acad. Sci. USA* **91**: 3438–3442.
- Wollnik, B., Schroeder, B. C., Kubisch, C., Esperer, H. D., Wieacker, P., and Jentsch, T. J. (1997). Pathophysiological mechanisms of dominant and recessive KVLQT1 K<sup>+</sup> channel mutations found in inherited cardiac arrhythmias. *Hum. Mol. Genet.* **6**: 1943–1949.

## CHAPTER 9

### NOVEL MUTATIONS IN LONG QT SYNDROME GENES:

#### *KVLQT1, HERG, SCN5A AND MINK*

##### Introduction

More than 300, 000 thousand people in the United States die suddenly each year, ventricular arrhythmias being responsible for most of these (Kannel et al., 1987; Willich et al., 1987). Despite their importance, presymptomatic diagnosis and treatment of life-threatening arrhythmias are difficult and in some cases medical therapy has increased the occurrence of arrhythmia. Until recently, the molecular mechanisms of cardiac arrhythmias were poorly understood.

Long QT is a cardiovascular disorder, characterized by an abnormality in cardiac repolarization, leading to prolonged QT interval on surface electrocardiograms. LQT causes episodic and abrupt loss of consciousness (syncope), seizures and sudden death, usually in young, otherwise healthy individuals (Jervell and Lange-Nielsen, 1957; Romano et al., 1963; Ward, 1964). The clinical features of LQT result from episodic ventricular tachyarrhythmias, such as *torsade de pointes* and ventricular fibrillation (Moss et al., 1991; Schwartz et al., 1975). Two inherited forms of LQT exist. The more common form, Romano-Ward syndrome, is not associated with other phenotypic abnormalities

and is inherited as an autosomal dominant trait (Romano et al., 1963; Ward, 1964). Jervell and Lange-Nielsen syndrome (JLN) is characterized by the presence of deafness, a phenotypic abnormality inherited as an autosomal recessive trait (Jervell and Lange-Nielsen, 1957).

In previous studies, we mapped LQT loci to chromosomes 11p15.5 (*LQT1*), 7q35-36 (*LQT2*), and *LQT3* to 3p21-24 (Jiang et al., 1994; Keating et al., 1991). A fourth locus (*LQT4*) was mapped to 4q25-27 (Schott et al., 1995). Our molecular genetic studies identified the genes responsible for the first three loci, *KVLQT1* (*LQT1*), *HERG* (*LQT2*), *SCN5A* (*LQT3*) and the gene for another LQT locus, *minK* (*LQT5*) at 21q22.1-22.2 (Curran et al., 1995; Splawski et al., 1997; Wang et al., 1996; Wang et al., 1995). These genes encode ion channels involved in the generation of the cardiac action potential, supporting the hypothesis that LQT results from delayed myocellular repolarization. *KVLQT1* and *minK* are also expressed in the inner ear (Neyroud et al., 1997; Vetter et al., 1996). We and others demonstrated that homozygous or compound heterozygous mutations in each of these genes can cause deafness and the severe cardiac phenotype of the Jervell and Lange-Nielsen syndrome (Duggal et al., 1998; Neyroud et al., 1997; Splawski et al., 1997; Tyson et al., 1997). The production of endolymph is apparently disrupted by the lack of functional channels in the ear, leading to deafness.

Presymptomatic diagnosis of LQT is currently based on prolongation of the QT interval on electrocardiograms. Genetic studies, however, have shown that diagnosis based solely on electrocardiogram reading is neither sensitive nor specific (Vincent et al., 1992). Genetic screening using mutational analysis can improve presymptomatic diagnosis. The presence of a mutation would unequivocally distinguish affected

individuals and identify the gene underlying LQT even in small families and sporadic cases. To improve genetic testing and enable genotype-phenotype correlation studies, we screened a pool of 350 unrelated individuals for mutations in the four defined genes.

## Methods

### Ascertainment and Phenotyping

Phenotypic criteria were identical to those used in our previous studies (Curran et al., 1995; Keating et al., 1991; Splawski et al., 1997). Individuals were evaluated for LQT based on QTc (the QT interval corrected for heart rate) and for the presence of syncope, seizures, and aborted sudden death. Individuals without any symptoms and a QTc of 0.41 seconds or less were classified as unaffected. Symptomatic individuals with QTc of 0.44 seconds or less and asymptomatic individuals with QTc between 0.41 seconds and 0.47 seconds were classified as uncertain. Symptomatic individuals with QTc of 0.45 seconds or greater and asymptomatic individuals with QTc of 0.47 seconds or greater were considered affected. Informed consent was obtained from all individuals or from their guardians in accordance with local institutional review board guidelines. Phenotypic data were interpreted without knowledge of genotype.

### SSCP Analysis

Genomic samples were amplified by PCR and used in SSCP analysis as previously described (Splawski et al., 1997). PCR was carried out with 75 ng DNA in a final volume of 10  $\mu$ l using a Perkin-Elmer Cetus 9600 thermocycler. Primer pairs for each exon and amplification conditions were the same as in Splawski et al., 1998.

Reactions were diluted with 40 µl of 0.1% SDS/10mM EDTA and with 30 µl of 95% formamide loading dye. The mixture was denatured at 94 °C for 5-10 min. and immediately placed on ice. Three µl of each sample was electrophoresed on 5% polyacrylamide gel (acrylamide:bisacrylamide 49:1) at 4°C and on 0.5X Mutation Detection Enhancement gel (MDE, FMC Bioproducts) at room temperature. Electrophoreses on the 5% gels were carried out at 40W for 3-5 hours and electrophoreses on 0.5X gels were run overnight at 350V. Gels were dried on 3MM filter paper and exposed to film for 18 hours at -70 °C.

### DNA Sequencing

Aberrant and normal SSCP bands were excised from the gel and eluted in 100 µl ddH<sub>2</sub>O at 65°C for 30 min. Ten µl of the eluted DNA was used as a template in a second 100 µl PCR reaction using the original primer pair. Products were washed 3X with 400 µl ddH<sub>2</sub>O in Microcon 100 microconcentrators (Amicon). DNA was directly sequenced in both directions by the dideoxy chain termination method, using the original primers, on an Applied Biosystems model 373A DNA sequencer (Applied Biosystems).

## Results

### *KVLQT1* Mutations Associated with LQT in 59 Cases

SSCP analysis was used to screen 350 unrelated individuals with inherited, sporadic or acquired LQT for mutations in *KVLQT1* (chromosome 11p15.5, LQT1). Seventeen primer pairs were used to amplify the 16 exons of *KVLQT* (Splawski et al.,

1998). PCR products were subjected to electrophoresis under two different conditions. Abnormal bands were sequenced and the cause of the mobility shift determined. *KVLQT1* mutations associated with LQT were identified in 59 individuals (bringing the total number of *KVLQT1* mutations that we have identified to 79, Figure 9.1, Tables 9.1 and 9.2). Twenty-seven had not been described before.

Most *KVLQT1* mutations associated with LQT were missense mutations. Forty five abnormal bands revealed single nucleotide changes leading to amino acid substitutions. Six nucleotide changes found in samples from unrelated individuals resulted in termination signals. These alleles would lead to the production of truncated KVLQT1 proteins. Seven abnormal conformers harbored single nucleotide changes in conserved splice junction sequences. These changes would impair intron excision leading to aberrant mRNAs. We also found a three base pair deletion leading to an in-frame deletion of a single amino acid.

#### *HERG* Mutations Associated with LQT in 70 Cases

Samples from the same group of 350 LQT patients were next screened for mutations in *HERG* (chromosome 7q36-36, *LQT2*). Twenty-one primer pairs were used to amplify the 16 exons of *HERG* (Splawski et al., 1998) and PCR products were subjected to electrophoresis under two conditions. *HERG* mutations were identified in members of 70 LQT families or sporadic cases (total number of *HERG* mutations that we have identified is 81; Figure 9.2, Tables 9.2 and 9.3). Fifty-seven of these mutations were novel. Most of them were missense or frameshift mutations. Sequencing of 44 aberrant SSCP conformers revealed single nucleotide changes resulting in amino acid substitutions.

**Figure 9.1** Schematic representation of the predicted topology of KVLQT1 and locations of LQT-associated mutations.

KVLQT1 consists of six putative transmembrane segments (S1 to S6) and a pore (Pore) region. The approximate location and type of LQT-associated mutations are shown with colored circles. Missense mutations are shown as black circles, red circles denote splice site mutations, pink circles - amino acid deletions, green circles - frameshift mutations, blue circles - nonsense mutations and orange circles illustrate common polymorphisms. The coding effect of each mutation is shown in the respective color. The number of mutations at each site is in parenthesis following the coding effect. Mutation information is summarized in Tables 9.1 and 9.2.



missense  
nonsense  
frameshift  
**splice**  
AA deletion

# KVLQT1

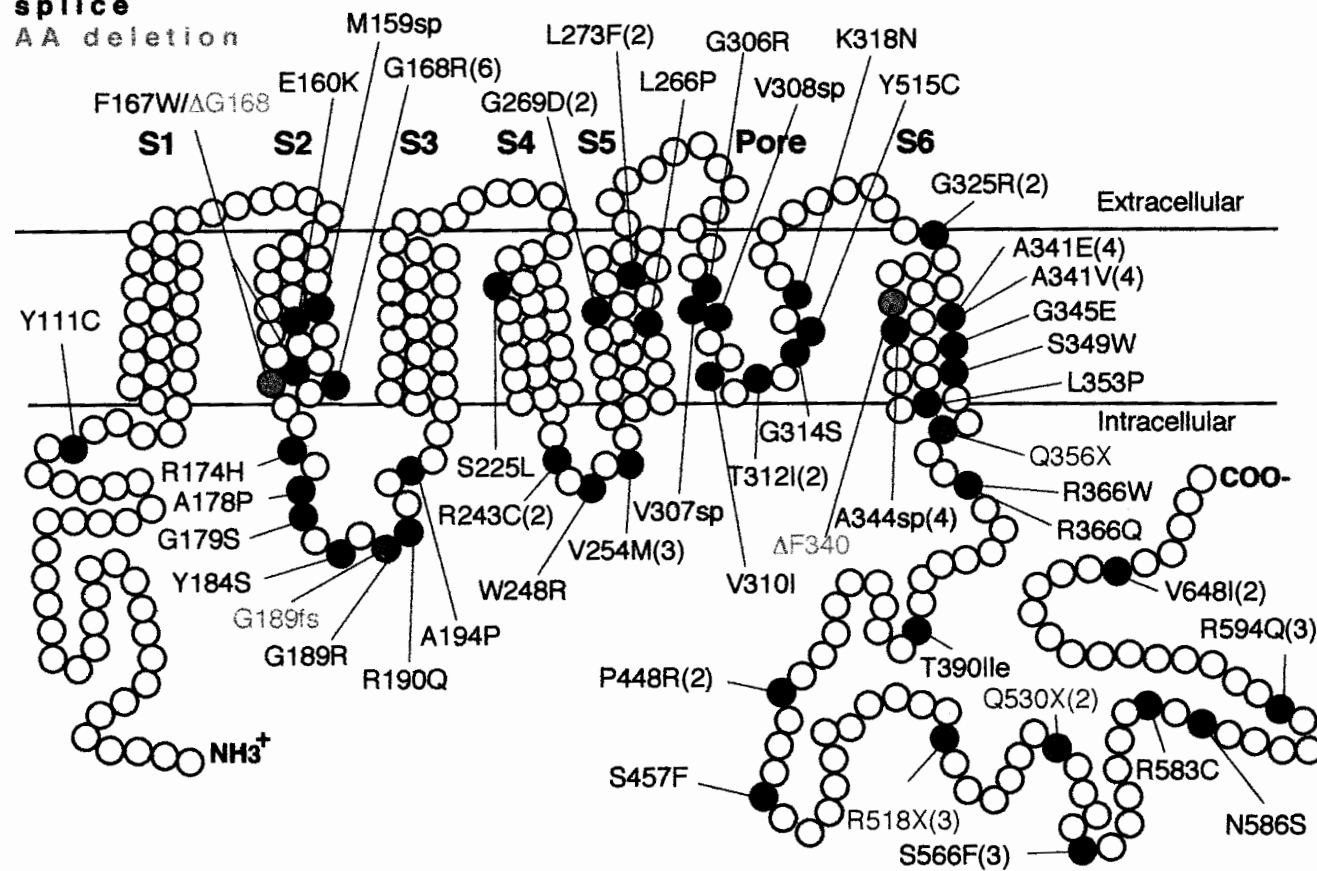


**Table 9.1**Summary of *KVLQT1* mutations

gene	nucleotide change	coding effect	position	exon	kindred	study
<i>KVLQT1</i>	A332G	Tyr111Cys*	N-term.	1	2994	This study
<i>KVLQT1</i>	G477+1A	splice*	S2	2	1789	This study
<i>KVLQT1</i>	G478A	Glu160Lys*	S2	3	1789	This study
<i>KVLQT1</i>	Δ500-502	F167W/ΔG168	S2	3	1789	Wang et al.(96)
<i>KVLQT1</i>	G502A	Gly168Arg	S2	3	1757	This study
<i>KVLQT1</i>	G502A	Gly168Arg	S2	3	2625	Splawski et al.(98)
<i>KVLQT1</i>	G502A	Gly168Arg	S2	3	2673	Splawski et al.(98)
<i>KVLQT1</i>	G502A	Gly168Arg	S2	3	2717	This study
<i>KVLQT1</i>	G502A	Gly168Arg	S2	3	2721	This study
<i>KVLQT1</i>	G502A	Gly168Arg	S2	3	3698	Splawski et al.(98)
<i>KVLQT1</i>	G521A	Arg174His*	S2/S3	3	FamC	This study
<i>KVLQT1</i>	G532C	Ala178Pro	S2/S3	3	1789	Wang et al.(96)
<i>KVLQT1</i>	G535A	Gly179Ser*	S2/S3	3	1796	This study
<i>KVLQT1</i>	A551C	Tyr184Ser*	S2/S3	3	3476	This study
<i>KVLQT1</i>	G565A	Gly189Arg	S2/S3	3	2557	Wang et al.(96)
<i>KVLQT1</i>	iG567-568	Gly189fs	S2/S3	3	2948	Splawski et al.(97b)
<i>KVLQT1</i>	G569A	Arg190Gln	S2/S3	3	1789	Wang et al.(96)
<i>KVLQT1</i>	G580C	Ala194Pro*	S2/S3	3	3433	This study
<i>KVLQT1</i>	C674T	Ser225Leu*	S4	4	3732	This study

Table 9.1 Continued

gene	nucleotide change	coding effect	position	exon	kindred	study
<i>KVLQT1</i>	C727T	Arg243Cys*	S4/S5	5	2836	This study
<i>KVLQT1</i>	C727T	Arg243Cys*	S4/S5	5	3547	This study
<i>KVLQT1</i>	T742C	Trp248Arg*	S4/S5	5	2911	This study
<i>KVLQT1</i>	G760A	Val254Met	S4/S5	5	1532	Wang et al.(96)
<i>KVLQT1</i>	G760A	Val254Met	S4/S5	5	1789	This study
<i>KVLQT1</i>	G760A	Val254Met	S4/S5	5	FamJ	This study
<i>KVLQT1</i>	T797C	Leu266Pro*	S5	6	3642	This study
<i>KVLQT1</i>	G806A	Gly269Asp	S5	6	1789	This study
<i>KVLQT1</i>	G806A	Gly269Asp	S5	6	2719	This study
<i>KVLQT1</i>	C817T	Leu273Phe	S5	6	1777	Wang et al.(96)
<i>KVLQT1</i>	C817T	Leu273Phe	S5	6	2804	This study
<i>KVLQT1</i>	G921+1T	splice*	Pore	6	2762	This study
<i>KVLQT1</i>	A922-2C	splice*	Pore	7	1789	This study
<i>KVLQT1</i>	G916A	Gly306Arg	Pore	7	1789	Wang et al.(96)
<i>KVLQT1</i>	G928A	Val310Ile*	Pore	7	3327	This study
<i>KVLQT1</i>	C935T	Thr312Ile	Pore	7	1789	Wang et al.(96)
<i>KVLQT1</i>	C935T	Thr312Ile	Pore	7	3546	This study
<i>KVLQT1</i>	G940A	Gly314Ser	Pore	7	1789	Splawski et al.(98)
<i>KVLQT1</i>	A944G	Tyr315Cys	Pore	7	1789	Splawski et al.(98)
<i>KVLQT1</i>	G955C	Lys318Asn	Pore	7	2762	Splawski et al.(98)

Table 9.1 Continued

gene	nucleotide change	coding effect	position	exon	kindred	study
<i>KVLQT1</i>	G973A	Gly325Arg	S6	7	2050	This study
<i>KVLQT1</i>	G973A	Gly325Arg	S6	7	2546	This study
<i>KVLQT1</i>	$\Delta$ 1017-1019	$\Delta$ F340*	S6	7	2628	This study
<i>KVLQT1</i>	C1022A	Ala341Glu	S6	7	1723	Wang et al.(96)
<i>KVLQT1</i>	C1022A	Ala341Glu	S6	7	1805	This study
<i>KVLQT1</i>	C1022A	Ala341Glu	S6	7	2931	This study
<i>KVLQT1</i>	C1022A	Ala341Glu	S6	7	3430	This study
<i>KVLQT1</i>	C1022T	Ala341Val	S6	7	1807	Wang et al.(96)
<i>KVLQT1</i>	C1022T	Ala341Val	S6	7	2737	This study
<i>KVLQT1</i>	C1022T	Ala341Val	S6	7	2807	This study
<i>KVLQT1</i>	C1022T	Ala341Val	S6	7	2819	This study
<i>KVLQT1</i>	G1032A	splice	S6	7	2613	This study
<i>KVLQT1</i>	G1032A	splice	S6	7	2815	This study
<i>KVLQT1</i>	G1032A	splice	S6	7	2950	This study
<i>KVLQT1</i>	G1032A	splice	S6	7	3770	This study
<i>KVLQT1</i>	G1034A	Gly345Glu	S6	8	2605	Wang et al.(96)
<i>KVLQT1</i>	C1046G	Ser349Trp*	S6	8	2924	This study
<i>KVLQT1</i>	T1058C	Leu353Pro	S6	8	3401	Splawski et al.(98)
<i>KVLQT1</i>	C1066T	Gln356Stop	C-term.	8	2917	This study
<i>KVLQT1</i>	C1096T	Arg366Trp	C-term.	8	2824	Splawski et al.(98)

Table 9.1 Continued

gene	nucleotide change	coding effect	position	exon	kindred	study
<i>KVLQT1</i>	G1097A	Arg366Gln*	C-term.	8	2813	This study
<i>KVLQT1</i>	C1172T	Thr390Ile*	C-term.	9	4021	This study
<i>KVLQT1</i>	C1343G	Pro448Arg*	C-term.	10	1789	This study
<i>KVLQT1</i>	C1343G	Pro448Arg*	C-term.	10	3335	This study
<i>KVLQT1</i>	C1370T	Ser457Phe*	C-term.	10	KTim	This study
<i>KVLQT1</i>	C1552T	Arg518Stop*	C-term.	12	1795	This study
<i>KVLQT1</i>	C1552T	Arg518Stop*	C-term.	12	2620	This study
<i>KVLQT1</i>	C1552T	Arg518Stop*	C-term.	12	2671	This study
<i>KVLQT1</i>	C1588T	Gln530Stop*	C-term.	12	2229	This study
<i>KVLQT1</i>	C1588T	Gln530Stop*	C-term.	12	4021	This study
<i>KVLQT1</i>	C1697T	Ser566Phe*	C-term.	14	1789	This study
<i>KVLQT1</i>	C1697T	Ser566Phe*	C-term.	14	2728	This study
<i>KVLQT1</i>	C1697T	Ser566Phe*	C-term.	14	4026	This study
<i>KVLQT1</i>	C1747T	Arg583Cys*	C-term.	15	3798	This study
<i>KVLQT1</i>	A1757G	Asn586Ser*	C-term.	15	KTim	This study
<i>KVLQT1</i>	G1781A	Arg594Gln*	C-term.	15	1789	This study
<i>KVLQT1</i>	G1781A	Arg594Gln*	C-term.	15	2020	This study
<i>KVLQT1</i>	G1781A	Arg594Gln*	C-term.	15	3327	This study
<i>KVLQT1</i>	G1942A	Val648Ile*	C-term.	16	2577	This study

**Table 9.1** Continued

gene	nucleotide change	coding effect	position	exon	kindred	study
<i>KVLQT1</i>	G1942A	Val648Ile*	C-term.	16	2795	This study

\* - denotes novel mutation

**Table 9.2**

Mutations identified in our laboratory

Locus	<i>LQT1</i>	<i>LQT2</i>	<i>LQT3</i>	<i>LQT5</i>	All
Gene	<i>KVLQT1</i>	<i>HERG</i>	<i>SCN5A</i>	<i>minK</i>	genes
Location	11p15.5	7q35-36	3p21	21q22	total
Mutations found in this study	59(37)*	70(61)	8(7)	1(1)	138(106)
Novel mutations	37(27)	63(57)	4(4)	1(1)	105(89)
Total mutations found	79(49)	81(69)	14(8)	3(3)	177(129)

\*Number in parenthesis denotes how many of the mutations were distinct

**Figure 9.2** Schematic representation of the predicted topology of HERG and locations of LQT-associated mutations.

HERG consists of six putative transmembrane segments (S1 to S6) and a pore (Pore) region. Symbols describing the mutations are the same as in Figure 9.1. Mutation information is summarized in Tables 9.2 and 9.3.



**missense**  
**nonsense**  
**frameshift**  
**splice**  
 AA deletion

# HERG

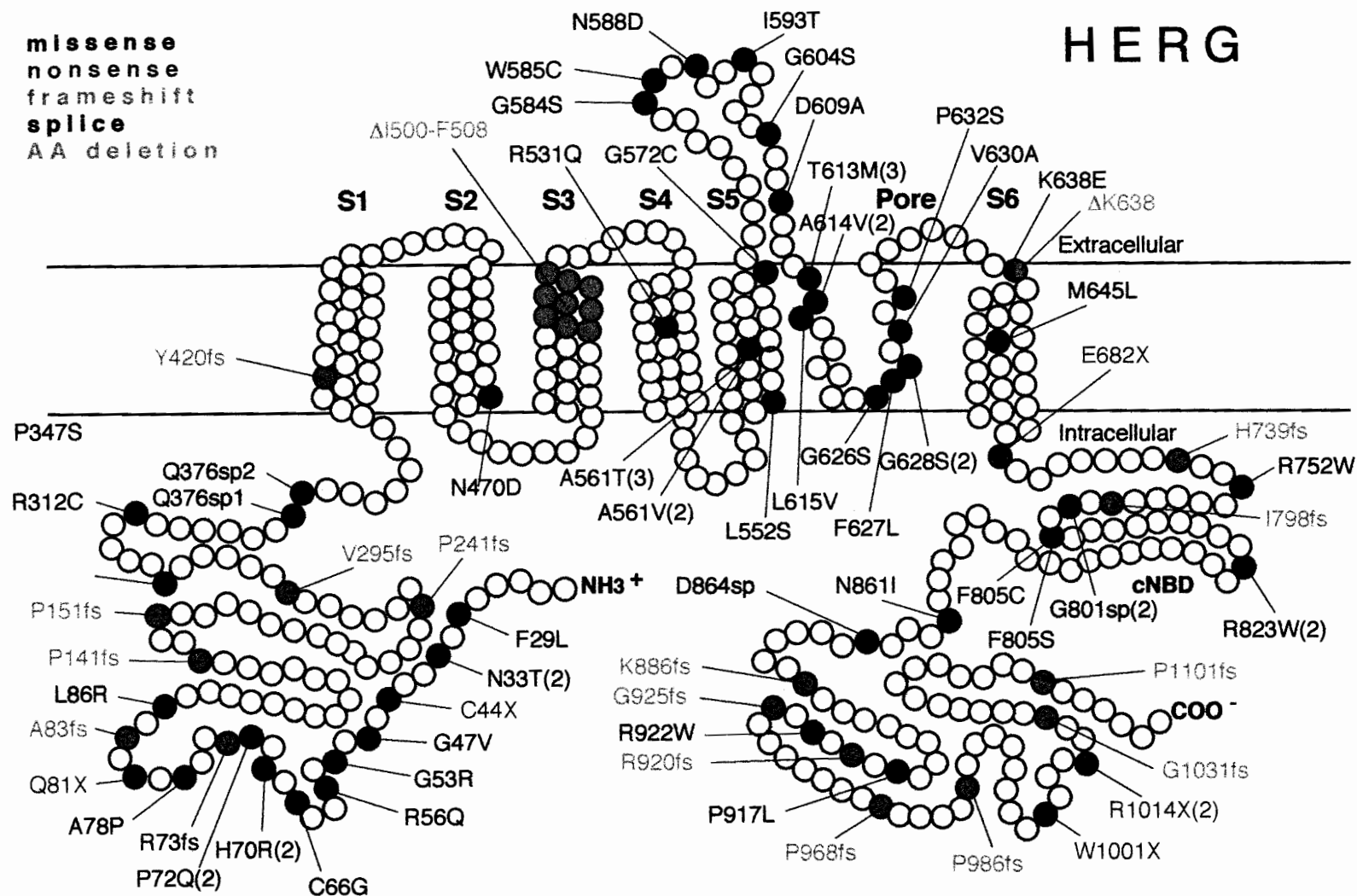


**Table 9.3**Summary of *HERG* Mutations

gene	nucleot. change	coding effect	position	exon	kindred	study
<i>HERG</i>	C87A	Phe29Leu*	N-term.	2	2228	This study
<i>HERG</i>	A98C	Asn33Thr*	N-term.	2	2254	This study
<i>HERG</i>	A98C	Asn33Thr*	N-term.	2	3378	This study
<i>HERG</i>	C132A	Cys44Stop*	N-term.	2	2751	This study
<i>HERG</i>	G140T	Gly47Val*	N-term.	2	2544	This study
<i>HERG</i>	G157C	Gly53Arg*	N-term.	2	1789	This study
<i>HERG</i>	G167A	Arg56Gln*	N-term.	2	2553	This study
<i>HERG</i>	T196G	Cys66Gly*	N-term.	2	2755	This study
<i>HERG</i>	A209G	His70Arg*	N-term.	2	2796	This study
<i>HERG</i>	A209G	His70Arg*	N-term.	2	2971	This study
<i>HERG</i>	C215A	Pro72Gln*	N-term.	2	2551	This study
<i>HERG</i>	C215A	Pro72Gln*	N-term.	2	2822	This study
<i>HERG</i>	D221-251	Arg73fs*	N-term.	2	2840	This study
<i>HERG</i>	G232C	Ala78Pro*	N-term.	2	2920	This study
<i>HERG</i>	dupl234-250	Ala83fs*	N-term.	2	1778	This study
<i>HERG</i>	C241T	Gln81Stop*	N-term.	2	2711	This study
<i>HERG</i>	T257G	Leu86Arg*	N-term.	2	1756	This study
<i>HERG</i>	iC422-423	Pro141fs*	N-term.	3	1740	This study
<i>HERG</i>	iC453-454	Pro151fs*	N-term.	3	2988	This study

**Table 9.3** Continued

gene	nucleot. change	coding effect	position	exon	kindred	study
<i>HERG</i>	iC724-725	Pro241fs*	N-term.	4	2172	This study
<i>HERG</i>	ΔG885	Val295fs*	N-term	4	2547	This study
<i>HERG</i>	C934T	Arg312Cys*	N-term.	5	2622	This study
<i>HERG</i>	C1039T	Pro347Ser*	N-term	5	2796	This study
<i>HERG</i>	G1128A	splice*	N-term	5	3332	This study
<i>HERG</i>	A1129-2G	splice*	N-term.	6	2941	This study
<i>HERG</i>	ΔA1261	Tyr420fs	S1	6	2595	Curran et al.(95)
<i>HERG</i>	A1408G	Asn470Asp	S2	6	2596	Curran et al.(95)
<i>HERG</i>	Δ1498-1524	Δ500-508	S3	6	2287	Curran et al.(95)
<i>HERG</i>	G1592A	Arg531Gln*	S4	7	1697	This study
<i>HERG</i>	T1655C	Leu552Ser*	S5	7	1816	This study
<i>HERG</i>	G1681A	Ala561Thr	S5	7	2985	This study
<i>HERG</i>	G1681A	Ala561Thr	S5	7	3414	This study
<i>HERG</i>	G1681A	Ala561Thr	S5	7	3985	This study
<i>HERG</i>	C1682T	Ala561Val	S5	7	1956	Curran et al.(95)
<i>HERG</i>	C1682T	Ala561Val	S5	7	3439	This study
<i>HERG</i>	G1714T	Gly572Cys	S5	7	1663	Splawski et al.(98)
<i>HERG</i>	G1750A	Gly584Ser*	S5/Pore	7	3651	This study
<i>HERG</i>	G1755T	Trp585Cys*	S5/Pore	7	1789	This study
<i>HERG</i>	A1762G	Asn588Asp	S5/Pore	7	2548	Splawski et al.(98)

Table 9.3 Continued

gene	nucleot. change	coding effect	position	exon	kindred	study
<i>HERG</i>	T1778C	Ile593Thr*	S5/Pore	7	3851	This study
<i>HERG</i>	G1810A	Gly604Ser*	S5/Pore	7	2750	This study
<i>HERG</i>	G1825A	Asp609Asn*	S5/Pore	7	1761	This study
<i>HERG</i>	C1838T	Thr613Met*	Pore	7	1789	This study
<i>HERG</i>	C1838T	Thr613Met*	Pore	7	1789	This study
<i>HERG</i>	C1838T	Thr613Met*	Pore	7	1989	This study
<i>HERG</i>	C1841T	Ala614Val	Pore	7	1697	Splawski et al.(98)
<i>HERG</i>	C1841T	Ala614Val	Pore	7	2554	Splawski et al.(98)
<i>HERG</i>	C1843G	Leu615Val	Pore	7	FamT	This study
<i>HERG</i>	G1876A	Gly626Ser*	Pore	7	2672	This study
<i>HERG</i>	C1881G	Phe627Leu*	Pore	7	2925	This study
<i>HERG</i>	G1882A	Gly628Ser	Pore	7	2011	This study
<i>HERG</i>	G1882A	Gly628Ser	Pore	7	2269	Curran et al.
<i>HERG</i>	T1889C	Val630Ala	Pore	7	1789	Splawski et al.(98)
<i>HERG</i>	C1894T	Pro632Ser*	Pore	7	2740	This study
<i>HERG</i>	A1912G	Lys638Glu*	S6	7	2814	This study
<i>HERG</i>	D1913-5	DLys638*	S6	7	3459	This study
<i>HERG</i>	A1933T	Met645Leu*	S6	7	3376	This study
<i>HERG</i>	G2044T	Glu682Stop*	S6/cNBD	8	1758	This study
<i>HERG</i>	iT2218-2219	His739fs*	S6/cNBD	9	2602	This study

Table 9.3 Continued

gene	nucleot. change	coding effect	position	exon	kindred	study
<i>HERG</i>	C2254T	Arg752Trp*	S6/cNBD	9	2974	This study
<i>HERG</i>	ΔC2395	Ile798fs*	cNBD	9	2961	This study
<i>HERG</i>	G2398+1C	splice	cNBD	9	2015	Curran et al.(95)
<i>HERG</i>	G2398+1C	splice	cNBD	9	2027	This study
<i>HERG</i>	T2414C	Phe805Ser*	cNBD	10	3354	This study
<i>HERG</i>	T2414G	Phe805Cys*	cNBD	10	1977	This study
<i>HERG</i>	C2467T	Arg823Trp*	cNBD	10	2103	This study
<i>HERG</i>	C2467T	Arg823Trp*	cNBD	10	2723	This study
<i>HERG</i>	A2582T	Asn861Ile*	C-term.	10	1815	This study
<i>HERG</i>	G2592+1A	splice*	C-term.	10	1805	This study
<i>HERG</i>	ΔG2660	Lys886fs*	C-term.	11	3351	This study
<i>HERG</i>	C2750T	Pro917Leu*	C-term.	12	1789	This study
<i>HERG</i>	ΔG2762	Arg920fs*	C-term.	12	3452	This study
<i>HERG</i>	C2764T	Arg922Trp*	C-term.	12	1754	This study
<i>HERG</i>	iG2775-2776	Gly925fs*	C-term.	12	2913	This study
<i>HERG</i>	ΔG2906	Pro968fs*	C-term.	12	2627	This study
<i>HERG</i>	Δ2959-2960	Pro986fs*	C-term.	12	2997	This study
<i>HERG</i>	G3003A	Trp1001Stop*	C-term.	13	2808	This study
<i>HERG</i>	ΔC3094	Gly1031fs*	C-term.	13	2600	This study
<i>HERG</i>	C3040T	Arg1014Stop*	C-term.	13	2662	This study

**Table 9.3** Continued

gene	nucleot. change	coding effect	position	exon	kindred	study
<i>HERG</i>	C3040T	Arg1014Stop*	C-term.	13	2754	This study
<i>HERG</i>	iC3303-3304	Pro1101fs*	C-term.	14	1789	This study

\* - denotes novel mutation

Thirteen single base pair deletions or insertions, one 31 bp deletion and a 17 bp duplication caused a frameshift and premature termination. Six nucleotide changes lead to nonsense mutations. Splice site sequences were mutated in four of the samples.

#### SCN5A Mutations Associated with LQT in Eight Cases

The cardiac sodium channel gene *SCN5A* (chromosome 3p21, *LQT3*) was screened for all 28 exons. Thirty-three primer pairs were used in SSCP analysis (Wang et al., 1996). *SCN5A* mutations were identified in the members of eight families or sporadic cases (total number of mutations found in our population is 14). Five of the aberrant conformers were observed in unrelated individuals and showed nucleotide changes that lead to amino acid substitutions (Figure 9.3, Tables 9.2 and 9.4). Two individuals had an in-frame deletion of nine base pairs leading to deletion of three amino acids in the DIII/DIV linker. Another in-frame deletion of three nucleotides caused the deletion of a single amino acid. Four of these mutations have not been described before. Another conformer was observed in multiple samples and in normal controls. It contained a nucleotide change resulting in the substitution of His588 for Arg in the DI/DII linker. The allele frequency of Arg588 is 25% and the heterozygosity 29%.

#### MinK Mutation Associated with LQT in One Case

Three primer pairs were used to screen the entire *minK* gene (*LQT5*) on chromosome 21q22.1-22.2 (Splawski et al., 1998). The sequence of an abnormal SSCP band identified in one sample revealed an A to G transition. The change caused an Arg32His substitution in the N-terminal region of the gene (Figure 9.4, Tables 9.2 and

**Figure 9.3** Schematic representation of the predicted topology of SCN5A and locations of LQT-associated mutations.

SCN5A consists of four domains (DI to DIV), each of which has six putative transmembrane segments (S1 to S6) and a pore (Pore) region. Symbols describing the mutations are the same as in Figure 9.1. Mutation information is summarized in Tables 9.2 and 9.4.



**missense**  
AA deletion  
common  
polymorphism

## SCN5A

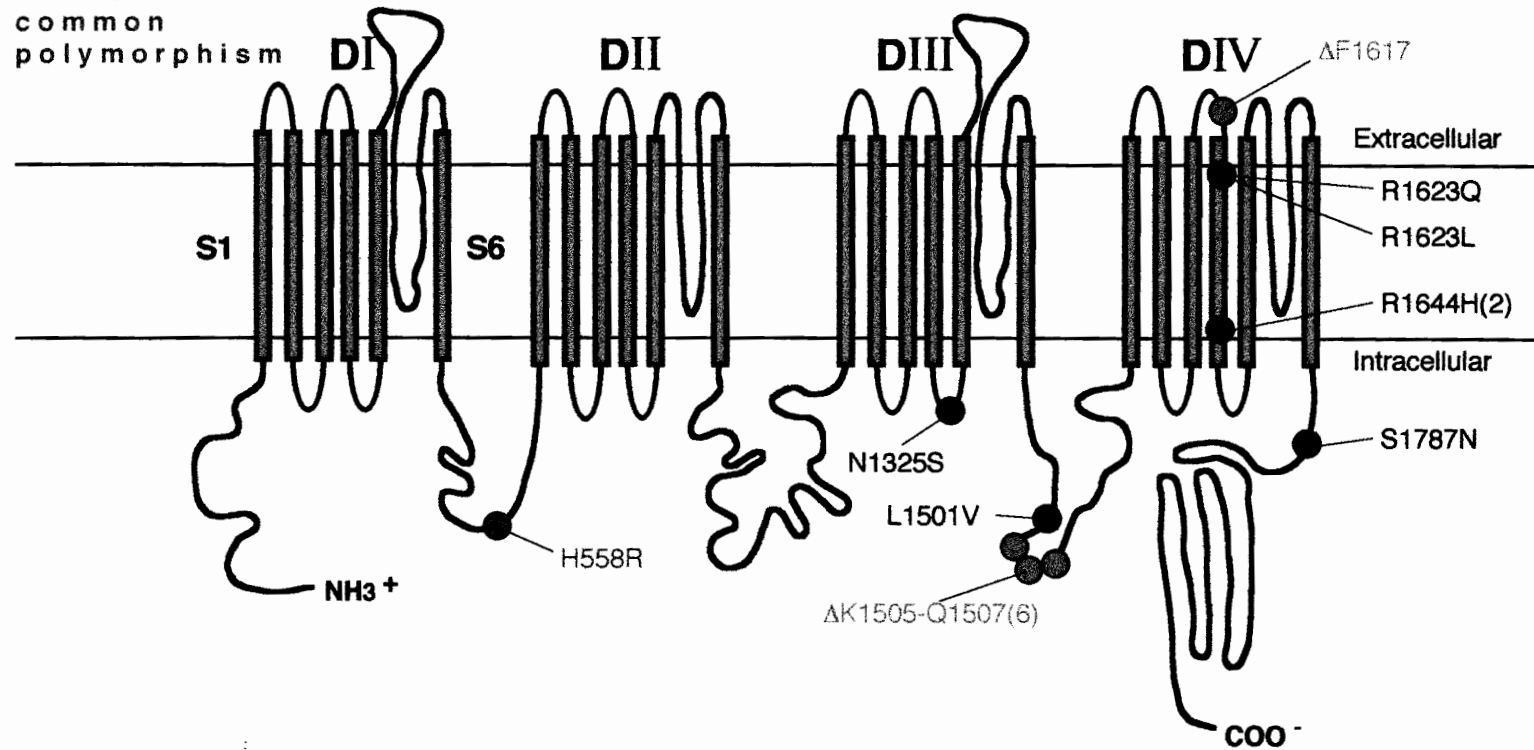


**Table 9.4**Summary of *SCN5A* mutations

gene	nucleot. change	coding effect	position	exon	kindred	study
<i>SCN5A</i>	A1673G	His588Arg	DI/DII	12	many	This study
<i>SCN5A</i>	A3974G	Asn1325Ser	DIII/S4/S5	23	2028	Wang et al.(95b)
<i>SCN5A</i>	C4501G	Leu1501Val*	DIII/DIV	26	3347	This study
<i>SCN5A</i>	Δ4511-4519	Δ1505-1507	DIII/DIV	26	1792	Wang et al.(95b)
<i>SCN5A</i>	Δ4511-4519	Δ1505-1507	DIII/DIV	26	2220	Wang et al.(95b)
<i>SCN5A</i>	Δ4511-4519	Δ1505-1507	DIII/DIV	26	2321	Wang et al.(95a)
<i>SCN5A</i>	Δ4511-4519	Δ1505-1507	DIII/DIV	26	2322	Wang et al.(95a)
<i>SCN5A</i>	Δ4511-4519	Δ1505-1507	DIII/DIV	26	3922	This study
<i>SCN5A</i>	Δ4850-4852	ΔPhe1617*	DIV/S3/S4	28	2943	This study
<i>SCN5A</i>	G4868A	Arg1623Gln	DIV/S4	28	2970	This study
<i>SCN5A</i>	G4868T	Arg1623Leu*	DIV/S4	28	3454	This study
<i>SCN5A</i>	G4931A	Arg1644His	DIV/S4	28	1775	Wang et al.(95b)
<i>SCN5A</i>	G4931A	Arg1644His	DIV/S4	28	2521	This study
<i>SCN5A</i>	G5360A	Ser1787Asn*	C-term.	28	1789	This study

\* - denotes novel mutation

**Figure 9.4** Schematic representation of the predicted topology of minK and locations of LQT-associated mutations.

MinK consists of one putative transmembrane domain (S1). Symbols describing the mutations are the same as in Figure 9.1. Rare polymorphisms not segregating with the disease or found in control individuals are presented in purple. Each LQT-associated mutation or rare polymorphism was found only in one family or single individual.

Mutation information is summarized in Tables 9.2 and 9.5.

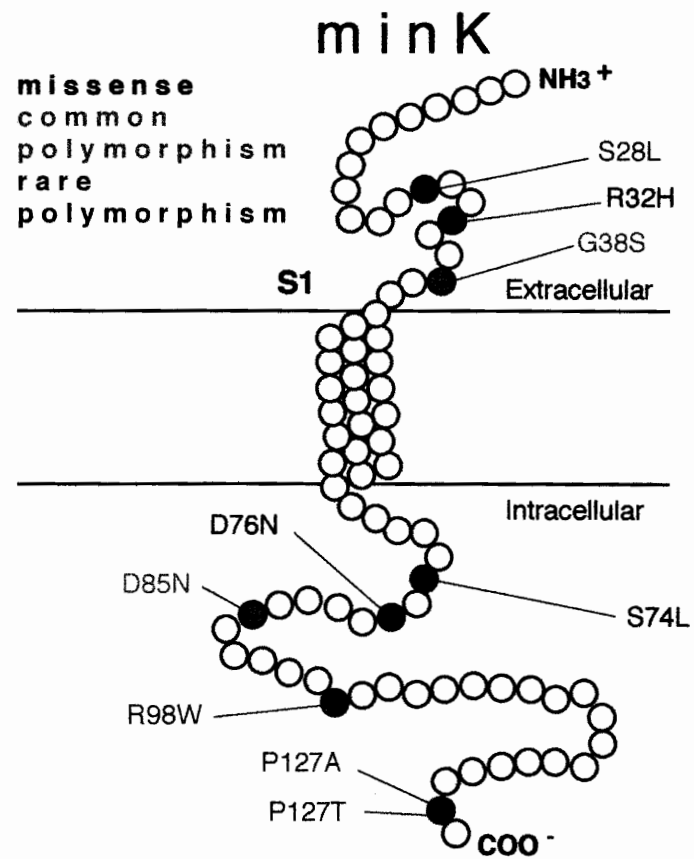


**Table 9.5**Summary of *minK* mutations

gene	nucleot. change	coding effect	position	exon	kindred	study
<i>minK</i>	C83G	Ser28Leu	N-term.	3	1789	This study
<i>minK</i>	G95A	Arg32His*	N-term.	3	2521	This study
<i>minK</i>	G112A	Gly38Ser	N-term.	3	many	This study
<i>minK</i>	C221T	Ser74Leu	C-term.	3	1754	Splawski et al.(97a)
<i>minK</i>	G226A	Asp76Asn	C-term.	3	1789	Splawski et al.(97a)
<i>minK</i>	G253A	Asp85Asn	C-term.	3	many	This study
<i>minK</i>	C292T	Arg98Trp	C-term.	3	2016	This study
<i>minK</i>	C379G	Pro127Ala	C-term.	3	2016	This study
<i>minK</i>	C379A	Pro127Thr	C-term.	3	2819	This study

\* - denotes novel mutation

9.5). This abnormal SSCP conformer was not observed in 200 control individuals. The analyses demonstrated six other conformers. Two of them were common polymorphisms - Gly38Ser and Asp85Asn. The allele frequency of Ser38 is 32% and the heterozygosity is 46%. The frequency of Asn85 is 2.5% and the heterozygosity is 5%. Both polymorphisms had the same frequency among affected and control individuals. Two amino acid changes, Ser28Leu and Pro127Thr, found in affected individuals did not segregate with the disease phenotype and did not have a functional effect when expressed in *Xenopus* oocytes (Dr. M. Sanguinetti, personal communication). Arg98Trp and Pro127Ala substitutions were identified in single control individuals.

### Discussion

*KVLQT1*, *HERG* and *minK* encode potassium channel subunits. Four KVLQT1 subunits coassemble with minK (stoichiometry is unknown) to form  $I_{Ks}$  channels underlying the slowly activating delayed rectifier potassium current in the heart (Barhanin et al., 1996; Sanguinetti et al., 1996). Four HERG subunits form  $I_{Kr}$  channels which underlie the rapidly activating delayed rectifier potassium current (Sanguinetti et al., 1995; Trudeau et al., 1995). It has been shown that, in most cases, expression of homomeric mutant KVLQT1 (with minK), HERG or minK (with KVLQT1) in *Xenopus* oocytes fails to produce functional channels (Chouabe et al., 1997; Sanguinetti et al., 1996; Shalaby et al., 1997; Splawski et al., 1997; Wollnik et al., 1997). Coexpression of mutant and normal subunits leads to reduction of  $I_{Ks}$  or  $I_{Kr}$  by a dominant-negative mechanism or loss of function. In a few of the cases, heteromeric channels show modified biophysical properties. *SCN5A* encodes the cardiac sodium channel which is responsible for  $I_{Na}$ , the

sodium current in the heart (Gellens et al., 1992). LQT-associated mutations in *SCN5A* resulted in gain of function (Bennett et al., 1995; Dumaine et al., 1996). The inactivation gate of mutant *SCN5A* is destabilized resulting in repetitive channel opening. In the heart, the reduced activity of  $I_{Ks}$  and  $I_{Kr}$  channels and the increased activity of  $I_{Na}$  channels will lead to prolongation of the cardiac action potential, lengthening of the QT interval on an electrocardiogram and increased risk of arrhythmia.

Since the initial identification of *KVLQTI*, *HERG*, *SCN5A* and *minK* as LQT genes, 67 different disease causing mutations have been reported (Akimoto et al., 1998; Benson et al., 1996; Curran et al., 1995; Dausse et al., 1996; Donger et al., 1997; Duggal et al., 1998; Kambouris et al., 1998; Li and al., 1998; Makita et al., 1998; Neyroud et al., 1997; Russell et al., 1996; Saarinen et al., 1998; Satler et al., 1998; Satler et al., 1996; Schulze-Bahr et al., 1995; Schulze-Bahr et al., 1997; Splawski et al., 1998; Splawski et al., 1997; Splawski et al., 1997; Tanaka et al., 1997; Tyson et al., 1997; van den Berg et al., 1997; Wang et al., 1996; Wang et al., 1995; Wang et al., 1995; Wollnik et al., 1997). Most of them are found in *KVLQTI* (39) and *HERG* (20), and fewer in *SCN5A* (4) and *minK* (4). These mutations were identified in regions of the genes for which the intron/exon structure was known, primarily the transmembrane segments and the pore domain. In this study, utilizing the complete genomic structure of the LQT genes, we screened for mutations in the entire coding regions of each gene. Samples from 350 unrelated individuals with inherited, sporadic or acquired LQT were used. We identified a total of 138 new mutations (59 in *KVLQTI*, 70 in *HERG*, 8 in *SCN5A* and 1 in *minK* (Figures 9.1-9.4 and Tables 9.1-9.5 show a summary of the newly discovered mutations and the

mutations reported in our previous papers). There were 89 different mutations that had not been published before.

*KVLQT1* mutations associated with LQT were identified in 59 individuals.

Twenty-seven were new and had not been described before. Missense mutations were most common, but we also found nonsense, splice, and deletion mutations (Figure 9.1, Tables 9.1 and 9.2). Most mutations in *KVLQT1* were found in the S2/S3 and S4/S5 linkers, the P region, transmembrane segment S6, and the C-terminus. Few or single mutations were identified in the N-terminus, S2, S4, S5 and no mutations were found in S1, S3 and the S5/Pore linker. *HERG* mutations were identified in the members of 70 LQT families or sporadic cases (Figure 9.2, Tables 9.2 and 9.3). Sixty-one were novel and had not been described before. Most of them were missense or frameshift mutations. The frameshifts resulted from one to several nucleotide insertions or deletions. We also detected splice and nonsense mutations, and an amino acid deletion. The majority of the mutations were found in the N-terminus, the S5/P linker, the P region and the C-terminus. Few mutations were identified in the transmembrane segments. There were no mutations in the S2/S3 and S4/S5 linkers.

The P region of potassium channels forms the outer pore and contains the selectivity filter. Transmembrane segment S6 (the inner helix) forms the inner 2/3 of the pore (Doyle et al., 1998). This structure of potassium channels is conserved from prokaryotes to higher eukaryotes (MacKinnon et al., 1998). Mutations in these regions will likely disrupt potassium transport. Indeed, multiple mutations common for *HERG* and *KVLQT1* were found in the pore and S6, and also in the C-terminus. Mutations in the C-terminus of *HERG* most likely lead to anomalies in tetramerization as it has been



proposed that the C-terminus of *eag* (related to HERG) is involved in this process (Ludwig et al., 1994). Currently, we are investigating the effects of mutations in the C-terminal region of *KVLQT1* to better understand its role in  $I_{Ks}$  channel function.

Multiple mutations were identified in other regions that were different for *HERG* and *KVLQT1*. More than 20 mutations were detected in the N-terminus of *HERG*. The N-terminus of HERG is thought to be involved in deactivation (Spector, 1996). HERG channels lacking this region deactivate faster and mutations in the region might have a similar effect. We are now testing this hypothesis. Multiple mutations in *KVLQT1*, were found in the S2/S3 and S4/S5 linkers. Coexpression of four S2/S3 mutants with WT KVLQT1 in *Xenopus* oocytes reduced  $I_{Ks}$  by simple loss of function or dominant-negative effect without significantly changing the biophysical properties of the channel (Chouabe et al., 1997; Shalaby et al., 1997; Wang et al., 1998). On the other hand, heteromultimeric channels formed by an S4/S5 mutant and WT KVLQT1 activated much faster and inactivated more effectively (Wang et al., 1998). This is suggestive of a role for the S4/S5 linker of KVLQT1 in channel activation and inactivation gating. The functional consequences of additional mutations in this region are now being studied.

Four of the *SCN5A* mutations (Figure 9.3 and Tables 9.2 and 9.4), identified in the members of eight families or sporadic cases, and the *minK* mutation (Figure 9.4 and Tables 9.2 and 9.5), detected in one individual, are novel. The mutations in the sodium channel most likely will be gain of function mutations, with effects similar to the previously described mutations. The Arg to His substitution in minK might alter the channel activity in response to changes in extracellular pH. We are now in the process of assessing the effects of *SCN5A* and *minK* mutations on channel function.

The catalogue of mutations will facilitate genotype-phenotype correlation analyses. It also has clinical implications for presymptomatic diagnosis and in some cases for effective drug therapy. Patients with mutations in *KVLQT1*, *HERG* and *minK*, for example, may benefit from potassium channel opener drugs. Sodium channel blockers, on the other hand, might be helpful in patients with *SCN5A* mutations. The identification of mutations is of importance for ion channel studies as well. The expression of mutant channels in *Xenopus* oocytes or mammalian cells can reveal how structural changes influence the behavior of the channel. These studies improve our understanding of channel function and provide insights into mechanisms of disease. Mutation identification will also contribute to future efforts in developing sensitive and effective screening tests.

In summary, we screened the entire coding sequence of the potassium channel subunit genes *KVLQT1*, *HERG* and *minK*, and the sodium channel gene *SCN5A*. We report the identification of 138 mutations associated with LQT, 89 of which are novel. The total number of mutations detected in the four genes in our population of 350 LQT patients is now 177. The sensitivity of the SSCP technique for mutation detection, however, is less than 100%. Mutations in *KVLQT1*, *HERG*, *SCN5A* and *minK*, therefore, would represent more than half of all LQT mutations. In our studies, *KVLQT1* (45%) and *HERG* (45%) accounted for 90% of the identified mutations, while *SCN5A* (8%) and *minK* (2%) accounted for the other 10%.

## References

- Akimoto, K., Furutani, M., Imamura, S., Furutani, Y., Kasanuki, H., Takao, A., Momma, K., and Matsuoka, R. (1998). Novel missense mutation (G601S) of *HERG* in a Japanese long QT syndrome family. *Hum. Mutat.* 1, S184-S186.
- Barhanin, J., Lesage, F., Guillemare, E., Fink, M., Lazdunski, M., and Romey, G. (1996). KvLQT1 and IsK (minK) proteins associate to form the  $I_{Ks}$  cardiac potassium current. *Nature* 384, 78-80.
- Bennett, P. B., Yazawa, K., Makita, N., and George, A. L. (1995). Molecular mechanism for an inherited cardiac arrhythmia. *Nature* 376, 683-685.
- Benson, D. W., MacRae, C. A., Vesely, M. R., Walsh, E. P., Seidman, J. G., Seidman, C. E., and Satler, C. A. (1996). Missense mutation in the pore region of *HERG* causes familial long QT syndrome. *Circulation* 93, 1791-1795.
- Chouabe, C., Neyroud, N., Guicheney, P., Lazdunski, M., Romey, G., and Barhanin, J. (1997). Properties of KvLQT1  $K^+$  channel mutations in Romano-Ward and Jervell and Lange-Nielsen inherited cardiac arrhythmias. *EMBO J.* 16, 5472-5479.
- Curran, M. E., Splawski, I., Timothy, K. W., Vincent, G. M., Green, E. D., and Keating, M. T. (1995). A molecular basis for cardiac arrhythmia: *HERG* mutations cause long QT syndrome. *Cell* 80, 795-803.
- Dausse, E., Berthet, M., Denjoy, I., Andre-Fouet, X., Cruaud, C., Bennaceur, M., Faure, S., Coumel, P., Schwartz, K., and Guicheney, P. (1996). A mutation in *HERG* associated with notched T waves in long QT syndrome. *J. Mol. Cell. Cardiol.* 28, 1609-1615.
- Donger, C., Denjoy, I., Berthet, M., Neyroud, N., Cruaud, C., Bennaceur, M., Chivoret, G., Schwartz, K., Coumel, P., and Guicheney, P. (1997). KvLQT1 C-terminal missense mutation causes a forme fruste long-QT syndrome. *Circulation* 96, 2778-2781.
- Doyle, D. A., Cabral, J. M., Pfuetzner, R. A., Kuo, A., Gublis, J. M., Cohen, S. L., Chait, B. T., and MacKinnon, R. (1998). The structure of the potassium channel: molecular basis of  $K^+$  conduction and selectivity. *Science* 280, 69-77.
- Duggal, P., Vesely, M. R., Wattanasirichaigoon, D., Villafane, J., Kaushik, V., and Beggs, A. H. (1998). Mutation of the gene for IsK associated with both Jervell and Lange-Nielsen and Romano-Ward forms of Long-QT syndrome. *Circulation* 97, 142-6.
- Dumaine, R., Wang, Q., Keating, M. T., Hartmann, H. A., Schwartz, P. J., Brown, A. M., and Kirsch, G. E. (1996). Multiple mechanisms of sodium channel-linked long QT syndrome. *Circ. Res.* 78, 914-924.

- Gellens, M., George, A., Chen, L., Chahine, M., Horn, R., Barchi, R., and Kallen, R. (1992). Primary structure and functional expression of the human cardiac tetrodotoxin-insensitive voltage-dependent sodium channel. *Proc. Natl. Acad. Sci. USA* 89, 554-558.
- Jervell, A., and Lange-Nielsen, F. (1957). Congenital deaf-mutism, functional heart disease with prolongation of the QT interval, and sudden death. *Am. Heart J.* 54, 59-68.
- Jiang, C., Atkinson, D., Towbin, J., Splawski, I., Lehmann, M., Li, H., Timothy, K., Taggart, R., Schwartz, P., Vincent, G. M., Moss, A., and Keating, M. (1994). Two long QT syndrome loci map to chromosome 3 and 7 with evidence for further heterogeneity. *Nat. Genet.* 8, 141-147.
- Kambouris, N. G., Nuss, H. B., Johns, D. C., Tomaselli, G. F., Marban, E., and Balser, J. R. (1998). Phenotypic characterization of a novel long-QT syndrome mutation (R1623Q) in the cardiac sodium channel. *Circulation* 97, 640-644.
- Kannel, W. B., Cupples, A., and D'Agostino, R. B. (1987). Sudden death risk in overt coronary heart diseases: the Framingham study. *Am. Heart J.* 113, 799-804.
- Keating, M., Atkinson, D., Dunn, C., Timothy, K., Vincent, G. M., and Leppert, M. (1991). Linkage of a cardiac arrhythmia, the long QT syndrome, and the Harvey *ras-1* gene. *Science* 252, 704-706.
- Li, H., Chen, Q., Moss, A. J., Robinson, J., Goytia, V., Perry, J. C., Vincent, G. M., Priori, S. G., Lehmann, M. H., Denfield, S. W., Duff, D., Kaine, S., Shimizu, W., Schwartz, P. J., Wang, Q., and Towbin, J. A. (1998). New mutations in the KVLQT1 potassium channel that cause long-QT syndrome. *Circulation* 97, 1264-1269.
- Ludwig, J., Terlau, H., Wunder, F., Bruggemann, A., Pardo, L., Marquardt, A., Stuhmer, W., and Pongs, O. (1994). Functional expression of a rat homologue of the voltage gated *ether a go-go* potassium channel reveals differences in selectivity and activation kinetics between the *Drosophila* channel and its mammalian counterpart. *EMBO J.* 13, 4451-4458.
- MacKinnon, R., Cohen, S. L., Kuo, A., Lee, A., and Chait, B. (1998). Structural conservation in prokaryotic and eukaryotic potassium channels. *Science* 280, 106-109.
- Makita, N., Shirai, N., Nagashima, N., Matsuoka, R., Yamada, Y., Tohse, N., and Kitabatake, A. (1998). A de novo missense mutation of human cardiac Na<sup>+</sup> channel exhibiting novel molecular mechanisms of long QT syndrome. *FEBS Lett.* 423, 5-9.
- Moss, A., Schwartz, P., Crampton, R., Tzivoni, D., Locati-Heilbron, E., MacCluer, Hall, W., Weitkamp, L., Vincent, G. M., Garson, A., Robinson, J., and Benhorin, J. (1991). The long QT syndrome: prospective longitudinal study of 328 families. *Circulation* 84, 1136-1144.

- Neyroud, N., Tesson, F., Denjoy, I., Leibovici, M., Donger, C., Barhanin, J., Faure, S., Gary, F., Coumel, P., Petit, C., Schwartz, K., and Guicheney, P. (1997). A novel mutation in the potassium channel gene *KVLQT1* causes the Jervell and Lange-Nielsen cardioauditory syndrome. *Nat. Genet.* 15, 186-189.
- Romano, C., Gemme, G., and Pongiglione, R. (1963). Artimie cardiach rare dell'eta pediatrica. II. Accessi sincopali per fibrillazione ventricolare parossitica. *Clin. Pediatr.* 45, 656-683.
- Russell, M. W., Dick, M., Collins, F. S., and Brody, L. C. (1996). KVLQT1 mutations in three families with familial or sporadic long QT syndrome. *Hum. Mol. Genet.* 5, 1319-1324.
- Saarinén, K., Swan, H., Kainulainen, K., Toivonen, L., Viitasalo, M., and Kontula, K. (1998). Molecular genetics of the long QT syndrome: two novel mutations of the KVLQT1 gene and phenotypic expression of the mutant gene in a large kindred. *Hum. Mutat.* 11, 158-165.
- Sanguinetti, M. C., Curran, M. E., Spector, P. S., and Keating, M. T. (1996). Spectrum of HERG K<sup>+</sup> channel dysfunction in an inherited cardiac arrhythmia. *Proc. Natl. Acad. Sci., USA* 93, 2208-2212.
- Sanguinetti, M. C., Curran, M. E., Zou, A., Shen, J., Spector, P. S., Atkinson, D. L., and Keating, M. T. (1996). Coassembly of KvLQT1 and minK (IsK) proteins to form cardiac I<sub>Ks</sub> potassium channel. *Nature* 384, 80-83.
- Sanguinetti, M. C., Jiang, C., Curran, M. E., and Keating, M. T. (1995). A mechanistic link between an inherited and an acquired cardiac arrhythmia: HERG encodes the I<sub>Kr</sub> potassium channel. *Cell* 81, 299-307.
- Satler, C. A., Vesely, M. R., Duggal, P., Ginsburg, G. S., and Beggs, A. H. (1998). Multiple different missense mutations in the pore region of HERG in patients with long QT syndrome. *Hum. Genet.* 102, 265-272.
- Satler, C. A., Walsh, E. P., Vesely, M. R., Plummer, M. H., Ginsburg, G. S., and Jacob, H. J. (1996). Novel missense mutation in the cyclic nucleotide-binding domain of HERG causes long QT syndrome. *Am. J. Med. Genet.* 65, 27-35.
- Schott, J., Charpentier, F., Peltier, S., Foley, P., Drouin, E., Bouhour, J., Donnelly, P., Vergnaud, G., Bachner, L., Moisan, J., Le Marec, H., and Pascal, O. (1995). Mapping of a gene for long QT syndrome to chromosome 4q25-27. *Am. J. Hum. Genet.* 57, 1114-1122.
- Schulze-Bahr, E., Haverkamp, W., and Funke, H. (1995). The Long-QT Syndrome. *N. Engl. J. Med.* 333, 1783-1784.

- Schulze-Bahr, E., Wang, Q., Wedekind, H., Haverkamp, W., Chen, Q., Sun, Y., Rubie, C., Hordt, M., Towbin, J., Borggrefe, M., Assmann, G., Qu, X., Somberg, J. C., Breithardt, G., Oberti, C., and Funke, H. (1997). *KCNE1* mutations cause Jervell and Lange-Nielsen syndrome. *Nat. Genet.* 17, 267-268.
- Schwartz, P. J., Periti, M., and Malliani, A. (1975). The long Q-T syndrome. *Am. Heart J.* 89, 378-390.
- Shalaby, F. Y., Levesque, P. C., Yang, W. P., Little, W. A., Conder, M. L., Jenkins-West, T., and Blann, M. A. (1997). Dominant-negative KvLQT1 mutations underlie the LQT1 form of long QT syndrome. *Circulation* 96, 1733-1736.
- Spector, P. S., Curran, M. E., Zou, A., Keating, M. T., and Sanguinetti, M. C. (1996). Fast inactivation causes rectification of the  $I_{K_r}$  channel. *J. Gen. Physiol.* 107, 611-619.
- Splawski, I., Shen, J., Timothy, K. W., Vincent, G. M., Lehmann, M. H., and Keating, M. T. (1998). Genomic structure of three long QT syndrome genes: *KVLQT1*, *HERG* and *KCNE1*. *Genomics* 51, 86-97.
- Splawski, I., Timothy, K. W., Vincent, G. M., Atkinson, D. L., and Keating, M. T. (1997). Molecular basis of the long-QT syndrome associated with deafness. *N. Engl. J. Med.* 336, 1562-1567.
- Splawski, I., Tristani-Firouzi, M., Lehmann, M. H., Sanguinetti, M. C., and Keating, M. T. (1997). Mutations in the hminK gene cause long QT syndrome and suppress  $I_{K_s}$  function. *Nat. Genet.* 17, 338-340.
- Tanaka, T., Nagai, R., Tomoike, H., Takata, S., Yano, K., Yabuta, K., Haneda, N., Nakano, O., Shibata, A., Sawayama, T., Kasai, H., Yazaki, Y., and Nakamura, Y. (1997). Four novel KVLQT1 and four novel HERG mutations in familial long-QT syndrome. *Circulation* 95, 565-567.
- Trudeau, M. C., Warmke, J. W., Ganetzky, B., and Robertson, G. A. (1995). HERG, a human inward rectifier in the voltage-gated potassium channel family. *Science* 269, 92-95.
- Tyson, J., Tranebjaerg, L., Bellman, S., Wren, C., Taylor, J. F. N., Bathen, J., Aslaksen, B., Sorland, S. J., Lund, O., Malcolm, S., Pembrey, M., Bhattacharya, S., and Bitner-Glindzicz, M. (1997). IsK and KvLQT1: mutation in either of the two subunits of the slow component of the delayed rectifier potassium channel can cause Jervell and Lange-Nielsen syndrome. *Hum. Mol. Genet.* 6, 2179-2185.
- van den Berg, M. H., Wilde, A. A., Robles de Medina, E. O., Meyer, H., Geelen, J. L., Jongbloed, R. J., Wellens, H. J., and Geraedts, J. P. (1997). The long QT syndrome: a novel missense mutation in the S6 region of the KVLQT1 gene. *Hum. Genet.* 100, 356-361.

Vetter, D. E., Mann, J. R., Wangemann, P., Liu, J., McLaughlin, K. J., Lesage, F., Marcus, D. C., Lazdunski, M., Heinemann, S. F., and Barhanin, J. (1996). Inner ear defects induced by null mutation of the *isk* gene. *Neuron* 17, 1251-1264.

Vincent, G. M., Timothy, K., Leppert, M., and Keating, M. (1992). The spectrum of symptoms and QT intervals in carriers of the gene for the long QT syndrome. *N. Engl. J. Med.* 327, 846-852.

Wang, Q., Curran, M. E., Splawski, I., Burn, T. C., Millholland, J. M., VanRaay, T. J., Shen, J., Timothy, K. W., Vincent, G. M., de Jager, T., Schwartz, P. J., Towbin, J. A., Moss, A. J., Atkinson, D. L., Landes, G. M., Connors, T. D., and Keating, M. T. (1996). Positional cloning of a novel potassium channel gene: KVLQT1 mutations cause cardiac arrhythmias. *Nat. Genet.* 12, 17-23.

Wang, Q., Shen, J., Li, Z., Timothy, K., Vincent, G. M., Priori, S. G., Schwartz, P. J., and Keating, M. T. (1995). Cardiac sodium channel mutations in patients with long QT syndrome, an inherited cardiac arrhythmia. *Hum. Mol. Genet.* 4, 1603-1607.

Wang, Q., Shen, J., Splawski, I., Atkinson, D., Zhizhong, L., Robinson, J., Moss, A., Towbin, J., and Keating, M. (1995). *SCN5A* mutations associated with an inherited cardiac arrhythmia, long QT syndrome. *Cell* 80, 805-811.

Wang, Q., Zhizhong, L., Shen, J., and Keating, M. T. (1996). Genomic organization of the human *SCN5A* gene encoding the cardiac sodium channel. *Genomics* 34, 9-16.

Wang, Z., Tristani-Firouzi, M., Xu, Q., Lin, M., Keating, M. T., and Sanguinetti, M. C. (1998). Functional effects of mutations in KVLQT1 that cause inherited long QT syndrome. *J. Cardiovasc. Electrophysiol.*

Ward, O. C. (1964). A new familial cardiac syndrome in children. *J. Ir. Med. Assoc.* 54, 103-106.

Willich, S. N., Levy, D., Rocco, M. B., Tofler, G. H., Stone, P. H., and Muller, J. O. E. (1987). Circadian variation in the incidence of sudden cardiac death in the Framingham heart study population. *Am. J. Cardiol.* 60, 801-806.

Wollnik, B., Schroeder, B. C., Kubisch, C., Esperer, H. D., Wieacker, P., and Jentsch, T. J. (1997). Pathophysiological mechanisms of dominant and recessive KVLQT1 K<sup>+</sup> channel mutations found in inherited cardiac arrhythmias. *Hum. Mol. Genet.* 6, 1943-1949.